Evolutionary conserved breakpoints in Old World Monkeys and New World Monkeys and their relation to fragile sites observed in Homo sapiens

Dissertation

in partial fulfilment of the requirements for the degree of doctor rerum naturalium (Dr. rer. nat.)

submitted to the Faculty Council of the School of Medicine at Friedrich Schiller University of Jena

by M.Sc. Fan Xiaobo

born on 28.09.1984 in Xu Zhou, China

Reviewers

1. **PD Dr. rer. nat. / med. habil. Thomas Liehr**

   Institute of Human Genetics, Friedrich Schiller University of Jena

2. **Prof. Dr. rer. nat. Wim Damen**

   Faculty of Biology and Pharmacy, Friedrich Schiller University of Jena

3. **PD Mag. Dr. rer. nat. Irmgard Verdorfer**

   Department of Pathology, Medical University of Innsbruck

Date of the public disputation: 06.07.2016

Dedication

To my beloved parents and to my future family.

To all of those, who supported and encouraged me.

To those who keep on advancing for pursuing a dream.

Contents

Abbreviations

ACA	*Alouatta caraya*
aCGH	Array-comparative genomic hybridization
AD	Alzheimer's disease
AIDS	Acquired immunodeficiency syndrome
BAC	Bacterial artificial chromosome
BrdU	Bromodeoxyuridine
CAE	*Chlorocebus aethiops*
CAP	*Cebus apella*
C-bands	Constitutive heterochromatin bands
cFSs	Common fragile sites
CGH	Comparative genomic hybridization
CJA	*Callithrix jacchus*
CML	Chronic myelogenous leukemia
CNI	*Cebus nigrivittatus*
CNVs	Copy number variations
CPA	*Cebus apella paraguayanus*
DNA	Deoxyribonucleic acid
DOP-PCR	Degenerate oligonucleotide primed polymerase chain reaction
ECBs	Evolutionary conserved breakpoints
FdU	Fluorodeoxyuridine
Fig.	Figure
FISH	Fluorescence in situ hybridization
FSs	Fragile sites
G-bands	Giemsa dye based bands
GGO	*Gorilla gorilla*
HCM-FISH	Heterochromatin mix fluorescence in situ hybridization
HLA	*Hylobates lar*
HSA	*Homo sapiens*
ITSs	Interstitial telomeric sequences
Kb	Kilobase
MAR	*Macaca arctoides*

MAS	*Macaca assamensis*
MCB	Multicolor banding
MFA	*Macaca fasciculars*
M-FISH	Multiplex-FISH using whole chromosome paints
MMU	*Macaca mulatta*
MNE	*Macaca nemestrina*
MSP	*Mandrillus sphinx*
MSY	*Macaca sylvanus*
NGS	Next-generation sequencing
NHPs	Non-human Primates
NORs	Nucleolus organizing regions (bands)
NWMs	New World Monkeys
OMIM	Online Mendelian Inheritance in Man
OWMs	Old World Monkeys
PACs	P1-derived artificial chromosome
PD	Parkinson's disease
PPY	*Pongo pygmeu*
PTR	*Pan troglodytes*
Q-bands	Quinacrine dihydrochloride
R-bands	Reverse staining bands
rFSs	Rare fragile sites
SBO	*Saimiri boliviensis*
SKY	Spectral karyotyping
SSC	*Saimiri sciureus*
STRs	Short tandem repeats
SubcenM-FISH	Subcentromeric multicolor fluorescence in situ hybridization
TB	Tuberculosis
T-bands	Telomeric bands
TCR	*Trachypithecus cristatus*
TSGs	Tumor suppressor genes
WBS	Williams–Beuren syndrome
WCP	Whole chromosome paints
YACs	Yeast artificial chromosome

Summary

Evolutionary conserved breakpoints (ECBs) in Old World Monkeys (OWMs) and New World Monkeys (NWMs) are localized in particular chromosomal bands and prone to breakage during the phylogeny. Similarly, fragile sites (FSs) are specific regions in *Homo sapiens* (HSA) which can be induced to form gaps or breaks. Notably, FSs can be involved in chromosomal rearrangements in cancer, owing as targets of carcinogens; also FSs have been positively correlated with breakpoints of constitutional rearrangements in human. Thus, a comparative study of the relation of ECBs and FSs is necessary to uncover the common underlying principles of chromosomal alterations in human diseases and evolution. Chromosomal homologies of HSA and OWMs/NWMs have previously been studied by chromosome banding and fluorescence in situ hybridization (FISH). However, due to limitations in resolution of such techniques, in this study I applied for the first time multicolor banding (MCB) probe sets complemented with selected locus-specific and heterochromatin specific probes to characterize ECBs in *Hylobates lar* (HLA; here also microdissection combined with array-techniques was applied), eight OWMs and four NWMs, such as *Trachypithecus cristatus* (TCR), *Macaca nemestrina* (MNE), *Macaca sylvanus* (MSY), *Macaca fascicularis* (MFA), *Chlorocebus aethiops* (CAE), *Alouatta caraya* (ACA), *Cebus apella* (CAP), *Callithrix jacchus* (CJA), *Saimiri sciureus* (SSC), *Macaca mulatta* (MMU), *Macaca arctoides* (MAR) and *Macaca assamensis* (MAS). Thus, numerous new ECBs were characterized for the first time in detail, and centromeric positions in several species could be redefined. In HLA 92 ECBs were accessible by the used approach and overall, this study identified 73 ECBs in TCR, 53 identical ECBs for all studied macaque species, 41 in CAE, 51 in ACA, 44 in CAP, 47 in CJA and 64 in SSC. Also the results showed that the monkey chromosomes homologous to human #3, #7 and #9 presented enhanced rates of ECBs both in OWMs and NWMs. ECBs of NWMs and OWMs could be followed during evolution and aligned with FSs observed in HSA. Most interestingly more than 60% of ECBs co-localized with known FSs and ~70% of ECBs corresponded to breakpoints that can be observed in human disorders. For medical field this data is important as FSs now clearly were aligned on molecular level with ECBs. In other words the disease associated chromosomal defects, seem at least in parts be due to breakage prone regions of the mammalian genome.

Zusammenfassung

Evolutionär konservierte Bruchpunkte (ECBs) in Alt- (OWMs) und Neuweltaffen (NWMs) sind in bestimmten chromosomalen Banden lokalisiert und anfällig für Bruchereignisse während der Phylogenie. Weiterhin gibt es sog. fragile Sites (FSs) die in bestimmten Regionen unter entsprechender Induktion im Genom von *Homo sapiens* (HSA) auftreten können, und sich als Lücken oder Brüche darstellen. Bemerkenswert ist, dass FSs mitkrebsassoziiertem Chromosomenaberrationen assoziiert wurden, wo sie als Ziele von Karzinogenen dienen können; außerdem wurden FSs auch schon positiv mit konstitutionellen Bruchpunkten von HSA korreliert. Somit ist eine vergleichende Studie über die Beziehung von ECBs und FSs dringend erforderlich, um gemeinsame zugrundeliegenden Prinzipien von chromosomalen Veränderungen beim Menschen und innerhalb der Evolution aufzudecken. Chromosomale Homologien von HSA und OWMs / NWMs wurden bereits früher mittels Chromosomenbänderungsanalyse und Fluoreszenz-in-situ-Hybridisierung (FISH) untersucht. Jedoch hatten derartige Studien nur ein beschränkte Auflösung, so dass ich in hier erstmals das hierfür besser geeignete multicolor-banding (MCB), ergänzt durch ausgewählte lokus- und Heterochromatin spezifische Sonden zur ECB-Charakterisierung einsetzte; und zwar bei *Hylobates lar* (HLA, hier wurde auch mit Array-Techniken kombinierte Mikrodissektion angewandt), acht OWMs und vier NWMs, namentlich *Trachypithecus cristatus* (TCR), *Macaca nemestrina* (MNE), *Macaca sylvanus* (MSY), *Macaca fascicularis* (MFA), *Chlorocebus aethiops* (CAE), *Alouatta caraya* (ACA), *Cebus apella* (CAP), *Callithrix jacchus* (CJA), *Saimiri sciureus* (SSC), *Macaca mulatta* (MMU), *Macaca arctoides* (MAR) und *Macaca assamensis* (MAS). Durch diesen Ansatz wurden zahlreiche neue ECBs erstmals detailliert charakterisiert und Zentromer-Positionen bei verschiedenen Spezies neu definiert. In HLA wurden 92 ECBs durch den verwendeten Ansatz zugänglich und insgesamt in dieser Studie identifiziert wurden 73 ECBs in TCR, 53 identische ECBs für alle untersuchten Makaken Arten, 41 in CAE, 51 in ACA, 44 in der CAP, 47 in CJA und 64 SSC. Darüber hinaus zeigten die Ergebnisse, dass diejenigen Affen-Chromosomen die homolog zu den Menschlichen #3, #7 und #9 sind, erhöhte Raten an ECBs sowohl in OWMs und NWMs aufwiesen. ECBs der NWMs und OWMs konnten im Verlauf ihrer Evolution verfolgt und die ECBs konnten mit FSs in HSA abgeglichen werden. Interessanterweise

kolokalisierten mehr als 60% der ECBs mit bekannten FSs und ~70% der ECBs entsprachen Bruchpunkten, die in bei menschlichen Erbkrankheiten beobachtet werden können. Für den medizinischen Bereich sind diese Daten deshalb wichtig weil FSs nun erstmals auf molekularer Ebene mit ECBs in Zusammenhang gebracht werden konnten. Mit anderen Worten, die krankheitsassoziiertem Chromosomendefekte scheinen zumindest teilweise aufgrund von bruchanfälligen Regionen des Säugetiergenoms zu entstehen.

1. Introduction

1.1 Cytogenetics

Cytogenetics is a field of genetics including studies on the numbers, structures, function and evolution of chromosomes in human, animals and plants. In 1882, Walther Flemming discovered the fibrous network within the nucleus, which was designated as chromosomes by Wilhelm von Waldeyer (O'Connor and Miko 2008). In the early of 1900s, Boveri postulated the linkage between chromosome and heredity. Finally it was Hunt Morgan who proved that genetic material is located on the chromosomes. Interestingly it was not before 1956, that the correct model chromosome number in man was determined as 46 (Tjio JH and Levan A. 1956). After this important finding the field of human cytogenetics was able to grow.

1.1.1 Classical and banding cytogenetics

The era of diagnostic cytogenetics started with the discovery that Down syndrome is due to trisomy 21 in 1958 (Lejeune et al.1958). From then on, cytogenetics played a significant role in human chromosomal aberration and disease diagnosis, which even became more important with the development of chromosome banding techniques such as Q-, G-, C- and NOR banding. In 1969, Q-banding as the first chromosome banding approach was able to characterize a complete human karyotype using quinicrine fluorescent staining (Caspersson et al.1969). Meanwhile, also C-banding was reported as being helpful to study constitutive heterochromatin (Pardue and Gall 1970). Giemsa staining in human chromosomes with trypsin modification was established in 1971 (Seabright 1971), distinguishing unique banding patterns of each chromosome under a bright field microscope. In 1975, Yunis and coworkers established experimental conditions to obtain high resolution of up to 1,000 bands per haploid chromosome set (Yunis and Sanehez 1975). Nowadays, G-banding has become the routine chromosome analysis technique. Besides above mentioned, there are other staining methods including reverse banding (R-banding) telomeric banding (T-banding) and nucleolus organizing regions (NORs) staining.

1.1.2 Fluorescence in situ hybridization (FISH) and FISH probes

Despite the high-resolution G-banding (resolution of ~3Mb) is effective in detection of chromosomal aberrations (Bishop 2010), small and complex chromosomal aberrations still could escape detection. To overcome this limitation, a new technique using fluorescence labeled DNA sequences to label specific chromosomal regions, was introduced in the 1980s to support banding cytogenetic analysis. This method was termed fluorescence in situ hybridization (FISH). Until now, many different kinds of FISH probes were introduced, as outlined below.

In 1986, Pinkel and coworkers used plasmid DNA labeled with fluorescent dyes to hybridize the whole human Y-chromosome (Pinkel et al. 1986). These probes were called whole chromosome paints (WCPs) and labeled by nick-translation. In 1992, WCP probes were generated by flow sorting and labeled by degenerate oligonucleotide primed polymerase chain reaction (DOP-PCR) to overcome limitations of plasmid libraries (Telenius et al. 1992). Afterwards, construction of WCP probes by microdissection was reported to be even more reliable (Guan et al. 1994). Overall, WCPs became an effective tool to identify chromosomal aberrations in wide range of clinical cytogenetics.

However, for detection all human chromosomes at the same time, in 1996, Speicher and coworkers labeled each chromosome via a different fluorochrome composition (Speicher et al. 1996); this technique was called multiplex-FISH (M-FISH). In parallel, Evelin Schröck and colleagues established multicolor spectral karyotyping (SKY), which is based on a different kind of image acquisition (Schröck et al. 1996). Both of them M-FISH and SKY served to characterize translocations and complex aberrations, but failed to identify intrachromosomal rearrangements (see Fig. 1).

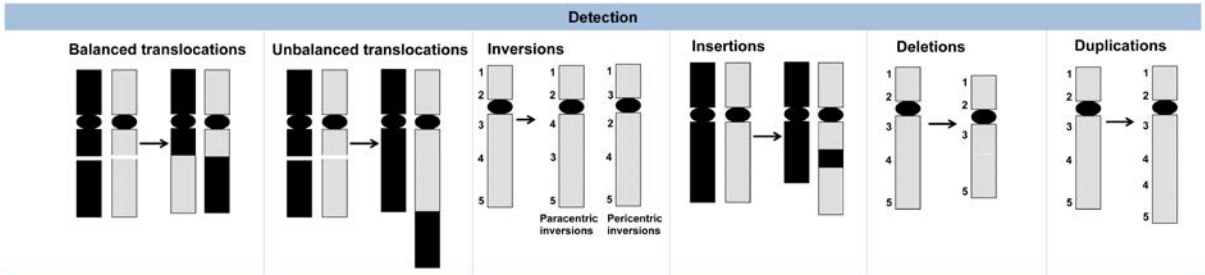

Technique						
Banding	Yes	Yes	Yes	Yes	Yes	Yes
M-FISH/SKY	Yes	Yes	No	Yes	Yes	Yes
CGH	No	Yes	No	No	Yes	Yes
aCGH	No	Yes	No	No	Yes	Yes
MCB	Yes	Yes	Yes	Yes	Yes	Yes

Figure 1. The pattern of chromosomal rearrangements and cytogenetic techniques for identifying them. Abbreviations: M-FISH, multiplex FISH; SKY, spectral karyotyping; CGH, comparative genomic hybridization; MCB, multicolor chromosome banding(adapted from Bakker et al. 2015).

In 2002 a new FISH probe set, called multicolor banding (MCB), was finalized and based on overlapping, sub-chromosomal band specific microdissection libraries that were labeled with a series of fluorescent combination along each chromosome (Liehr et al. 2002). In the contrast to WCP-based M-FISH, MCB is suitable for characterization of interchromosomal and intrachromosomal rearrangements in clinical cytogenetics (Fig. 1), but also works well in the field of comparative cytogenetic interspecies studies (Mrasek et al. 2003).

Besides M-FISH and MCB, comparative genomic hybridization (CGH) is another basic FISH-approach. For CGH whole genomic test and normal control DNA labeled with different colors are applied to normal human chromosome preparations and thus enable detection of chromosomal deletions and duplications (Kallioniemi et al. 1992). In 1998 array-based CGH (aCGH) was developed enabling a much higher resolution than CGH (Pinkel et al. 1998); still neither CGH nor aCGH could be used yet in interspecies studies reasonably.

Finally, locus specific probes that bind to DNA sequences of specific chromosomal regions are available; they can be used e.g. for breakpoint location. It is noteworthy that the different size of specific sequences depend on the used cloning vectors and range from cosmid (average 45kb) to bacterial artificial chromosome (BACs), P1-derived artificial chromosome (PACs) and yeast artificial chromosome (YACs) (80 kb±1 Mb). Locus specific probes are widely applied to provide information of genetic rearrangements, deletions, and amplifications (Kearney 2001). Additionally, establishing marker order and determining centromere repositioning were also conducted by BAC-based FISH (Rocchi et al. 2012, Graphodatsky et al. 2012).

1.1.3 Chromosomal rearrangements and breakpoints

Chromosomal rearrangements contain two main subtypes: balanced and unbalanced ones. Balanced rearrangements can e.g. be inversions, insertions or balanced translocations. Furthermore, inversion can be pericentric, i.e. include the centromere or paracentric involving only one chromosome arm. Reciprocal translocations and

Robertsonian translocations are the two major types of balanced translocations. Unbalanced chromosomal rearrangements comprise deletions, duplications and unbalanced translocations, and cause dosage changes of chromosomal material (Griffiths et al. 1999, Huang et al. 2004). Any kind of chromosomal rearrangements can be observed in as constitutional or acquired changes in human (Abeysinghe et al. 2003). Chromosomal rearrangements are also one major driver of evolution and speciation (Ehrlich et al. 1997, Rieseberget al. 2001). Some of them involved breakpoints remain stable during evolution, and are recognized as evolutionary makers of structural chromosomal changes (Ruiz-Herrera and Robinson 2008); such break events are termed evolutionary conserved breakpoints (ECBs). The reasons why specific regions in the human genome are more breakpoint prone than other ones is a yet understudied field of research.

1.2 Fragile sites

Fragile sites (FSs) are inducible microscopically visible gaps, constrictions or breaks on chromosomes, which are distributed non-randomly along the human genome. FSs are caused by inhibition of DNA synthesis when cells are induced to grow under specific culture requirements and the presence of certain chemical agents. In the 1970, the term ‘fragile site’ was initially used for a heritable polymorphic condition of a human chromosome 16. Until now, there are more than 200 FSs identified in human (Ruiz-Herrera et al. 2006, Mrasek et al. 2010). FSs are discussed to play a role in tumor chromosomal rearrangements, for example generation of cancer-specific translocations and also are discussed for a few ECBs in primates (Burrow et al. 2011, Arlt et al. 2006). According to their frequency in the human population, FSs are classified as two groups: common fragile sites (cFSs) present in all individuals as a part of normal chromosomal structure, and rare fragile sites (rFSs), found in small portion of population with frequencies of 5% (Aqeilan 2014).

1.2.1 Common fragile sites and rare fragile sites

According to different chemical inducible agents, cFSs are subdivided into 3 groups: aphidicolin, 5-azacytidine and bromodeoxyuridine (BrdU) inducible ones (Durkin and Glover 2007). cFSs in the different chromosomal regions present different

frequencies; thus the most frequent FSs are in FRA3B at 3p14.2, FRA2G at 2q31, FRA6E at 6q26, FRA7H at 7q32.3, FRA16D at 16q23 and FRAXB at Xp22.3 with frequencies of ~ 15%, even up to 30% in some individuals (Lukusa and Fryns 2008). In contrast to cFSs, rare fragile sites (rFSs) are detectable much less frequently, e.g. 1.2% for FRA10B or 2.5% for FRA16B. According to their different modes of induction in cells, rFSs are further subdivided into two groups: folate sensitive and non-folate sensitive fragile sites, folate sensitive rFSs are expressed in folic acid-deficient medium, and non-folate sensitive rFSs are induced after cell growth with BrdU and/or distamycin A (Lukusa and Fryns 2008).

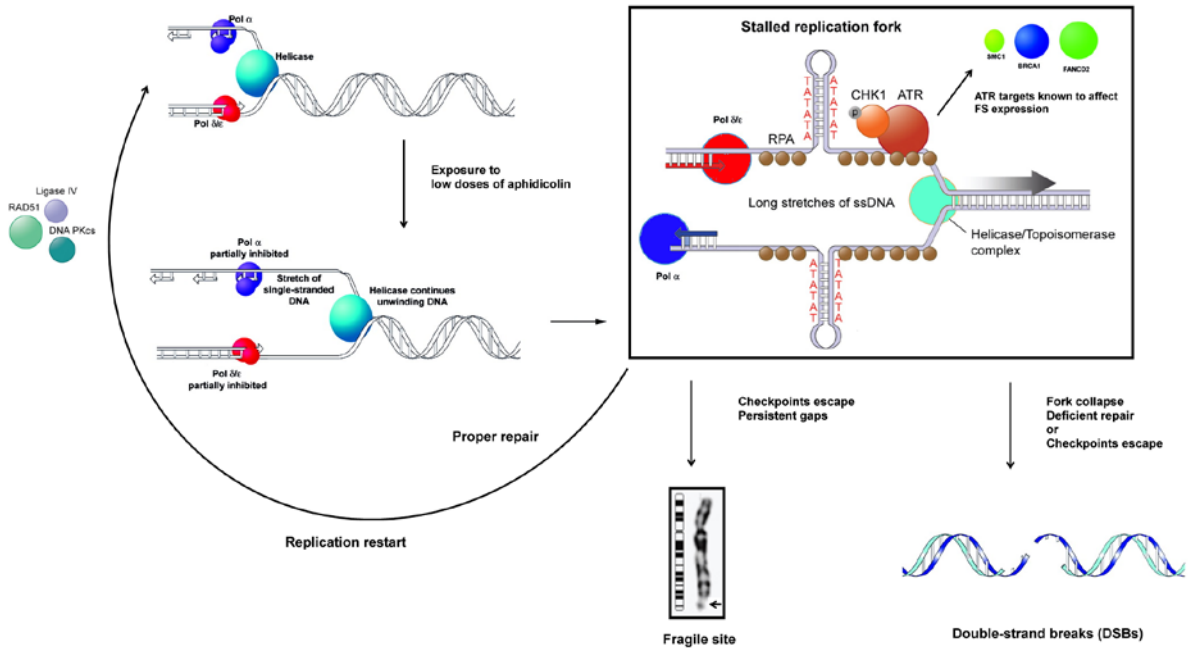

Figure 2. Model of common fragile site (cFS) expression. This model shows that cFSs come from regions of unreplicated single-stranded DNA (ssDNA) that appear at a stalled replication fork due to treatment with aphidicolin. In the box, RPA (the ssDNA binding protein) coats the unreplicated ssDNA regions to recruit ATR, which plays a role in DNA damage response checkpoints. BRCA1, SMC1 and the Fanconi anemia (FA) pathway proteins could target or modify the ATR-regulated pathway to influence FS formation. RAD51 and DNA-PK proteins restore the replication fork to properly repair these regions, but if these regions escape checkpoint control, this results in an unreplicated region. Thus, escaping repair will lead to appearance of an FS or a DSB (adapted from Glover et al. 2005 and Durkin et al. 2007).

The putative mechanism of cFS formation is shown in Fig. 2. AT-rich-dinucleotide flexibility islands can serve here as aphidicolin-inducible cFSs. Additionally,

aphidicolin plays a role in further delay in replication of the fragile region, while the AT-rich repeat sequences increase superhelical density and cause deficiency of topoisomerase activity. Finally, nonreplicated DNA regions make chromosomal structures unstable and lead to microscopically visible gaps or breaks (Lukusa and Fryns 2008).

Similar to cFSs, the molecular basis of rFSs has been presented for folate sensitive rFSs: those are caused by CCG/CGG-repeat expansion. Non-folate sensitive rFSs are due to high repeat expansion of AT-rich minisatellite. These expanded di- or trinucleotide repeats sequences can cause superhelical density change and form stable secondary non-B DNA structures to perturb the replication progression and result in breaks (Arlt et al. 2006).

1.2.2 Fragile site in primates

Besides inducible FSs in HSA, also FSs have been reported in some primate species. In 1984, blood of chimpanzee (*Pan troglodytes*; PTR) and gorilla (*Gorilla gorilla*; GGO) was induced by fluorodeoxyuridine (FdU) and caffeine, and resulted in fifty and forty-six FSs, respectively (Yunis and Soreng 1984). In 1990, PTR, GGO and orangutan (*Pongo pygmeu*; PPY) were induced by aphidicolin to form forty-one, fifty-five and twenty-seven FSs, respectively (Smeets et al. 1990). Furthermore, in 2000, twenty-one FSs in *Saimiri boliviensis* (SBO) and twenty-four FSs in *Alouatta caraya* (ACA) were induced by FdU and compared with previously published eleven FSs in *Cebus apella paraguayanus* (CPA) (Fundia et al. 2000). In 2002, ninety-five cFSs were induced by aphidicolin in *Macaca fasciculars* (MFA) and thirty-eight of them corresponded to human cFSs (Ruiz-Herrera et al. 2002). Additionally, in 2005, 53 FSs in CAP, 16 FSs in *Cebus nigrivittatus* (CNI) and 50 FSs in *Mandrillus sphinx* (MSP) were also induced by aphidicolin (Ruiz-Herrera et al. 2005a). Although primate FSs are conserved and homologous to human FSs, the relationship between ECBs and primate FSs still remain unclear on the molecular cytogenetic level; their relation will be further evaluated in this study.

1.2.3 Fragile sites in human disease

cFSs were shown to colocalize with chromosomal aberrations associated with tumorigenesis (Debacker and Kooy 2007). Most available studies are on FRA3B (*FHIT* gene) in human lung and breast cancer, FRA16D (*WWOX* gene) in prostate carcinoma and breast cancer, as well as FRA6E, FRA7G and FRA9E in ovarian cancer. However, the function of cFSs associated cancer genes remains still unclear and needs further to be validated. Folate sensitive rFSs mainly include FRAXA at Xq27.3 within *FMR1* gene related to fragile X syndrome. FRAXE at Xq28 in *FMR2* gene and FRA12A at 12q13.1 in the *DIP2B* gene are associated with mental retardation, and FRA11B at 11q23.3 is associated with Jacobsen syndrome. However, some rFSs have not correlated with any disease, yet, such as FRA10A, FRA12A and FRA16A (Durkin and Glover 2007, Lukusa and Fryns 2008). In the non-folate sensitive rFSs, FRA10B at 10q25.2 and FRA16B at 16q22.1 are the most frequent (Schwartz et al. 2006). Due to expression in normal individuals and no clinical phenotypic effects, non-folate sensitive rFSs have not been considered to be associated with human diseases but should be considered as a kind of chromosomal heteromorphism (Sutherland 2003, Lukusa and Fryns 2008).

1.3 Cytogenetics in New and Old World Monkeys

Non-human primates (NHPs) include prosimians, Old World Monkeys (OWMs), New World Monkeys (NWMs), lesser apes and great apes. There are ~354 primate species recognized by Groves (Groves 2001) but still new primate species are reported these days like Indochinese silvered langur and banded langur (Supanuam et al. 2015, Tanomtong et al. 2015). Numerous NHPs as experimental animals have been widely utilized in preclinical researches, and thus are critical to prevention and treatment of human diseases, for example for acquired immunodeficiency syndrome (AIDS), hepatitis virus, tuberculosis (TB), influenza virus, Parkinson's disease (PD), Alzheimer's disease (AD) and malaria (Vallender and Miller 2013). Taking into account that NHPs have a high degree of similarities to humans in terms of genetic mechanisms, developmental, immunologic and physiological features (Sibal and Samson 2001), OWMs and NWMs are considered as main choice of NHPs models in biomedical experiments.

To our knowledge, nowadays over 110 species and 95 subspecies of NWM are recognized and comprise of over 16 genera, commonly classified in 3 families: Cebidae, Atelidae and Pitheciidae. NWMs-OWMs split occurred about 37 million years ago, as based on African Catarrhini fossils (Kay 2015). OWMs contain two main subfamilies (Cercopithecinae and Colobinae), with ~132 species. Cercopithecinae comprise two tribes: one tribe is Cercopithecini, all members in Africa, having a variable range of chromosomal numbers from 48 to 72; the other tribe is Papionini and is the main NHPs models. Most Papionini distribute in Asian, besides few species in Africa. Notably, this tribe has conserved diploid chromosome number (2n = 42) (Groves 2001). Until now, numerous OWM and NWM species have been studied by G-banding or whole chromosome painting (Fig. 3). Due to such molecular cytogenetic data, first hints were found that ECBs could be useful markers for a better understanding of the relationships between chromosomal rearrangements in NHPs and chromosomal alterations in human diseases (Ruiz-Herrera et al. 2005b).

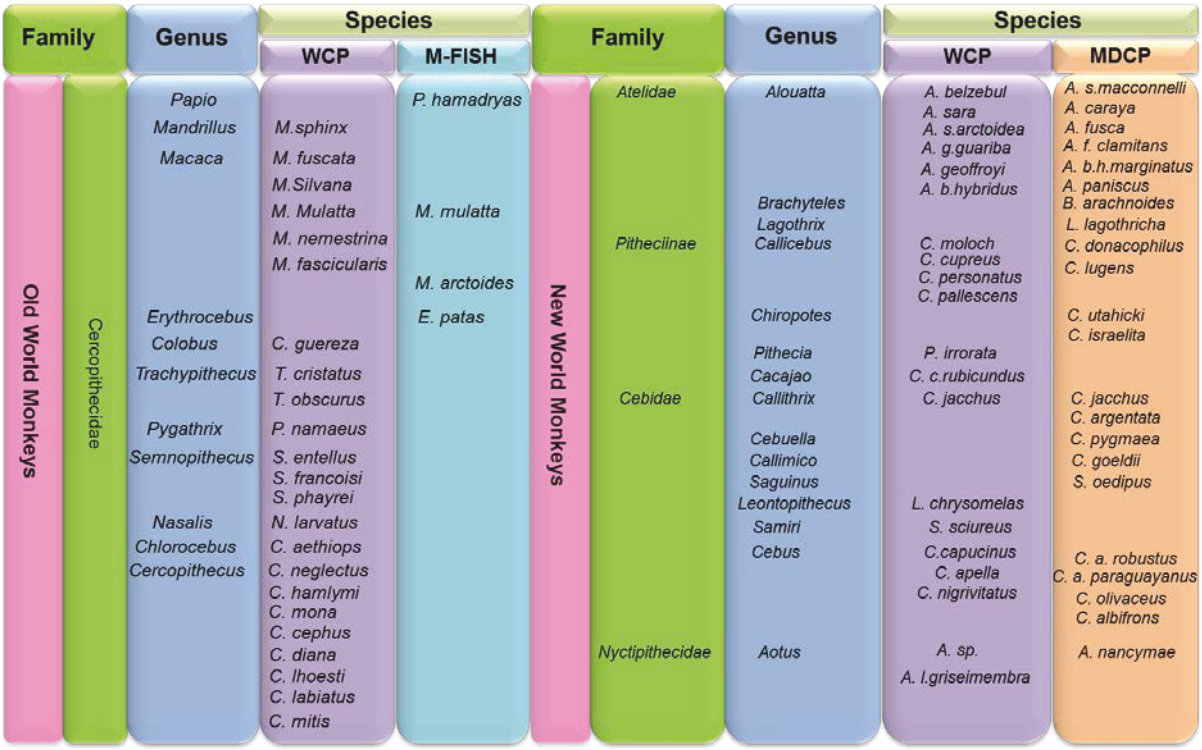

Figure 3. Summary of OWM and NWM species analyzed by whole chromosome painting using human probes. Abbreviations: WCP: whole chromosome painting, MDCP: multi-directional chromosome painting. Data according to previous reports by Picone et al. 2010 and De Oliveira et al. 2012.

OWMs and NWMs show high variation in their chromosomal constitutions, both between the two groups as well as within their groups. As it would lead too far to discuss this variety for all species below there is just given an overview on the karyotypes of the here studied species before this work was done.

1.3.1 Old World Monkeys

In present work, white-handed gibbon and eight OWMs species were studied and are presented below.

1.3.1.1 Macaques

The genus Macaca is divided into six species-groups (*M. sylvanus, M. nemestrina, Sulawesi, M. fascicularis, M. mulatta* and *M. sinica*), including twenty species and twenty-eight subspecies (Groves 2001). Macaca species are distributed in Asia and Northern Africa, inhabiting various environments such as rainforests, mountains, and even cities (Fig. 4A, B and D). In present study, six species comprising *M. fascicularis* (MFA), *M. arctoides* (MAR), *M. assamensis* (MAS), *M. nemestrina* (MNE), *M. Sylvanus* (MSY) and *M. mulatta* (MMU) were studied.
The diploid chromosome number was reported as 2n = 42 in MMU and MNE (Darlington et al. 1955). Y-chromosome is acrocentric and the smallest one on the basis of relative length and arm ratio (Rothfels et al. 1958). High-resolution G-banding and Ag-NOR staining was done in MMU (Goodpasture et al. 1975, Small et al. 1985). Homologies of human and *Macaca fuscata* (MFU) were identified using all WCPs (Wienberg et al. 1992). Furthermore some chromosomal rearrangements in MFU were characterized by human locus-specific DNA probes (Ried et al. 1993) and over 600 bacterial artificial chromosome (BAC) clone probes were applied on MMU to reveal centromere position shift and the chromosomal rearrangements (Ventura et al. 2007). Additionally, whole-genome sequencing and assembly of the genome of the MMU and MFA were reported (Gibbs et al. 2007, Higashino et al. 2012).

1.3.1.2 White-handed gibbon (*Hylobates lar*; HLA, (Linnaeus, 1771))

HLA, known as ”lar gibbon” or white-handed gibbon, is placed in genus Hylobates that belongs to family Hylobatidae, and genus Hylobates is divided into four subgenus (*Hylobates*, *Bunopithecus*, *Symphalangus* and *Nomascus*) including 14 species with overall 14 subspecies (Groves 2001). HLA mainly found in Southeast Asia such as Indonesia, Laos, Malaysia, Myanmar, most of Thailand and marginally into southern China (Fig. 4A).

The karyotype of HLA was described as 2n = 44 (Hamerton et al. 1963). G-banding, quinacrine and Ag-NOR staining were applied in HLA (Tantravahi et al. 1975 and 1976). Afterwards, chromosomal rearrangements of HLA were identified by DNA probes derived from all human chromosomes and showed a high degree of karyotype reshuffling (Jauch et al. 1992). Furthermore, reciprocal chromosome painting was introduced to establish homology maps between human and HLA (Müller et al. 2002). Mrasek and coworkers revealed 71 breakpoints present in HLA compared to HSA using MCB approach (Mrasek et al. 2003). Additionally, the extension, reciprocal arrangement, and orientation of chromosomal segments of HLA were characterized by over 1000 human BAC clones, involving a total number of 86 ECBs (Misceo et al. 2008). Recently, the whole mitochondrial genome of HLA was sequenced to reconstruct phylogenetic relationships among three gibbon genus (Matsudaira and Ishida 2010), and also the next-generation whole genome sequencing was performed in genus Hylobates (Carbone et al. 2014).

1.3.1.3 Silvery leaf monkey (*Trachypithecus crisata*; TCR, (Raffles, 1821))

Genus Trachypithecus belongs to subfamily Colobinae (family Cercopithecidae), and this genus comprises five groups (*T. vetulus, T. cristatus, T. obscurus, T. pileatus* and *T. francoisi*) including 17 species with overall 26 subspecies (Groves 2001). TCR is also known as silvery leaf monkey or the silvery langur (Fig. 4A), which widely inhabits continental Southeast Asia, such as Myanmar, West-central Thailand, Cambodia, Laos, Vietnam and Southern China (Harding 2010, Fooden 1973, Roos et al. 2008).

The karyotype of TCR was described as 2n = 44 (Hsu et al. 1970). G-, R- and Q-banding were analyzed in TCR (Dutrillaux et al. 1981, Ponsa et al. 1983, Muleris et al. 1986). Furthermore, karyotype analysis of male TCR revealed a translocation involving homologues of human Y chromosome and two autosomes (Dutrillaux et al.

1983). Additionally, chromosomal homologies between some but not all human and TCR chromosomes have been established using WCP (Bigoni et al. 1997).

1.3.1.4 Grivet monkey (*Chlorocebus aethiops*; CAE, (Linnaeus, 1758))

CAE known as grivet or African green monkey is placed in genus Chlorocebus that is divided into six species (C *sabaeus, C. aethiops, C. djamdjamensis, C. tantalus*, *C. pygerythrus* and *C. cynosures*) involving eight subspecies (Groves 2001). CAE is the most widespread African monkey and presents in Sudan, Djibouti, Ethiopia and Eritrea (Fig. 4D). In this study, CAE was chosen to consider the assumption that NWM ancestors came from Africa on the basis of morphological resemblance between NWM and the African anthropoid fossils (Schrago et al. 2003) and the African rafting source theory (Kay 2015); additionally a close similarity of single arms

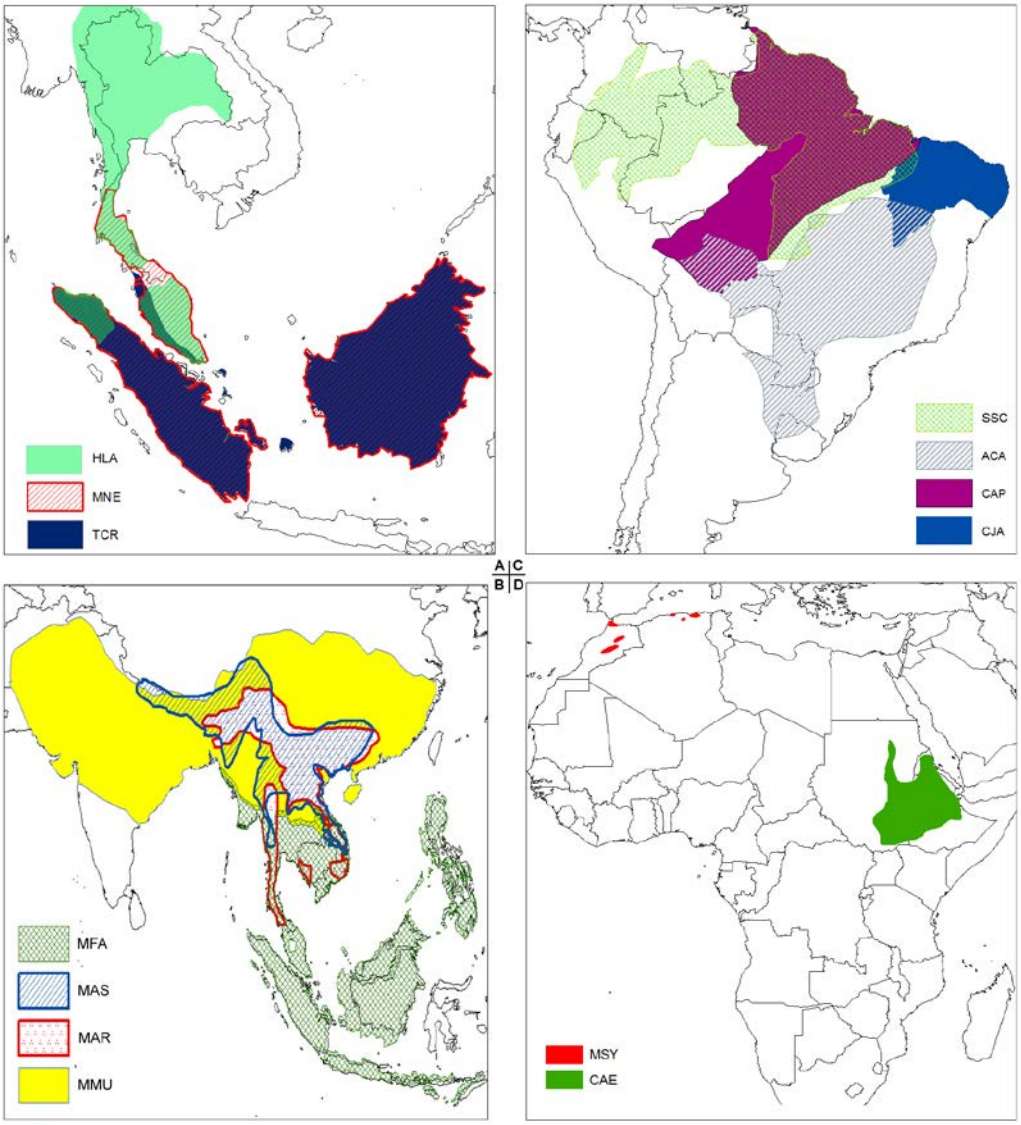

Figure 4. The distribution of HLA, OMWs and NWMs species studied in this work. Geographic data taken from the International Union for the Conservation of Nature Red List of Threatened Species (http://www.iucnredlist.org/).

of human and macaque banded chromosomes was reported for CAE chromosomes (Finelli et al. 1999).

Comparative analysis of chromosomal banding between CAE and other monkeys was applied using G-, C-banding and Ag-NOR staining (Stock and Hsu 1973, Estop et al. 1978). Reciprocal chromosome painting was carried out by both CAE and human chromosome specific DNA probes (Finelli et al. 1999). A comparative genetic map between CAE and human autosomes was established by 360 human orthologous short tandem repeats (STRs) markers (Jasinska et al. 2007). Recently, whole-genome sequencing and de novo assembly for CAE genome (GCA_000409795.2) have been completed and published (Warren et al. 2015).

1.3.2 New World Monkeys

In this work the four following NWMs species were studied.

1.3.2.1 Brown Howler (*Alouatta caraya*; ACA, (Humboldt, 1812))

ACA is one of howler monkey species, classified in genus Alouatta (Atelinae, Platyrrhini). The species numbers range in literature between 9 and 14. Here it is referred to Groves who proposed the classification of 10 species and 5 subspecies in this genus (Groves 2001). Their geographic distribution is so wide that they are found in Argentina, Bolivia, Brazil and Paraguay (Fig. 4C).

The first cytogenetic studies by standard staining reported that ACA chromosome numbers are 52 (Egozcue et al. 1966). Mudry and colleagues applied G-, C- and Ag-NOR banding on ACA, respectively, and suggested a conserved karyotype in this genus (Mudry et al. 1984). Furthermore, ACA has a multiple sex chromosome system of the X1X1X2X2/X1X2Y1Y2 (Rahn et al. 1996). Afterwards, human and monkey chromosome-specific probes were applied in ACA, and revealed ACA-Y derived from translocations of regions being homologous to HSA#3 and HSA#15 (De Oliveira et al. 2002). Yet not all homologies of HSA and ACA chromosomes were characterized.

1.3.2.2 Tufted capuchin (*Cebus apella*; CAP, (Linnaeus, 1758))

This genus consists at least of *Cebus capucinus* and *Cebus apella* groups, including eight different species and nineteen subspecies (Groves 2001). CAP is one of several species in *Cebus apella* group. The geographic distribution is in South America, such as Peru, Bolivia, Brazil, French Guyana, Suriname, Guyana, and Venezuela (Fig. 4C).

Cytogenetic studies revealed that CAP has 54 chromosomes (Bender et al. 1958). Afterwards, constitutive heterochromatin was further characterized by C-banding and Ag-NOR staining (Freitas et al. 1982). Furthermore, chromosomal homologies between humans and CAP were identified by WCP-FISH (Richard et al. 1996; Garcia et al. 2000).

1.3.2.3 Common marmoset (*Callithrix jacchus*; CJA, (Linnaeus, 1758))

The genus Callithrix comprises three subgenera (subgenus *Callithrix*, *Mico* and *Gebuella*) that include 18 species and two subspecies (Groves 2001). CJA is one of six species in Callithrix subgenus. CJA are widespread in Brazil. They distribute in the Northeastern and central forests of Atlantic coast and island, even living within cities (Fig. 4).

The karyotype of CJA was firstly reported in 1962 and revealed chromosome numbers of 46 (Benirschke et al. 1962). Afterwards, R-banding was carried out and a basic nomenclature was proposed (Perrotez 1974). In 1977, C-banding and Ag-NOR staining was applied in CJA (Bedard et al. 1977). Furthermore, all human chromosome-specific probes were applied in CJA (Sherlock et al. 1996). Recently whole-genome sequencing and assembly of the genome of CJA as the first NWM have been done (Marmoset Genome Sequencing and Analysis Consortium 2014).

1.3.2.4 Common squirrel monkey (*Saimiri sciureus*; SSC, (Linnaeus, 1758))

Squirrel monkeys comprise different South American species and central American ones. The genus Saimiri has been divided into two groups (*S. sciureus* and *S. boliviensis*), which include five species and eight subspecies (Groves 2001). In this study, SSC as one of three species in *S sciureus* group was included. The

distribution of SSC is in Brazil, Colombia, Ecuador, French Guyana and Bolivia (Fig. 4C).

Uniform karyotypes of SSC have been described as 2n = 44 from five different South American regions (Jones et al. 1973). Furthermore, chromosomal banding analyses in SSC revealed 21 pairs of autosomes with XY sex system and polymorphisms in C-banding and NORs (Jones et al. 1975, Goodpasture et al. 1975, Lau et al. 1977). In 2000, FISH based with human chromosome paints in SSC was reported (Stanyon et al. 2000). Genome sequencing projects for SSC are underway or planned (Bosinger et al. 2011).

1.4 Goals of study/questions worked on

The present study was based on previous work of our group on human FSs (Mrasek et al. 2010) and their putative relationship with ECBs, which was yet only studied in detail for one species (*Hylobates lar*; HLA; Mrasek et al., 2003). Thus, here the first detailed molecular cytogenetic analyses for four NWM species and eight OWM species, such as CAP (2n = 54), CJA (2n = 46), ACA (2n = 50) and SSC (2n = 44), CAE (2n = 60), TCR (2n=44) and six macaque subspecies (2n=42, MFA, MAR, MAS, MNE, MSY and MMU) was done to determine the ECBs of those species in detail. Also HLA was further studied here by microdissection and aCGH to characterize ECBs more precisely. Based on this data the following questions should be answered here:

1) **Are the detected ECBs and chromosomal rearrangements in concordance with previous published data?**
2) **Are FSs really colocalized with ECBs?**
3) **Are there different rates of ECB and FS colocalization in OWMs and NWMs?**
4) **Can be examples found for ECBs of the studied species and human disease?**

2. Results

Here the list of published original papers is provided:

1. Z Li, Q Zhang, J-H Mao, A Weise, K Mrasek, **X Fan**, X Zhang, T Liehr, KH Lu, A Balmain, W-W Cai. 2010. **A HDAC1-binding domain within FATS bridges p21 turnover to radiation-induced tumorigenesis**. Oncogene, 29:2659-2671.
2. **X Fan**, K Pinthong, H Mkrtchyan, P Siripiyasing, N Kosyakova, W Supiwong, A Tanomtong, A Chaveerach, T Liehr, M de Bello Cioffi, A Weise. 2013. **First detailed reconstruction of the karyotype of *Trachypithecus cristatus* (Mammalia: Cercopithecidae)**. Mol Cytogenet, 6:58.
3. **X Fan**, W Sangpakdee, A Tanomtong, A Chaveerach, K Pinthong, S Pornnarong, W Supiwong, VA Trifonov, GG Hovhannisyan, RM Aroutouinian, T Liehr, A Weise. 2014. **Molecular cytogenetic analysis of Thai southern pig-tailed macaque (*Macaca nemestrina*) by multicolor banding**. Proceedings of Yerevan State University, 2014:46-50.
4. **X Fan**, W Sangpakdee, A Tanomtong, A Chaveerach, K Pinthong, S Pornnarong, W Supiwong, V Trifonov, G Hovhannisyan, K Loth, C Hensel, T Liehr, A Weise. 2014. **Comprehensive molecular cytogenetic analysis of Barbary macaque (*Macaca sylvanus*)**.Biol J Arm, 66:98-102.
5. **X Fan**, A Tanomtong, A Chaveerach, K Pinthong, S Pornnarong, W Supiwong, T Liehr, A Weise. 2014. **High resolution karyotype of Thai crab-eating macaque *(Macaca fascicularis*)**. Genetika, 46:877-882.
6. A Weise, N Kosyakova, M Voigt, N Aust, K Mrasek, S Löhmer, N Rubtsov, T Karamysheva, V Trifonov, D Hardekopf, T Jancuková, S Pekova, K Wilhelm, T Liehr, **X Fan.** 2015.**Comprehensive analyses of white handed gibbon chromosomes enables access to 92 evolutionary conserved breakpoints compared to the human genome**. Cytogenet Genome Res, 145:42-49.
7. **X Fan**, W Supiwong, A Weise, K Mrasek, N Kosyakova, A Tanomtong, K Pinthong, VA Trifonov, M de Bello Cioffi, P Grothmann, T Liehr, EHC de Oliveira. 2015. **Comprehensive characterization of evolutionary conserved breakpoints in four New World Monkey karyotypes compared to *Chlorocebus aethiops* and *Homo sapiens***. Helyon, Article No ~ e00042.

Seven articles are bases of this work (Table 1). According to these articles mentioned above, they will be further discussed in the following for four aspects:

1. Effectiveness and availability of molecular cytogenetic approaches to characterize new ECBs in OWMs and NWMs.
2. Relation between ECBs in OWMs and NWMs with FSs observed in *Homo sapiens*.
3. Is there a clinical significance between enhanced rates of ECBs, FSs and chromosomal breakpoints observed in human disorders.
4. Chromosomal evolution of ECBs in OWMs and NWMs.

Tab. 1 Seven articles relied on above standpoints.

Articles No.	**Methodology**	**ECBs**		**FSs**	**Breakpoints in human disorders**	**Evolution**
		in OWMs	**in NWMs**			
1	+	-	-	+	+	-
2	+	+	-	+	+	+
3	+	+	-	-	-	+
4	+	+	-	-	-	+
5	+	+	-	-	-	+
6	+	-	-	+	+	+
7	+	+	+	+	-	+

Finally, the questions from 1.4 are answered.

2.1 Article No. 1

Z Li, Q Zhang, J-H Mao, A Weise, K Mrasek, **X Fan**, X Zhang, T Liehr, KH Lu, A Balmain, W-W Cai. 2010. **A HDAC1-binding domain within FATS bridges p21 turnover to radiation-induced tumorigenesis**. Oncogene, 29:2659-2671.

Abstract: There is a gap between the initial formation of cells carrying radiation-induced genetic damage and their contribution to cancer development. Herein, we reveal a previously uncharacterized gene FATS through a genome wide approach and demonstrate its essential role in regulating the abundance of p21 in surveillance of genome integrity. A large exon coding the NH2-terminal domain of FATS, deleted in spontaneous mouse lymphomas, is much more frequently deleted in radiation-induced mouse lymphomas. Its human counterpart is a fragile site gene at a previously identified loss of heterozygosity site. FATS is essential for maintaining steady-state level of p21 protein and sustaining DNA damage checkpoint. Furthermore, the NH2-terminal FATS physically interacts with histone deacetylase 1 (HDAC1) to enhance the acetylation of endogenous p21, leading to the stabilization of p21. Our results reveal a molecular linkage between p21 abundance and radiation-induced carcinogenesis.

Oncogene (2010) 29, 2659–2671

www.nature.com/onc

ORIGINAL ARTICLE

An HDAC1-binding domain within FATS bridges p21 turnover to radiation-induced tumorigenesis

Z Li[1], Q Zhang[2], J-H Mao[3], A Weise[4], K Mrasek[4], X Fan[1], X Zhang[1], T Liehr[4], KH Lu[2], A Balmain[3] and W-W Cai[5]

[1]*Department of Biochemistry and Molecular Biology, Key Laboratory of Ministry of Education for Breast Cancer Prevention and Treatment, Tianjin Medical University Cancer Institute and Hospital, Tianjin, China;* [2]*Department of Gynecologic Oncology, University of Texas, MD Anderson Cancer Center, Houston, TX, USA;* [3]*Cancer Research Institute, University of California at San Francisco, San Francisco, CA, USA;* [4]*Institute for Human Genetics and Anthropology, Jena, Germany and* [5]*Department of Molecular and Human Genetics, Baylor College of Medicine, Houston, TX, USA*

There is a gap between the initial formation of cells carrying radiation-induced genetic damage and their contribution to cancer development. Herein, we reveal a previously uncharacterized gene FATS through a genome-wide approach and demonstrate its essential role in regulating the abundance of p21 in surveillance of genome integrity. A large exon coding the NH2-terminal domain of FATS, deleted in spontaneous mouse lymphomas, is much more frequently deleted in radiation-induced mouse lymphomas. Its human counterpart is a fragile site gene at a previously identified loss of heterozygosity site. FATS is essential for maintaining steady-state level of p21 protein and sustaining DNA damage checkpoint. Furthermore, the NH2-terminal FATS physically interacts with histone deacetylase 1 (HDAC1) to enhance the acetylation of endogenous p21, leading to the stabilization of p21. Our results reveal a molecular linkage between p21 abundance and radiation-induced carcinogenesis.
Oncogene (2010) **29,** 2659–2671; doi:10.1038/onc.2010.19; published online 15 February 2010

Keywords: radiation; p21; acetylation; carcinogenesis

Introduction

Ionizing radiation (IR) is a well-known complete carcinogen that is able to initiate and promote neoplastic progression, resulting from its induction of a broad spectrum of DNA lesions including damage to nucleotide bases, crosslinking, and DNA single-strand breaks and DNA double-strand breaks (DSBs) that impairs chromosomal stability (van Gent *et al.*, 2001). The latent period between radiotherapy and the appearance of second primary tumor or recurrence ranges from a few years to several decades (Holm, 1990), which is particularly the case in patients treated for childhood Hodgkin's disease (Magrath, 1997; Schellong, 1998). With the increasing use of diagnostic radiation for various conditions, concern is growing that the risk/benefit ratio for such exposure needs to be weighed, and cancer is considered the major long-term contributor to health risk at doses below causing acute tissue injury (Brenner *et al.*, 2003). Recently, Genome-wide analysis of chromosomal aberrations has verified the similarities and differences between spontaneous and IR-induced tumorigenesis. In particular, radiation-induced tumors exhibit a high frequency of localized deletion events (Mao *et al.*, 2005). However, mechanistic understanding of radiation-induced carcinogenesis remains a major challenge.

Common fragile sites (CFSs) are site-specific loci that are found on most human chromosomes and can be induced in all individuals of the population under replication stress. Aphidicolin, an inhibitor of DNA polymerase that can cause DNA lesions including DSBs, is an efficient inducer of CFSs. CFSs are evolutionarily conserved regions that are AT-rich and late replicating (Mangelsdorf *et al.*, 2000; Glover *et al.*, 2005; Schwartz *et al.*, 2006; Zhang and Freudenreich, 2007). In general, CFSs are now being implicated as regions of high genomic instability associated with cancer (Buttel *et al.*, 2004; Durkin and Glover, 2007). However, much less is known about their molecular nature and functional characterization of CFS genes in DNA damage signaling.

Defects in cell-cycle checkpoints result in genomic instability and the initiation of tumorigenesis (van Gent *et al.*, 2001; Maser and DePinho, 2002; Rouse and Jackson, 2002; Kastan and Bartek, 2004). In eukaryotic DNA damage signaling pathways, tumor suppressor p53 and its transcriptional target *CDKN1A* (p21) have an essential role in monitoring cell-cycle checkpoints (Brugarolas *et al.*, 1995; Deng *et al.*, 1995; Bunz *et al.*, 1998). The cell-cycle inhibitor p21 is an unstable protein that is subjected to proteasome-dependent degradation in both ubiquitin-dependent (Bloom *et al.*, 2003; Bendiennat *et al.*, 2003; Coulombe *et al.*, 2004) and ubiquitin-independent manners (Sheaff *et al.*, 2000; Li *et al.*, 2007; Chen *et al.*, 2007). Unbound p21 is directly degraded by proteasome independently of ubiquitination, as the endogenous p21 is fully acetylated at its amino terminus (Chen *et al.*, 2004) and is therefore not a substrate for N-end rule ubiquitination (Varshavsky *et al.*, 2000). Ubiquitin-independent turnover of p21 results from the interaction of its C terminus with the C8 α-subunit of 20S proteasome (Touitou *et al.*, 2001) or proteasome activator REGγ (Chen *et al.*, 2007). In addition, the inhibition of histone deacetylases (HDACs) has been known to selectively induce p21 (Johnstone, 2002; Dokmanovic *et al.*, 2007), although the impact of acetylation on p21 turnover remains uncertain. Precise control of p21 abundance is required for its role in cell-cycle regulation, thus further elucidating the regulatory mechanism of p21 stabilization is an important priority toward a greater understanding of p21 deregulation in human cancer (Abbas and Dutta, 2009).

Here, we report the identification of a previously uncharacterized and evolutionarily conserved gene, FATS (for Fragile-site Associated Tumor Suppressor), at a frequently deleted region in IR-induced tumors. FATS functions as a regulator of p21 abundance. Furthermore, the NH2-terminal domain of FATS binds to HDAC1 and suppresses its binding to p21, leading to the enhanced acetylation of endogenous p21. We also provide new evidence for a tight functional link between acetylation and stability of p21. This study thus brings new insights into our understanding of radiation-induced carcinogenesis.

Correspondence: Dr Z Li, Department of Biochemistry and Molecular Biology, Key Laboratory of Ministry of Education for Breast Cancer Prevention and Treatment, Tianjin Medical University Cancer Institute and Hospital, Huan-Hu-Xi Road, He-Xi District, Tianjin 300030, China.
E-mail: zhengli@tijmu.edu.cn or Dr W Cai, Department of Molecular and Human Genetics, Baylor College of Medicine, One Baylor Plaza, Houston, TX 77030, USA.
E-mail: wcai@bcm.tmc.edu
Received 18 September 2009; revised 2 January 2010; accepted 18 January 2010; published online 15 February 2010

Results

FATS is a key component of radiation-induced tumorigenesis

IR-induced mouse thymic lymphoma is one of the classic models in radiation carcinogenesis, and p53 insufficiency accelerates IR-induced tumor progression (Kemp *et al.*, 1994). Our previous results demonstrated the markedly difference of genome-wide aberations between IR-induced and spontaneous mouse tumors (Mao *et al.*, 2005), allowing us to systematically analyze the deletion events specific to IR-induced tumorigenesis. Using microarrays containing over 19 200 bacterial artificial chromosome (BAC) clones with insert size in the range of 170–210 kb and maximized coverage of mouse genome (Cai *et al.*, 2002), we performed microarray-based comparative genomic hybridization analysis and identified a deletion site close to the end of mouse chromosome 7 in IR-induced tumors (Figure 1a). The DNA region, corresponding to the contig of RP23-35I7, was deleted in 15% of spontaneous tumors ($n=20$). Remarkably, the same region was deleted in 21 out of 29 (72.4%, $P<0.001$) IR-induced tumor samples (Figure 1b). Bioinformatics analysis revealed a

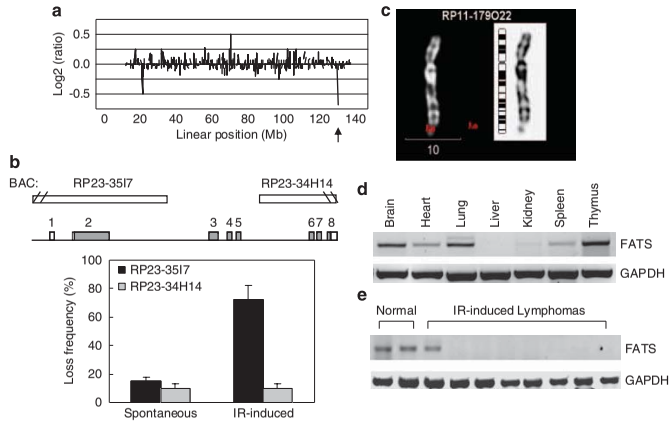

Figure 1 Identification of FATS. (**a**) A BAC array comparative genomic hybridization profile of chromosome 7 for a radiation-induced mouse lymphoma. An arrow indicates a deletion region of interest. (**b**) A BAC contig map of the FATS gene in the deleted region in panel a, and the frequencies of copy number loss of BAC contigs in spontaneous ($n=20$) and IR-induced ($n=29$) mouse thymic lymphomas. Boxes indicate exons and shaded boxes indicate coding regions. Genbank database accession number of FATS is NM_001081331. (**c**) Co-localization of BAC clone RP11-179O22 with a common fragile site FRA10F at 10q26. Fluorescence *in situ* hybridization image (red) on human chromosome 10 represents RP11-179O22 that spans 170 kb and contains all sequences of FATS ortholog. (**d**) The expression of FATS mRNA in normal tissues. The primer set for reverse transcription (RT)–PCR targets exon 2 and 4 respectively. (**e**) The mRNA levels of FATS in normal thymus and IR-induced thymic lymphomas. The same primer set as in panel d was used for RT–PCR analysis.

previously uncharacterized open reading frame in this frequently deleted region as a candidate tumor suppressor. This open reading frame, encoding a protein consisting of 365 amino-acid residues, overlapped (99.4%) the largest coding exon of a previously uncharacterized gene comprised by 8 exons (Figure 1b). Its human counterpart was mapped to a CFS FRA10F at 10q26 (Figure 1c), spanning a region of allelic loss associated with cancers (Maier *et al*., 1997; Nagase *et al*., 1997). Therefore, we called it FATS for fragile-site associated tumor suppressor.

We next evaluated whether FATS was an expressed gene that was involved in IR-induced mouse tumors. Indeed, FATS mRNA was expressed in various tissues including thymus, brain, heart, lung, spleen and kidney, but undetectable in liver (Figure 1d). The expression of FATS was extensively silent in IR-induced lymphomas (Figure 1e), indicating its involvement in IR-induced tumorigenesis.

An exon, encoding the NH2-terminal region of FATS, is enveloped in sequences of genetic instability

Genetic instability is an important facet of carcinogenesis. We next analyzed whether the DNA sequences of FATS gene exhibit features of DNA fragility. Noncoding sequences of FATS gene are AT-rich. Interestingly, exon 2 of mouse FATS, encoding the NH2-terminal domain of FATS that is evolutionarily conserved (Figure 2a), is surrounded by AT-rich sequences inserted with AT-dinucleotide repeats (Figure 2b), which is a feature of CFSs instability (Schwartz *et al*., 2006; Zhang and Freudenreich, 2007). Unusually, additional dinucleotide repeats such as $(CA)_n$ and $(TG)_n$ are distributed in AT-rich sequences of both upstream and downstream of FATS exon 2 (Figure 2b). A secondary structure model was further derived by free energy data calculated using the mFOLD program (http://www.mfold.bioinfo.rpi.edu/cgi-bin/dna-form1.cgi). The structure of $(CA)_{15}$-$(TG)_{21}$ repeat in intron 1 appears as a succession of three independent stem-loop structures (Figure 2c), which exhibit a tendency to induce replication pausing. The structure of $(AT)_{24}$ in intron 2 appears as a succession of two independent stem-loop structures that are separated by a short single-stranded region (Figure 2d), which is similar to an AT-rich fragment causing DNA fragility (Zhang and Freudenreich, 2007). These dinucleotide repeats inserted in AT-rich sequences thus confer genetic instability that are susceptible to DNA lesions induced by replication-blocking and radiation (Pearson *et al*., 2005; Bichara *et al*., 2006).

FATS deficiency results in hypersensitivity to DNA damage and severe defects in G_2/M checkpoint

To provide a physiological context for our findings, we next examined whether FATS has a role in DNA damage response. We took RNA interference approach using a small interfering RNA (siRNA) that specifically knockdowned the expression of FATS mRNA (Figure 3a). The phosphorylation of Chk1 kinase, a mediator of DNA damage signaling, was more pronounced after knockdown of FATS expression in mouse embryonic fibroblast (MEF) cells after IR treatment (Figure 3b). To further verify this observation, we examined the effect of FATS knockdown on IR-induced nuclear foci of 53BP1, a mediator of DNA damage signaling (DiTullio *et al*., 2002). The nuclear staining of 53BP1 in unstressed cells was diffused, and a few nuclear foci of 53BP1 were observed 3 h after IR treatment in MEF cells. In contrast, FATS deficiency significantly increased the number of 53BP1 nuclear foci under the same conditions (Figure 3c). These results demonstrated that knockdown of FATS expression resulted in sensitivity to DNA damage response induced by IR.

Because radiosensitivity and cancer susceptibility are hallmarks of many genomic instability syndromes (Shiloh, 2003), and cell-cycle checkpoint machinery has a pivotal role in guarding genomic stability and suppressing carcinogenesis, we next investigated the mitotic entry after DNA damage in FATS-inhibited MEF cells. After irradiation, cells were treated with nocodazole, a microtubule-disrupting agent that can trap cells in mitosis for several hours. In normal cells, the mitotic index was very low after irradiation. However, FATS-inhibited cells exhibited significantly higher mitotic index after irradiation (Figure 3d). For those FATS-deficient cells entering mitosis under IR-induced genotoxic stress, severe mitotic defects in nuclear division and centrosome duplication were observed (Figure 3e), confirming that FATS is required to sustain G_2/M checkpoint after DNA damage.

FATS regulates cell-cycle inhibitor p21

We further evaluated the effect of FATS expression on cell proliferation. Knockdown of FATS expression led to a significant increase in nuclear staining of Ki-67, a well-known proliferation marker (Figure 4a). In line with this observation, the growth rate of NIH3T3 cells stably transfected with a FATS-expressing vector was significantly decreased than those stably transfected with an empty vector pcDNA3 (Figure 4b). Because p21 is not only a cyclin-dependent kinase (CDK) inhibitor but also essential to sustain G_2 checkpoint after DNA damage, we determined whether FATS by itself could upregulate p21. Indeed, the protein level of p21 was significantly increased in the presence of overexpressed FATS. Interestingly, FATS did not affect the protein level of p27, another CDK inhibitor (Figure 4c). To gain further insight into the properties of the NH2-terminal region of FATS, namely FATS(1–363), whose coding region was frequently deleted in IR-induced tumors and susceptible to DNA lesions caused by repeat instability (Figures 1 and 2), we generated an FATS(1–363)-expressing vector and performed similar experiments. The overexpression of FATS(1–363) alone in NIH3T3 cells was sufficient to induce p21 (Figure 4c). The activities of cyclinE-associated CDK2 kinase and cyclinB1-associated CDK1 kinase, which stimulates the progression of G_1 to S phase and G_2 to M phase of cell cycle, respectively (Sherr and Roberts, 1999;

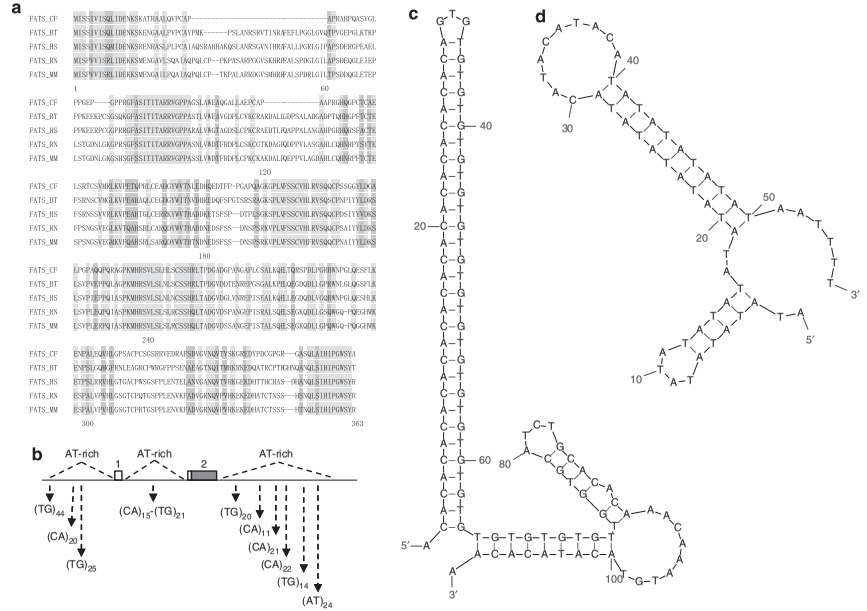

Figure 2 NH2-terminal sequences of FATS protein and secondary structures of DNA surrounding its coding region. (**a**) Sequence alignment of NH2-terminal domains of FATS orthologs. Entrez database accession numbers are as follows: FATS_CF, GI: 73998998; FATS_BT, GI: 119917909; FATS_HS, GI: 52145312; FATS_RN, GI: 253735807; FATS_MM, GI: 124486743. CF, *Canis familiaris*; BT, *Bos Taurus*; HS, *Homo sapiens*; RN, *Rattus norvegicus*; MM, *Mus musculus*. (**b**) Genomic organization of dinucleotide repeats in AT-rich sequences surrounding exon 2 of mouse FATS gene. A shaded box indicates the coding region for NH2 terminus in panel a. (**c**) Secondary structure of a dinucleotide repeat in intron 1. (**d**) Secondary structure of a $(AT)_{24}$ repeat in intron 2.

Ohi and Gould, 1999), were significantly suppressed after overexpression of FATS(1–363) (Figures 4d and e), supporting the role of FATS in regulating cell cycle. The overexpression of FATS induced a dominant effect on G_1 arrest (Supplementary Figure S1a and S1b). However, the overexpression of FATS(1–363) in p21-null cells failed to induce G_1 arrest (Figure 4f), indicating that FATS-mediated effect on cell cycle is p21-dependent.

Expression of the NH2-terminal region of FATS is sufficient to stabilize p21 independently of ubiquitination

Interestingly, the expression of FATS(1–363) was capable of increasing p21 protein level in p53-null cells (Figure 5a), indicating that FATS induces p21 protein in a p53-independent manner. Because p21 is an unstable protein and its abundance is also tightly regulated post-transcriptionally, we next evaluated whether FATS could stabilize p21. In the presence of cycloheximide (CHX), an inhibitor of protein synthesis, the expression of p21 protein was diminished after CHX treatment for 4 h in cells. However, the protein level of p21 only slightly decreased after CHX treatment for 12 h in the presence of overexpressed FATS(1–363) (Figure 5b), indicating that FATS inhibits the degradation of p21. To investigate the effect of FATS on p21 abundance after DNA damage without the influence of p53-mediated transcriptional activation, we performed immunoblotting analysis to determine the expression level of p21 protein in HeLa cancer cells, which carry inactive p53 (Hoppe-Seyler and Butz, 1993). The half-life of endogenous p21 in HeLa cells was shorter than 1 h, and the expression of p21 protein in HeLa cells was abolished within 3 h after IR treatment. In contrast, the protein level of p21 in the presence of FATS(1–363) under the same conditions was not significantly changed even 24 h after IR treatment (Figure 5c), strongly suggesting that FATS is important to regulate p21 abundance under genotoxic stress. To gain more definitive insight into the mechanism of FATS-mediated stabilization of p21, we investigated the effect of FATS on p21 ubiquitination. His-tagged ubiquitin and a p21-expressing vector were co-transfected with FATS(1–363) or an empty vector into p53-null cells, respectively. Ubiquitinated proteins were subsequently

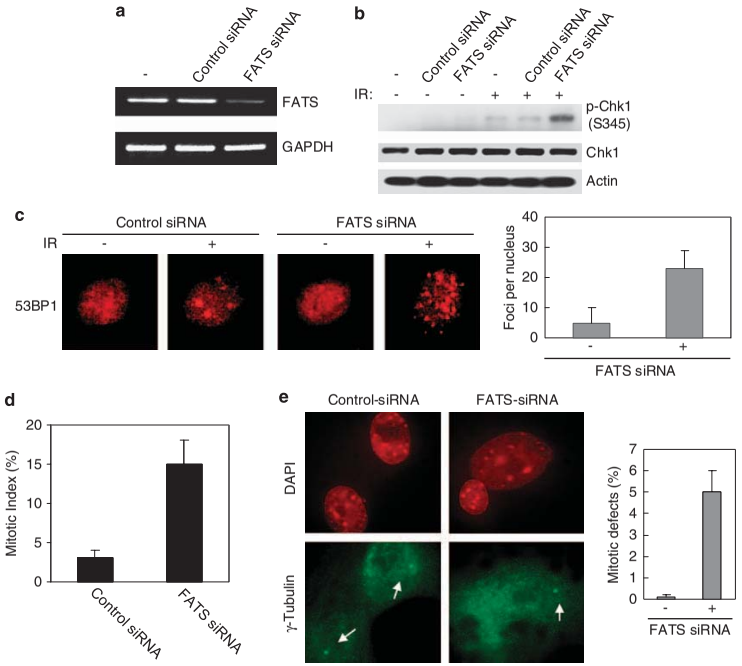

Figure 3 Involvement of FATS in DNA damage response and functional cell-cycle checkpoint. (**a**) MEF cells were untreated or transfected with either FATS siRNA or control siRNA, respectively. Expression of endogenous FATS was detected by reverse transcription (RT)–PCR after 48 h. (**b**) MEF cells with or without FATS siRNA transfection were exposed to 10 Gy dose of IR. Cell lysates were prepared 6 h after IR and subjected to western blot analysis using an antibody to phospho-Chk1 on Serine 345. (**c**) Representative microscope images of IR-induced nuclear foci of 53BP1 in MEF cells with or without FATS inhibition. At least 200 cells were examined and 53BP1 foci formation was quantified. (**d**) Mitotic entry of FATS-inhibited MEF cells after IR. After siRNA transfection, cells were subjected to IR treatment and incubated with nocodazole (0.2 μg/ml) for 24 h. Cells were then fixed, stained and examined by fluorescence microscopy to determine the mitotic index as described earlier (Bunz *et al*., 1998). (**e**) Representative microscope images of FATS-inhibited cells entering mitosis after IR-induced DNA damage. The siRNA-treated MEF cells were subjected to IR (10 Gy) exposure. After 24 h, cells were fixed and stained with an antibody to γ-tubulin component of centrosome, and nuclear DNA was stained with DAPI (red).Arrows indicate centrosomes (green). At least 200 cells were examined and the percentage of mitotic defects after IR was shown.

purified and subjected to immunoblotting using an antibody against p21. The expression of FATS(1–363) did not inhibit the ubiquitination of p21 in p53-null cells (Figure 5d), indicating that FATS-mediated stabilization of p21 is ubiquitin-independent. These results were in agreement with our observation (Figure 4c) that FATS did not change the protein level of p27, whose turnover was strictly ubiquitin-dependent (Pagano *et al*., 1995).

The NH2-terminal FATS contains one HDAC1-binding domain

To explore the mechanism by which FATS inhibited p21 turnover, we determined the cellular localization of p21 induced by FATS. We performed cell fractionation analysis and found that FATS-induced p21 was localized in nucleus (Supplementary Figure S2). Given that p21 is selectively induced by HDAC inhibitors (Johnstone, 2002; Dokmanovic *et al*., 2007) and that HDAC1 is a major deacetylase localized predominantly to the nucleus (Lagger *et al*., 2002; Supplementary Figure S2), we hypothesized that FATS might stabilize p21 through interacting with HDAC1. To this end, we performed coimmunoprecipitation assay to assess whether a physical association could be observed between FATS and HDAC1 in cells. A Flag-tagged HDAC1 and a myc-tagged FATS(1–363) were co-transfected into HeLa cells, and cellular proteins binding to HDAC1 were immunoprecipitated using a

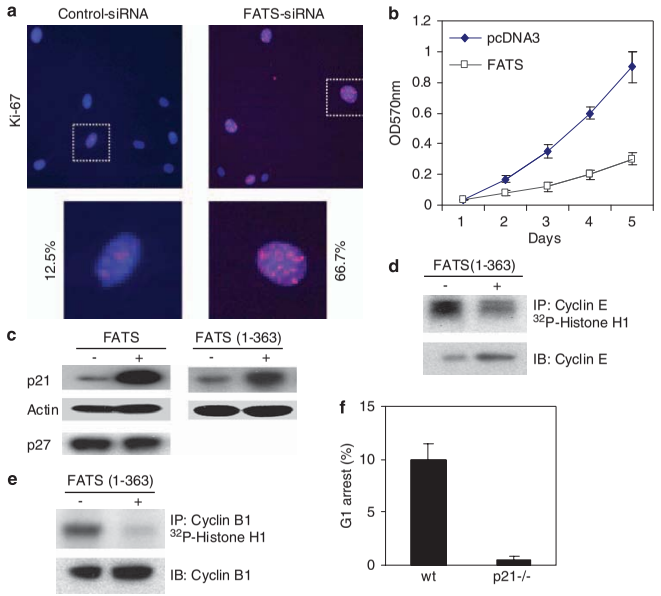

Figure 4 Overexpression of the NH2-terminal FATS is sufficient to induce p21. (**a**) Proliferation index of cells after FATS knockdown. Cells were fixed 24 h later and stained for a proliferation marker Ki-67 (red). The nuclei were stained with DAPI. The representative images were shown and Ki-67 staining was quantified. (**b**) Growth rates of NIH3T3 cells after stable transfection of a FATS-expressing vector and an empty vector pcDNA3, respectively. (**c**) Induction of p21 by FATS and FATS (1–363) in NIH3T3 cells. (**d**) CyclinE-associated kinase activity in the absence or presence of FATS(1–363). After transfection, cell lysates were subjected to immunoprecipitation (IP), and Histone H1 was used as a substrate for *in vitro* kinase assay. The protein level of CyclinE in lysate was examined by immunoblotting (IB). (**e**) CyclinB1-associated kinase activity in the absence or presence of FATS(1–363). Histone H1 was used as a substrate for *in vitro* kinase assay. (**f**) Effect of FATS (1–363) on G_1 phase in the absence of p21. Wild-type (wt) and p21 null MEF cells were transfected with FATS(1–363) or an empty vector pcDNA3, respectively. After 48 h, cells were fixed and subjected to flow cytometry analysis. The percentage of G_1 cells in wt MEFs and p21-null MEFs before FATS(1–363) transfection was 62.5 and 55.0%, respectively. The increase in G_1 is depicted in the bar graph. Each value is the average of three independent experiments and error bars represent the s.d.

Flag antibody, followed by immunoblotting with a myc antibody. Indeed, the NH2-termianl region of FATS protein coimmunoprecipitated with a significant amount of HDAC1, whereas a nonspecific immunoglobulin G (IgG) did not (Figure 6a), indicating that the NH2-terminal region of FATS specifically binds HDAC1 *in vivo*. Such conclusion was confirmed by the results using a reciprocal immunoprecipitation and immunoblotting procedure (Figure 6a). To determine whether FATS might directly interact with HDAC1, FATS(1–363) region was tagged with glutathione-*S*-transferase (GST), and purified fusion protein was subjected to pull down an *in vitro*-translated HDAC1. GST–FATS(1–363), but not GST alone, was found to bind a significant amount of HDAC1 (Figure 6b), indicating a direct interaction between the NH2-termianl region of FATS and HDAC1.

In order to gain additional insight into the interaction between FATS and HDAC1, we generated truncated FATS mutants and performed GST pull-down assay. We found that FATS(67–363) and FATS (1–288) bound to HDAC1, whereas FATS(175–363) did not (Figures 6c and d). Therefore, FATS(67–175) domain within the NH2-terminal region of FATS is required for efficient interaction between FATS and HDAC1.

The NH2-terminal FATS inhibits HDAC1 binding to p21 and facilitates the acetylation of p21

We next assessed the effect of FATS–HDAC1 interaction on FATS-mediated induction of p21. Given that endogenous p21 undergoes acetylation (Chen *et al*., 2004), we sought to determine whether FATS(1–363) could have an impact on acetylation of endogenous p21. After transfection of FATS(1–363) into cells, the acetylated p21 was examined by immunoprecipitation with an antibody to acetylated lysine residue, followed by immunoblotting using a p21 antibody. The acetyla-

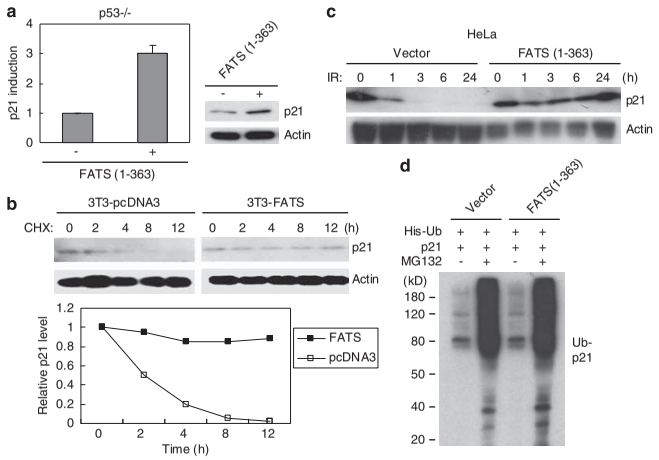

Figure 5 Inhibition of p21 turnover by the NH2-terminal region of FATS independently of p53. (**a**) Induction of p21 by FATS(1-363) in the absence of p53. MEF cells (p53−/−) were transfected with FATS (1–363) or an empty vector, respectively. The protein level of p21 was evaluated by immunoblotting using an antibody to p21. Results of three independent experiments were averaged and plotted as relative p21 induction. Error bars refer to ± s.d. A representative result of western blot was shown. (**b**) Degradation of endogenous p21 in the presence of FATS(1–363). The stable transfectants 3T3-FATS and its control, 3T3-pcDNA3, were treated with 50 μg/ml of cycloheximide (CHX) for different periods of time as indicated, followed by immunoblotting using a p21 antibody. The results were quantified and plotted against the indicated time course. (**c**) Protein levels of p21 after IR treatment in p53-inactivated cells. HeLa cells were transfected with FATS(1–363) or an empty vector, respectively. After 24 h, cells were treated with 10 Gy dose of IR. Protein levels of p21 were evaluated by immonublotting at the indicated time points. (**d**) p53−/− cells were transfected with p21 in combination with His-tagged ubiquitin in the absence or presence of FATS (1–363). At 48 h after transfection, cells were incubated with MG132 (20 μM) for 6 h. Ubiquitinated proteins were purified with Ni-NTA (Qiagen, Hilden, Germany) beads, followed by immunoblotting against p21.

tion of p21, which was barely detectable in the absence of FATS(1–363), was much more pronounced after the overexpression of FATS(1–363) (Figure 7a), indicating that FATS-mediated stabilization of p21 is associated with enhanced acetylation modification of p21. Furthermore, a significant amount of HDAC1 was physically associated with GST–p21 protein, whereas GST protein did not bind to HDAC1 (Figure 7b), indicating that HDAC1 protein is directly associated with p21. We next examined the effect of the NH2-terminal FATS on HDAC1 binding to p21 *in vivo*. The interaction between HDAC1 and endogenous p21 was observed *in vivo*. However, such interaction was abolished in the presence of FATS(1–363) (Figure 7c). The effect of FATS(1–363) on inhibiting HDAC1 binding to p21 *in vivo* was further substantiated by the observation that much less amount of HDAC1 was coimmunoprecipitated with an HA-tagged p21 in the presence of the NH2-terminal FATS, in comparison with that in the absence of the NH2-terminal FATS (Figure 7d). To further characterize the role of HDAC1 in FATS-mediated regulation of p21, we used RNA interference to inhibit the expression of HDCA1. Although knockdown of HDAC1 led to an increase in basal level of p21 protein, the fold induction of p21 protein level by the NH2-terminal FATS was significantly attenuated (Figure 7e), demonstrating that FATS targets HDAC1 to stabilize p21.

Acetylation of p21 suppresses its ubiquitin-independent proteasomal turnover linked to FATS-mediated control of p21 function

To gain further insight into the biological significance of acetylation modification of p21, we asked whether acetylation of p21 could suppress its proteasomal degradation. The treatment of trichostatin A (TSA), a HDAC inhibitor, has been known to selectively induce p21 (Johnstone, 2002; Dokmanovic *et al*., 2007). To rule out the possibility that p53-dependent induction of p21 under TSA treatment was involved, we investigated the effect of TSA treatment on p21 stability in HeLa cells, which carry inactive p53. Consistent with the results in Figure 5c, endogenous p21 protein in HeLa cells quickly diminished under CHX treatment and only about 10% of p21 protein was remained after CHX treatment for 1 h (Figures 8a and b). However, TSA treatment in advance for 2 h, followed by CHX treatment under the same conditions, significantly increased the protein stability of endogenous p21 and 80% of p21 protein remained intact after CHX treatment for 1 h (Figures 8a and b), indicating the relevance of p21 actetylation to its

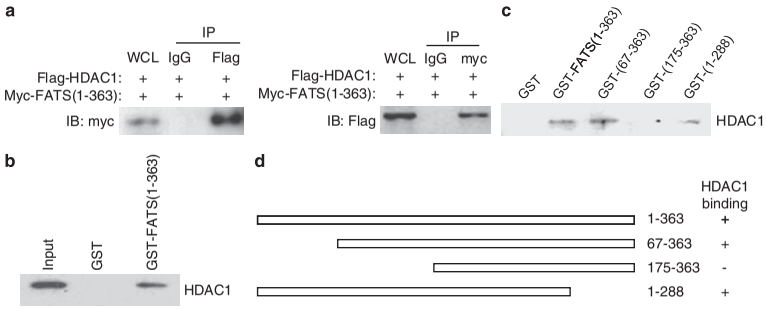

Figure 6 FATS as an HDAC1-binding protein. (**a**) Physical association of FATS(1–363) with HDAC1 *in vivo*. Cells were co-transfected with 1 μg of Flag-tagged HDAC1 and 1 μg of myc-tagged FATS (1–363). Cell lysates were subjected to immunoprecipitation (IP) followed by western blot analysis using a myc antibody. A reciprocal IP with a myc antibody followed by immunoblotting is shown in the right panel. (**b**) The NH2-terminal region of FATS directly interacts with HDAC1. Purified GST-FATS(1–363) protein was incubated with ^{35}S-labeled *in vitro* translated HDAC1. Protein interaction was detected by autoradiography. (**c**) GST pull-down assay for delineation of an HDAC1-binding domain within NH2-terminal FATS. (**d**) Schematic diagram of FATS truncated mutants and the summarized results in panel c indicate FATS(67–175) as the binding domain to HDAC1.

stability *in vivo*. The complete degradation of endogenous p21 after CHX treatment for 2 h in the presence of TSA (Figure 8a) suggested the transient effect of TSA on p21 stability in the presence of CHX and the dynamic mechanism underlying p21 acetylation.

It is noteworthy that the C terminus of p21, namely p21 (139–164), which was bound to both C8 α-subunit of 20S proteasome (Touitou *et al*., 2001) and REGγ proteasome activator (Chen *et al*., 2007), has an essential role in direct degradation of p21 by proteasome (Sheaff *et al*., 2000; Chen *et al*., 2007; Li *et al*., 2007). In addition, there are four lysine residues (K141, K154, K161 and K163) in the C terminus of p21 protein, which raising the possibility that FATS-mediated acetylation might be directly correlated with p21 stabilization. Owing to the difficulties in obtaining a constitutively acetylated protein *in vivo*, we generated an HA-tagged Ac-p21(139–164) peptide, in which K141, K154, K161 and K163 were *in vitro* acetylated. The HA-tagged p21(139–164) peptide was also generated as its control (Figure 8c). The same amount of Ac-p21(139–164) or p21(139–164) peptide was incubated with purified 20S proteasome, respectively, in the absence of adenosine triphosphate and ubiquitin. After incubation at 37 °C for 10 min, p21(139–164) peptide was completely degraded. In contrast, the amount of Ac-p21(139–164) peptide only slightly decreased after incubation with 20S proteasome for 10 min, and Ac-p21(139–164) was detectable even after incubation with 20S proteasome for 60 min (Figure 8d), strongly demonstrating that acetylation of p21 is critical to extend the half-life of free p21. To further validate this mechanism, we performed GST pull-down assay to evaluate the binding of C8 subunit to p21(139–164) peptide with or without acetylation. Purified GST-C8 protein strongly associated with p21(139–164) peptide. However, only tiny amount of Ac-p21(139–164) peptide was bound to GST-C8, which did not bind a nonspecific BSA protein (Figure 8e). Therefore, acetylation of lysine residues (K141, K154, K161 and K163) in the C terminus of p21 remarkably suppresses the direct binding of C8 α-subunit of 20S proteasome to p21, leading to significantly increased stability of p21 protein.

Specifically, knockdown of FATS mRNA expression significantly decreased the steady-state level of p21 protein (Figure 8f), and reduced protein levels of p21 in thymic lymphomas were observed in those samples with downregulated expression of FATS (Figure 8g), which strongly demonstrate the essential role of FATS in controlling p21 abundance. Furthermore, in contrast to control cells that exhibit G_1 arrest and significantly decreased S phase entry after IR treatment, the inhibition of S phase entry after DNA damage was significantly compromised in cells after FATS knockdown (Figure 8h), indicating that G_1 cell-cycle arrest after DNA damage is defective in FATS-deficient cells. These observations were consistent with our results as shown in Figures 3 and 4, emphasizing that the tumor suppressor role of FATS is linked to, at least in part, its control of p21 function in cell-cycle checkpoints.

Discussion

Identifying cancer genes and understanding their involvement in tumorigenesis are critical steps in controlling this disease. Despite tremendous works in genome-wide screening, these attempts were often hampered by the relatively low resolution of banded chromosomes and a plethora of genomic alterations in late-stage human tumors with genetic heterogenicity, making it difficult in identifying events at early stages of tumorigenesis. The identification and functional characterization of FATS suggest the values of dissecting frequent

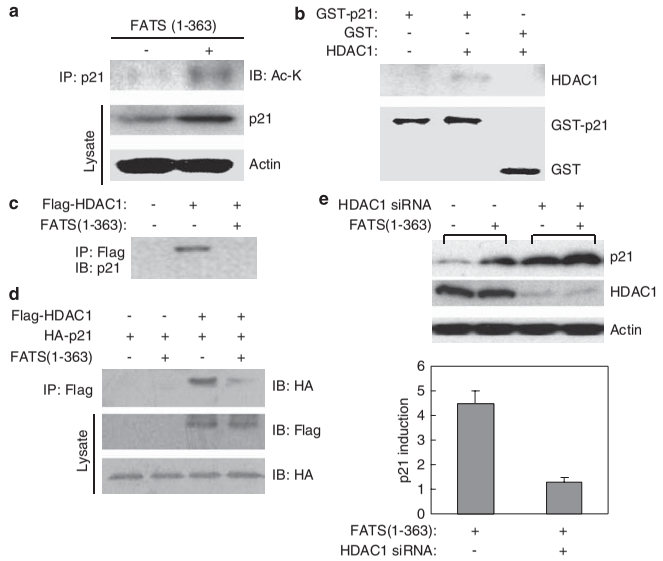

Figure 7 The interaction between FATS and HDAC1 enhances acetylation modification of endogenous p21. (**a**) HeLa cells were transfected with FATS(1–363) or an empty vector. After transfection for 48 h, cell lysates were immunoprecipitated with an antibody specific to acetyl-lysine (Ac-K) or an immunoglobulin G control, followed by immunoblotting with a p21 antibody. (**b**) GST pull downs using purified GST-p21 and *in vitro* translated HDAC1. GST-p21 proteins in pull-down assay system were analyzed by coomasie blue staining. (**c**) Effect of FATS(1–363) expression on HADC1 binding to p21 *in vivo*. HeLa cells were untreated or transfected with Flag-tagged HDAC1 alone or in combination of FATS(1–363). After transfection for 48 h, cell extracts were subjected to immunoprecipitation with a Flag antibody, followed by immnoblotting using an antibody to p21. (**d**) HA-p21 was transfected into HeLa cells alone, or co-transfected with Flag-tagged HDAC1, in the absence or presence of FATS(1–363). Cell extracts were subjected to immunoprecipitation with a Flag antibody, followed by immnoblotting using an antibody to HA tag. (**e**) FATS(1–363)-mediated induction of p21 after knockdown of HDAC1 expression. HeLa cells were transfected with HDAC1 siRNA or a non-targeting control siRNA for 24 h. siRNA-transfected cells were subsequently transfected with FATS(1–363) and an empty vector, respectively. After 24 h, cellular p21 was examined by immunoblotting using an antibody to p21. Results from three individual experiments were plotted for comparison. The data are represented as means ± s.d.

changes in IR-induced mouse tumors (Mao *et al*., 2005), which will allow us to uncover new cancer genes involved in early tumorigenesis. We verify that human ortholog of FATS is a CFS gene at FRA10F, one of 76 aphidicolin-induced CFSs that have previously not been cloned and characterized at the molecular level (Durkin and Glover, 2007). CFS stability is regulated by DNA damage checkpoints ATR (Casper *et al*., 2002), indicating that some level of replication stalling occurs at CFS regions and they could be prone to cause DSBs after radiation treatment in normal cells. Interestingly, CFS stability is not regulated by another checkpoint kinase ATM (for ataxia-telangiectasia mutated) that responds primarily to DSBs (Casper *et al*., 2002). As DSBs are the principal lesions of importance in the induction of chromosomal abnormalities and gene mutations, our study brings new insight into the function of some CFS genes, if not all, in linking DSBs sensor to DNA damage checkpoint machinery, and provides the first evidence that a CFS gene actively monitors DNA damage response and genomic stability. The discovery of a radiation-susceptible gene FATS that has an important role in maintaining genomic stability through regulating p21 abundance adds new insights into our understanding of radiation-associated cancer risks.

As a negative regulator of the cell cycle, p21 is uniquely positioned to function as a central inhibitor of CDK1 and CDK2, both in unstressed cells and after genotoxic stresses, leading to growth arrest in the G_1 and G_2 phase of cell cycle. The abundance of cellular p21 is tightly controlled at both transcriptional and post-transcriptional levels. Given that p21 is unstable and its transcription can be activated by many oncogenic factors other than p53 tumor suppressor (Macleod *et al*., 1995), the stabilization of p21 protein has a critical role in regulating p21 abundance and its function in cell-cycle control. Our finding reveals FATS as a potent regulator of p21 abundance. Following induction of DSBs by IR, FATS-inhibited cells exhibit radiosensitivity as shown by more pronounced Chk1

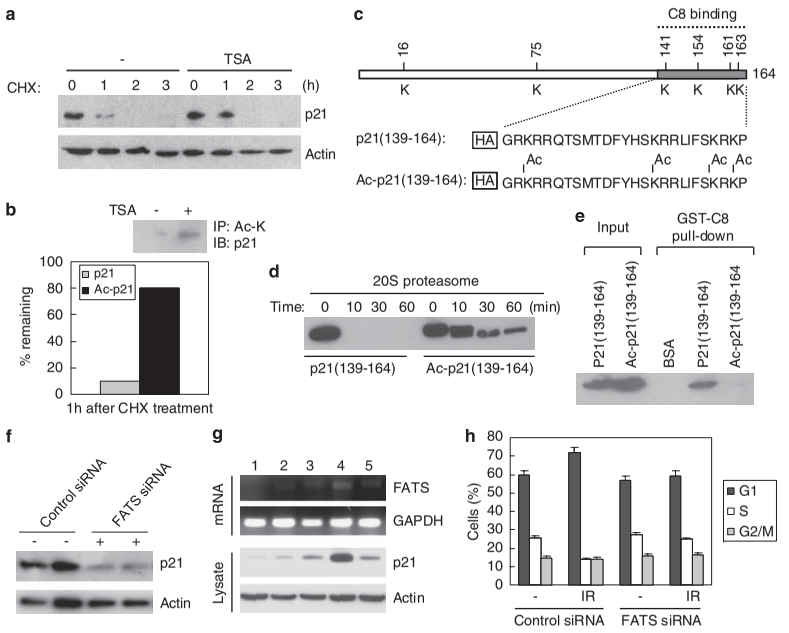

Figure 8 Acetylation of p21 suppresses its ubiquitin-independent proteasomal turnover linked to FATS-mediated control of p21 function. (**a**) Effect of HDAC inhibitor on p21 protein stability. HeLa cell were incubated with or without TSA (10 μM) treatment for 2 h, and subsequently treated with CHX at 100 μg/ml for indicated times. The endogenous p21 was evaluated by immunoblotting. (**b**) The effect of TSA and CHX treatment on p21 degradation as described in panel a. Cells with or without TSA treatment for 2 h in panel a were subjected to immunoprecipitation with an antibody specific to Ac-K, followed by immunoblotting using an antibody to p21. (**c**) Schematic diagram showing the position of lysine residues in C-terminal region of p21 protein. The sequences of HA-tagged p21(139–164) peptide with or without acetylation modification on K141, K154, K161 and K163 are indicated. (**d**) *In vitro* proteolytic analysis to compare the stability of p21(139-164) and Ac-p21(139-164) in the presence of activated 20S proteasome (Chemicon) and in the absence of ATP and ubiquitin. (**e**) Effect of acetylation on C8-binding to p21(139–164). GST pull-down assay was performed and bound polypeptides were analyzed by immunoblotting using an HA antibody. (**f**) The abundance of p21 after FATS knockdown. MEF cells were transfected with FATS siRNA or control siRNA, respectively. After transfection for 24 h, the steady-state level of p21 protein was analyzed by immunoblotting. (**g**) The protein levels of p21 in mouse thymic lymphomas were measured by immunoblotting. The total RNA was extracted from a portion of the same sample and the mRNA levels of FATS were examined by reverse transcription–PCR. (**h**) Flow cytometry analysis of FATS-inhibited MEF cells after IR (10 Gy) treatment. The percentage of the population of cells was summarized. Each value is the average of three independent experiments and error bars represent the s.d.

phosphorylation (Figure 3b) and distinct 53BP1 foci formation at the sites of DNA damage (Figure 3c), a character of a group of inherited chromosomal instability syndromes including ataxia telangiectasia (AT) and Nijmegen breakage syndrome with a predisposition to cancer. In addition, defects in mitosis and centrosome duplication after IR in FATS-deficient cells (Figure 3e) are more severe than that in p21-deficient cells (Bunz *et al*., 1998), supporting that FATS acts upstream of p21 and is required for G_2/M checkpoint function. The tumor suppressor activity for p21 is demonstrated by the genetic evidence (Martin-Caballero *et al*., 2001), and p21 is a major determinant of tumor suppression by p53, especially in case p53 loses its capacity in inducing apoptosis (Barboza *et al*., 2006; Efeyan *et al*., 2007). It is noteworthy that p21 is often deregulated in cancer, which is frequently associated with its cytoplasmic expression due to phosphorylation at Thr145 (Zhou *et al*., 2001; Winter *et al*., 2003; Xia *et al*., 2004). FATS-mediated acetylation of p21 may not only inhibit p21 degradation by proteasome, but also interfere with its phosphorylation by some oncogenic kinase to retain its nuclear localization and proper function to regulate cell cycle. The importance of acetylation modification of p21 is further emphasized by the fact that the C terminal p21 interacts with PCNA, a proliferating cell nuclear antigen (Touitou *et al*., 2001). The stabilization of p21 by FATS may also facilitate p21-mediated regulation of cell-cycle progression by inhibiting PCNA, independently of CDK inhibition.

HDAC1 is a major deacetylase whose genetic deletion causes a significant reduction in total HDAC activity (Zupkovitz *et al*., 2006), and its involvement in cancer has been established (Lin *et al*., 1998). In addition, HDAC1 has been implicated in ATM-mediated sensing of IR-induced DNA damage (Kim *et al*., 1999), implying the potential crosstalk between FATS and ATM. Although we cannot rule out the possibility that the interaction between FATS and HDAC1 may also abolish HDAC1-mediated repression of p21 transcription, which acts through a general transcription factor Sp1 (Lagger *et al*., 2002; Lagger *et al*., 2003), such effect on FATS-mediated induction of p21 is negligible, as FATS did not affect the expression of p27, whose expression is also mediated by Sp1 (Wei *et al*., 2003; Cen *et al*., 2008). Finally, FATS may have potential application in cancer therapeutics and the development of new generation of HDAC inhibitors.

Materials and methods

Microarray-based comparative genomic hybridization
Mouse whole-genome BAC arrays consisting of more than 19200 BAC clone DNAs were used to perform comparative genomic hybridization as previously described (Cai *et al*., 2002). Heterozygous p53 + /− mice were exposed to a single dose of 4 Gy by whole-body γ-radiation to induce tumors as previously described (Mao *et al*., 2005). Mouse C_0t-1 DNA was used for blocking repetitive sequences in BAC clones and genomic probes. The Cy5/Cy3 ratios were plotted along individual chromosomes. For each mouse tumor sample, two experiments were carried out with reversal of Cy3/Cy5 labeling to remove any ratio artifact.

Reagents, plasmids and cell culture
NIH3T3 and HeLa cells were obtained from American Type Culture Collection (ATCC, Manassas, VA, USA), MEF and p53-null cells were obtained from Dr A Balmain (San Francisco, CA, USA). p21-null cells were kindly provided by Dr Lozano G (Houston, TX, USA). Cells were grown in Dulbecco's modified Eagle's medium (Invitrogen, Carlsbad, CA, USA) supplemented with 10% fetal calf serum.

To generate pcDNA3-FATS, a FATS fragment from MEF cDNA was generated by PCR using the following primers: 5′-CACACTCCTGGGAGCCTTAC-3′ and 5′-CAGATCCA GGGCTAGCAGAG-3′ and subsequently inserted into pcDNA3.1/Topo vector (Invitrogen). A FATS(1–363) fragment was obtained by PCR amplification from MEF cDNA using the following primers: 5′-CTGGCATCACAGAACACA AGAATGA-3′ and 5′-CTACTCACCAGCCCTGTAACTCC AG-3′, and subsequently inserted into pcDNA3.1/Topo vector to generate pcDNA3-FATS(1–363). All the constructs were verified by sequence analysis. GST-FATS(1–363) plasmid was produced by in-frame inserting a FATS(1–363) fragment from pcDNA3-FATS (1–363) into *Eco*RI/*Xho*I sites of pGex-6p1 vector (Amersham Biosciences, Buckinghamshire, UK). A vector pCMV-Tag5 (Stratagene, La Jolla, CA, USA) was used to generate myc-FATS(1–363). 3T3-FATS and 3T3-pcDNA3 cells were generated by transfecting pcDNA3-FATS or pcDNA3 (Invitrogen) into NIH3T3 cells, respectively, followed by G418 selection. Plasmids were transfected into cells by lipofectamine (Invitrogen) or an electroporator (Amaxa, Cologne, Germany). Flag-HDAC1 was kindly provided by Dr RA DePinho (Boston, MA, USA). GST-p21 and HA-p21 were gifts from Dr H Lu (Indianapolis, IN, USA). GST-C8 was kindly provided by Dr Y Long (Shanghai, China). Antibodies including anti-p21, anti-p27, and anti-Ki-67 were purchased from BD Pharmigen (San Diego, CA, USA); antibodies to Flag, β-actin, and γ-tubulin were from Sigma (Buchs, Switzerland); an antibody to cyclinB1 was from Santa Cruz Biotechnology (Santa Cruz, CA, USA); an antibody to acetyl-lysine was from Upstate (Charlottesville, VA, USA). The antibodies to Chk1 and Chk1 (phospho S345) were purchased from Abcam (Cambridge, UK). HA-tagged p21(139–164) and Ac-p21(139–164) peptides were synthesized by Shanghai Science Peptide Biological Technology (Shanghai, China). The sequences were as follows: YPYDVPDY AGRKRRQTSMTDFYHSKRRLIFSKRKP and YPYDVP-DYAGRK(Ac)RRQTSMTDFYHSK(Ac)RRLIFSK(Ac)RK (Ac)P. TSA, MG132 and CHX were purchased from Sigma.

RNA interference
FATS siRNA was generated using a Block-iT RNAi topo transcription kit (Invitrogen) and Block-iT dicer RNAi kits (Invitrogen) following the manufacturer's instructions. The primers for FATS were 5′-CTCAGCCTCCGCTGTAGTT C-3′ and 5′-CCTTCCAGTGACCACCTTGT-3′. The siRNA pool for FATS was obtained by cleaving ds-RNA with Dicer enzyme. Purified FATS-siRNA was diluted to 0.1 μg/μl and stored at −80 °C. A non-targeting siRNA pool from Dharmacon (D-001206-13, Lafayette, CO, USA) was used as control. Lipofectamine (Invitrogen) was used for siRNA transfection.

Reverse transcription–PCR
First-strand cDNA was synthesized using M-MuLV reverse transcriptase (New England BioLabs, Ipswich, MA, USA) from 0.5 μg of total RNA. The primers specific to mouse FATS were as follows: 5′-GTGACAGTGGGGTCTTCGTT-3′ and 5′-GGTGTTGAAGTCCCAGCAAT-3′. The primers specific to a housekeeping gene glyceraldehyde-3-phosphate dehydrogenase were as follows: 5′-TGCCTCCTGCACCAC CAACT-3′ and 5′-CGCCTGCTTCACCACCTT-3′.

GST pull-down assay
GST fusion proteins were expressed and purified as described previously (Li *et al*., 2004).

Immunoprecipitation and western blot
Immunoprecipitation and western blot analysis was performed as described previously (Li *et al*., 2004).

Fluorescence in situ *hybridization and immunofluorescence microscopy*
Peripheral blood lymphocytes from two healthy individuals were cultured and treated with aphidicolin (0.2 μM) for 24 h. Then metaphase chromosomes were prepared according to standard procedures. A BAC clone RP11-179O22 was selected from the UCSC database (http://genome.ucsc.edu) for fluorescence *in situ* hybridization analysis as described (Liehr *et al*., 2002).

Cells were fixed with 4% paraformaldehyde for 20 min, permeabilized with 0.1% Triton X-100 solution, and then immunostained with a primary antibody (1:100 dilution) overnight at 4 °C, then incubated with a fluorescein isothiocyanate- or cy3-conjugated secondary antibody (1:200 dilution) for 1 h. Images were taken with a deltavision deconvolution microscope (Olympus, Tokyo, Japan).

MTT assay
Cells (1×10^4) were plated onto 24-well plates. At the indicated times, 5 mg/ml of MTT [3-(4, 5-dimethylthiazolyl-2)-2, 5-diphenyltetrazolium bromide] (Sigma) was added into media at 1:10 dilution and incubated for 5 h. Then supernatants were removed, and 1 ml of acidic isopropanol containing 0.04 M HCl was added to dissolve intracellular purple formazan. Absorbance was measured at 570 nm. The reference wavelength was 650 nm.

Flow cytometry analysis
Cells were harvested and fixed in 70% cold ethanol for 30 min at room temperature. Cells were stored at 4 °C until ready to stain. Cells were recovered by centrifugation, then stained with propidium iodide containing 100 μg/ml of RNAse and subjected to analysis with a flow cytometer (Becton Dickinson, Franklin Lakes, NJ, USA).

In vitro *proteolytic analysis*
The proteolytic analysis was performed using a 20S proteasome activity assay kit (Chemicon, Cat. no. APT280, Temecula, CA, USA). In brief, 2 μg of purified HA-tagged p21(139–164) or Ac-p21(139–164) peptides was incubated with 1 μl of 20S proteasome (Chemicon, Part no. 90205) in assay buffer (25 mM HEPES, (pH 7.5), 0.5 mM EDTA, 0.05% NP-40 and 0.001% SDS) at 37 °C for different time course. The reaction was stopped by adding 10 μl of SDS sample buffer (65 mM Tris, pH 8.0; 10% glycerol, 2% SDS, 1% DTT, 0.01% bromophenol blue) and heating at 95 °C for 5 min. An aliquot of the reaction was analyzed by western blotting using an antibody against HA.

In vitro *kinase assay*
Cell extracts were harvested and subjected to immunoprecipitation using an antibody against cyclin B1 at 4 °C overnight. Immnuocomplex was then suspended in buffer containing 25 mM Tris (pH 7.5), 10 mM $MgCl_2$, 10 μCi [γ-^{32}P]-adenosine triphosphate and 0.1 μg histone H1. After incubation at 30 °C for 30 min, samples were boiled and loaded on SDS–polyacrylamide gel electrophoresis gel. The phosphorylation of histone H1 was detected by autoradiography.

Conflict of interest

The authors declare no conflict of interest.

Acknowledgements

We are grateful to Mien-Chi Hung for critical discussions. We thank Xiangwei He and Qi Gao for assistance in microscopic imaging; Tao Jiang and Qian Li for technical assistance. This study was supported in part by the following grants: Tianjin Medical University Cancer Institute and Hospital Start-up 08Y01 (to Z Li); Ministry of Science and Technology of China 973-program Concept Award 2009CB526407 (to Z Li); Tianjin Municipal Science and Technology Foundation (to Z Li); Department of defense of United States FG02-03ER63630 (to A Balmain); IZKF Jena Start-up S16 (to T Liehr).

References

Abbas T, Dutta A. (2009). p21 in cancer: intricate networks and multiple activities. *Nat Rev Cancer* **9**: 400–414.
Barboza JA, Liu G, Ju Z, El-Naggar AK, Lozano G. (2006). p21 delays tumor onset by preservation of chromosomal stability. *Proc Natl Acad Sci USA* **103**: 19842–19847.
Bendiennat M, Boulaire J, Jascur T, Brickner H, Barbier V, Sarasin A *et al.* (2003). UV irradiation triggers ubiquitin-dependent degradation of p21(WAF1) to promoter DNA repair. *Cell* **114**: 599–610.
Bichara M, Wagner J, Lambert IB. (2006). Mechanisms of tandem repeat instability in bacteria. *Mut Res* **598**: 144–163.
Bloom J, Amador V, Bartolini F, DeMartino G, Pagano M. (2003). Proteasome-mediated degradation of p21via N-terminal ubiquitinylation. *Cell* **115**: 71–82.
Brenner DJ, Doll R, Goodhead DT, Hall EJ, Land CE, Little JB *et al.* (2003). Cancer risks attributable to low doses of ionizing radiation: assessing what we really know. *Proc Natl Acad Sci USA* **100**: 13761–13766.
Brugarolas J, Chandrasekaran C, Gordon JI, Beach D, Jacks T, Hannon GJ. (1995). Radiation-induced cell cycle arrest compromised by p21 deficiency. *Nature* **377**: 552–557.
Bunz F, Dutriaux A, Lengauer C, Waldman T, Zhou S, Brown JP *et al.* (1998). Requirement for p53 and p21 to sustain G2 arrest after DNA damage. *Science* **282**: 1497–1501.
Buttel I, Fechter A, Schwab M. (2004). Common fragile sites and cancer: targeted cloning by insertional mutagenesis. *Ann NY Acad Sci* **1028**: 14–27.
Cai WW, Mao JH, Chow CW, Damani S, Balmain A, Bradley A. (2002). Genome-wide detection of chromosomal imbalances in tumors using BAC microarrays. *Nat Biotechnol* **20**: 393–396.
Casper AM, Nghiem P, Arlt MF, Glover TW. (2002). ATR regulates fragile site stability. *Cell* **111**: 779–789.
Cen B, Deguchi A, Weinstein IB. (2008). Activation of protein kinase G increases the expression of p21CIP1, p27KIP1, and histidine triad protein 1 through Sp1. *Cancer Res* **68**: 5355–5362.
Chen X, Chi Y, Bloecher A, Aebersold R, Clurman BE, Roberts JM. (2004). N-acetylation and ubiquitin-independent proteasomal degradation of p21(Cip1). *Mol Cell* **16**: 839–847.
Chen X, Barton LF, Chi Y, Clurman BE, Roberts JM. (2007). Ubiquitin-independent degradation of cell-cycle inhibitos by the REGγ proteasome. *Mol Cell* **26**: 843–852.
Coulombe P, Rodier G, Bonneil E, Thibault P, Meloche S. (2004). N-terminal ubiquitination of extracellular signal-regulated kinase 3 and p21 directs their degradation by the proteasome. *Mol Cell Biol* **24**: 6140–6150.
Deng C, Zhang P, Harper JW, Elledge SJ, Leder P. (1995). Mice lacking p21CIP1/WAF1 undergo normal development, but are defective in G1 checkpoint control. *Cell* **82**: 675–684.
DiTullio Jr RA, Mochan TA, Venere M, Bartkova J, Sehested M, Bartek J *et al.* (2002). 53BP1 functions in an ATM-dependent checkpoint pathway that is constitutively activated in human cancer. *Nat Cell Biol* **4**: 998–1002.
Dokmanovic M, Clarke C, Marks PA. (2007). Histone deacetylase inhibitors: overview and perspectives. *Mol Cancer Res* **5**: 981–989.
Durkin SG, Glover TW. (2007). Chromosome fragile sites. *Annu Rev Genet* **41**: 169–192.
Efeyan A, Collado M, Velasco-Miguel S, Serrano M. (2007). Genetic dissection of the role of p21$^{Cip1/Waf1}$ in p53-mediated tumor suppression. *Oncogene* **26**: 1645–1649.
Glover TW, Arlt MF, Casper AM, Durkin SG. (2005). Mechanisms of common fragile site instability. *Hum Mol Genet* **14**: R197–R205.
Holm LE. (1990). Cancer occurring after radiotherapy and chemotherapy. *Int J Radiat Oncol Biol Phy* **19**: 1303–1308.
Hoppe-Seyler F, Butz K. (1993). Repression of endogenous p53 transactivation function in HeLa cervical carcinoma cells by human papillomavirus type 16 E6, human mdm-2, and mutant p53. *J Virol* **67**: 3111–3117.
Johnstone RW. (2002). Histone-deacetylase inhibitors: novel drugs for the treatment of cancer. *Nat Rev Drug Discov* **1**: 287–299.

Kastan MB, Bartek J. (2004). Cell-cycle checkpoints and cancer. *Nature* **432**: 316–323.
Kemp CJ, Wheldon T, Balmain A. (1994). p53-deficient mice are extremely susceptible to radiation-induced tumorigenesis. *Nat Genet* **8**: 66–69.
Kim GD, Choi YH, Dimtchev A, Jeong SJ, Dritschilo A, Jung M. (1999). Sensing of ionizing radiation-induced DNA damage by ATM through interaction with histone deacetylase. *J Biol Chem* **274**: 31127–31130.
Lagger G, O'Carroll D, Rembold M, Khier H, Tischler J, Weitzer G *et al*. (2002). Essential function of histone deacetylase 1 in proliferation control and CDK inhibitor repression. *EMBO J* **21**: 2672–2681.
Li X, Amazit L, Long W, Lonard DM, Monaco JJ, O'Malley BW. (2007). Ubiquitin- and ATP-independent proteolytic turnover of p21 by the REGγ-proteasome pathway. *Mol Cell* **26**: 831–842.
Li Z, Day CP, Yang JY, Tsai WB, Lozano G, Shih HM *et al*. (2004). Adenoviral E1A targets Mdm4 to stabilize tumor suppressor p53. *Cancer Res* **64**: 9080–9085.
Liehr T, Heller A, Starke H, Claussen U. (2002). FISH banding methods: applications in research and diagnosis. *Expert Rev Mol Diagn* **2**: 217–225.
Lin RJ, Nagy L, Inoue S, Shao W, Miller WH, Evans RM. (1998). Role of the histone deacetylase complex in acute promyelocytic leukaemia. *Nature* **391**: 811–814.
Macleod KF, Sherry N, Hannon G, Beach D, Tokino T, Kinzler K *et al*. (1995). P 53-dependent and independent expression of p21 during cell growth, differentiation, and DNA damage. *Genes Dev* **9**: 935–944.
Magrath IT. (1997). The treatment of pediatric lymphomas: paradigms to plagiarize? *Ann Oncol* **8**: 7–14.
Maier D, Comparone D, Taylor E, Zhang Z, Gratzl O, van Meir EG *et al*. (1997). New deletion in low-grade oligodendroglioma at the glioblastoma suppressor locus on chromosome 10q25-26. *Oncogene* **15**: 997–1000.
Mangelsdorf M, Ried K, Woollatt E, Dayan S, Eyre H, Finnis M *et al*. (2000). Chromosomal fragile site FRA16D and DNA instability in cancer. *Cancer Res* **60**: 1683–1689.
Mao JH, Li J, Jiang T, Li Q, Wu D, Perez-Losada J *et al*. (2005). Genomic instability in radiation-induced mouse lymphoma from p53 heterozygous mice. *Oncogene* **24**: 7924–7934.
Martin-Caballero J, Flores JM, Garcia-Palencia P, Serrano M. (2001). Tumor susceptibility of p21(Waf1/Cip1)-deficient mice. *Cancer Res* **61**: 6234–6238.
Maser RS, DePinho RA. (2002). Connecting chromosomes, crisis, and cancer. *Science* **297**: 565–569.
Nagase S, Yamakawa H, Sato S, Yajima A, Horii A. (1997). Identification of a 790-kilobase region of common allelic loss in chromosome 10q25-q26 in human endometrial cancer. *Cancer Res* **57**: 1630–1633.
Ohi R, Gould KL. (1999). Regulating the onset of mitosis. *Curr Opin Cell Biol* **11**: 267–273.
Pagano M, Tam SW, Theodoras AM, Beer-Romero P, Del Sal G, Chau V *et al*. (1995). Role of the ubiquitin-proteasome pathway in regulating abundance of the cyclin-dependent kinase inhibitor p27. *Science* **269**: 682–685.
Pearson CE, edamura KN, Cleary JD. (2005). Repeat instability: mechanisms of dynamic mutations. *Nat Rev Genet* **6**: 729–742.
Rouse J, Jackson SP. (2002). Interfaces between the detection, signaling, and repair of DNA damage. *Science* **297**: 547–551.
Schellong G. (1998). Pediatric Hodgkin's disease: treatment in the late 1990s. *Ann Oncol* **9**: S115–S119.
Sherr CJ, Roberts TM. (1999). CDK inhibitors: positive and negative regulators of G1-phase progression. *Genes Dev* **13**: 1501–1512.
Shiloh Y. (2003). ATM and related protein kinase: safeguarding genome integrity . *Nat Rev Cancer* **3**: 155–168.
Schwartz M, Zlotorynski E, Kerem B. (2006). The molecular basis of common and rare fragile sites. *Cancer Lett* **232**: 13–26.
Sheaff RJ, Singer JD, Swanger J, Smitherman M, Roberts JM, Clurman BE. (2000). Proteasomal turnover of p21Cip1 does not require p21Cip1 ubiquitination. *Mol Cell* **5**: 403–410.
Touitou R, Richardson J, Bose S, Nakanishi M, Rivett J, Allday MJ. (2001). A degradation signal located in the C-terminus of p21WAF1/CIP1 is a binding site for the C8 alpha-subunit of the 20S proteasome. *EMBO J* **20**: 2367–2375.
Van Gent DC, Hoeijmakers JH, Kanaar R. (2001). Chromosomal stability and the DNA double-stranded break connection. *Nat Rev Genet* **2**: 196–206.
Varshavsky A, Turner G, Du F, Xie Y. (2000). Felix HoppeSeyler Lecture 2000. The ubiquitin system and the N-end rule pathway. *Biol Chem* **381**: 779–789.
Wei Q, Miskimins WK, Miskimins R. (2003). The Sp1 family of transcription factor is involved in p27(Kip1)-mediated activation of myelin basic protein gene expression. *Mol Cell Biol* **23**: 4035–4045.
Winter ZE, Leek RD, Bradburn MJ, Norbury CJ, Harris AL. (2003). Cytoplasmic $p21^{WAF1/CIP1}$ expression is correlated with HER-2/neu in breast cancer and is an independent predictor of prognosis. *Breast Cancer Res* **5**: R242–R249.
Xia W, Chen JS, Zhou X, Sun PR, Lee DF, Liao Y *et al*. (2004). Phosphorylation/cytoplasmic localization of p21Cip1/WAF1 is associated with HER2/neu overexpression and provided a novel combination predictor for poor prognosis in breast cancer patients. *Clin Cancer Res* **10**: 3815–3824.
Zhang H, Freudenreich CH. (2007). An AT-rich sequence in human common fragile site FRA16D causes fork stalling and chromosome breakage in S. cerevisiae. *Mol Cell* **27**: 367–379.
Zhou BP, Liao Y, Xia W, Spohn B, Lee MH, Hung MC. (2001). Cytoplasmic localization of $p21^{Cip1/WAF1}$ by Akt-induced phosphorylation in HER-2/neu-overexpressing cells. *Nat Cell Biol* **3**: 245–252.
Zupkovitz G, Tischler J, Posch M, Sadzak I, Ramsauer K, Egger G *et al*. (2006). Negative and positive regulation of gene expression by mouse histone deacetylase 1. *Mol Cell Biol* **26**: 7913–7928.

Supplementary Information accompanies the paper on the Oncogene website (http://www.nature.com/onc)

2.2 Article No. 2

X Fan, K Pinthong, H Mkrtchyan, P Siripiyasing, N Kosyakova, W Supiwong, A Tanomtong, A Chaveerach, T Liehr, M de Bello Cioffi, A Weise. 2013. **First detailed reconstruction of the karyotype of *Trachypithecus cristatus* (Mammalia: Cercopithecidae)**. Mol Cytogenet, 6:58.

Abstract: The chromosomal homologies of human (*Homo sapiens* = HSA) and silvered leaf monkey (*Trachypithecus cristatus* = TCR) have been previously studied by classical chromosome staining and by fluorescence in situ hybridization (FISH) applying chromosome-specific DNA probes of all human chromosomes in the 1980s and1990s, respectively. However, as the resolution of these techniques is limited we used multicolor banding (MCB) at ~250-band level, and other selected human DNA probes to establish a detailed chromosomal map of TCR. Therefore it was possible to precisely determine evolutionary conserved breakpoints, orientation of segments and distribution of specific regions in TCR compared to HSA. Overall, 69 evolutionary conserved breakpoints including chromosomal segments, which failed to be resolved in previous reports, were exactly identified and characterized. This work also represents the first molecular cytogenetic one characterizing a multiple sex chromosome system with a male karyotype 44,XY1Y2. The obtained results are compared to other available data for old world monkeys and drawbacks in hominoid evolution are discussed.

MOLECULAR CYTOGENETICS

RESEARCH Open Access

First detailed reconstruction of the karyotype of Trachypithecus cristatus (Mammalia: Cercopithecidae)

Fan Xiaobo[1], Krit Pinthong[2], Hasmik Mkrtchyan[3], Pornnarong Siripiyasing[4], Nadezda Kosyakova[1], Weerayuth Supiwong[5], Alongkoad Tanomtong[5], Arunrat Chaveerach[5], Thomas Liehr[1], Marcelo de Bello Cioffi[6] and Anja Weise[1,7*]

Abstract

Background: The chromosomal homologies of human (Homo sapiens = HSA) and silvered leaf monkey (*Trachypithecus cristatus* = TCR) have been previously studied by classical chromosome staining and by fluorescence in situ hybridization (FISH) applying chromosome-specific DNA probes of all human chromosomes in the 1980s and 1990s, respectively.

Results: However, as the resolution of these techniques is limited we used multicolor banding (MCB) at an ~250-band level, and other selected human DNA probes to establish a detailed chromosomal map of TCR. Therefore it was possible to precisely determine evolutionary conserved breakpoints, orientation of segments and distribution of specific regions in TCR compared to HSA. Overall, 69 evolutionary conserved breakpoints including chromosomal segments, which failed to be resolved in previous reports, were exactly identified and characterized.

Conclusions: This work also represents the first molecular cytogenetic one characterizing a multiple sex chromosome system with a male karyotype 44,XY_1Y_2. The obtained results are compared to other available data for old world monkeys and drawbacks in hominoid evolution are discussed.

Keywords: Evolutionary conserved breakpoints, Multicolor banding, Old world monkeys, XY_1Y_2 sex system

Background

Trachypithecus cristatus (TCR) [1], also known as silvered lutung, silvered leaf monkey or the silvery langur, belongs to superfamily Cercopithecoidea, family Cercopithecidae, subfamily Colobinae. The colobines divided during evolution into an African clade and an Asian clade [2]. TCR is widely distributed in continental Southeast Asia including Myanmar, West-central Thailand, Cambodia, Laos, Vietnam and Southern China [2-4]. Recently, four species groups were recognized (*T. pileatus*, *T. francoisi*, *T. obscurus* and *T. cristatus*), including 18 species only in the Asian colobine of *Trachypithecus*. Genus TCR was initially denominated with various Latin names between 1821 and 1962, like *Simia cristata*, *Semnopithecus cristata*, *Pygathrix cristata*, *Presbytis cristata*, before the current name *Trachypithecus cristatus* was introduced [2].

The karyotype of TCR was described in 1970 as 2n = 44 [5]. In the 1980s, chromosome banding analysis were used in TCR [6-8], including comparative R-banding of three different species of *Colobus* genus [6]. In 1983, G and Q banding were applied to analyze the banding patterns of a female TCR [7]. One year later, male TCR was characterized as carrying an evolutionary conserved translocation involving the Y chromosome and two autosomes [9]. Furthermore, since 1997 chromosomal homologies between human chromosomes and TCR has been established by fluorescence in situ hybridization (FISH) applying human whole chromosome paintings. Thus, up to now, unique reciprocal translocations corresponding to HSA Y & 5, HSA 1 & 19, and HSA 6 & 16 as well as fusions of HSA 14 & 15 and HSA 21 & 22, were characterized [10]. However, as whole chromosome paints have only a limited resolution [11], we established a detailed comparative chromosome map of TCR primarily based on multicolor banding (MCB). The potential of this approach in order to clarify and to resolve evolutionary conserved chromosomal rearrangements was already shown by our group for other primates [12-14].

* Correspondence: Anja.Weise@med.uni-jena.de
[1]Institute of Human Genetics, Jena University Hospital, Friedrich Schiller University, Kollegiengasse 10, Jena D-07743, Germany
[7]Institut für Humangenetik, Postfach, Jena D-07740, Germany
Full list of author information is available at the end of the article

Results

MCB results are summarized in Figure 1 and in Tables 1 and 2. Representative results of probes specific for all acrocentric short arms in HSA, the NOR-region and SRY are also shown in Figure 1. As outlined in Table 1 the majority of TCR chromosomes are completely homologous to one of the human chromosomes, exceptions are only TCR 5 (homologous to HSA 14 and 15), TCR 6 and 8 (homologous to HSA 1 and 19), TCR 9 and 16 (homologous to HSA 6 and 16), TCR 15 (homologous to HSA 21 and 22), and TCR Y1 and Y2 (homologous to HSA Y and 5).

The centromeric positions could be narrowed down to the subband level for all 24 TCR chromosomes (Table 1). In the following chromosomes the TCR centromeric

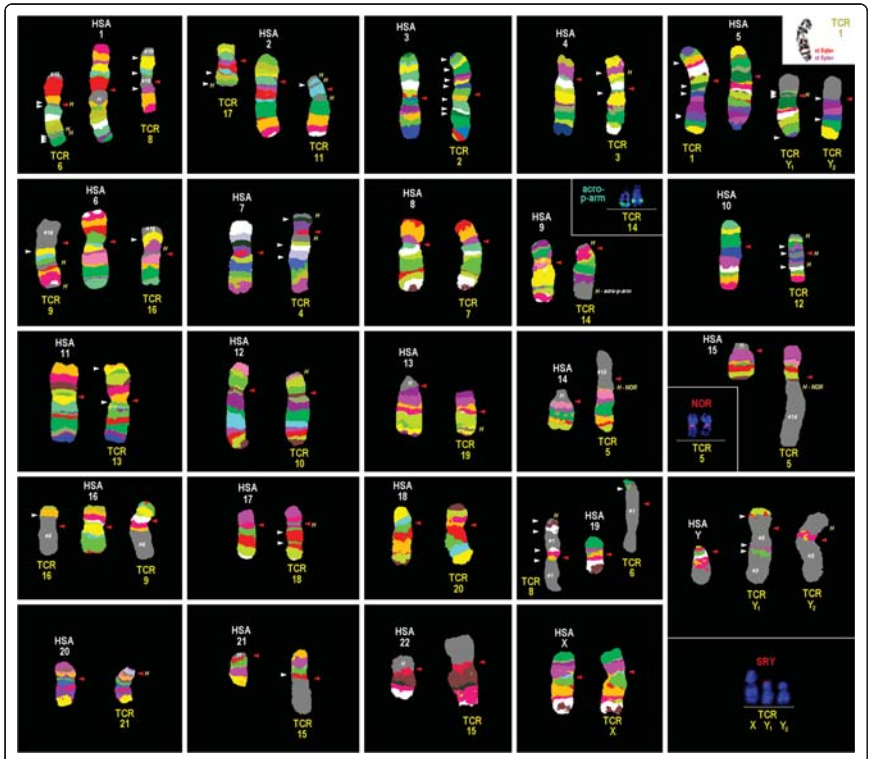

Figure 1 Representative results from this study using human MCB probes on TCR in comparison to HSA chromosomes are depicted as pseudo-colored results of HSA and TCR, at an ~250-band level. HSA chromosomes are numbered by white figures, TCR chromosomes by yellow figures. The chromosomes are sorted here according to the HSA-chromosomes. In subfigures for HSA 5, 9, 14 and Y there are additional FISH-results shown using probes as indicated. Red arrows stand for TCR centromeres and white arrows for HSA-centromeres. Abbreviations # = number of a human chromosome – region not stained by MCB probe; acro-p-arm = probe for all acrocentric short arms in HSA; H = heterochromatin, HSA = *Homo sapiens*; NOR = HSA specific FISH-probe for nucleolus organizing region; st = subtelomere; SRY = HSA specific FISH-probe for sex determining region Y; TCR = *Trachypithecus cristatus*.

Table 1 Homologous regions, centromere position and heterochromatic inserts observed in this study of TCR compared to HSA chromosomes

TCR chromosome	Homologous HSA-regions (for rearrangements see Table 2)	Centromere position	Heterochromatic inserts in
TCR 1	HSA 5pter-5qter	like in HSA 5	n.d.i.t.s.
TCR 2	HSA 3pter-3qter	HSA 3q26	n.d.i.t.s.
TCR 3	HSA 4pter-4qter	like in HSA 4	n.d.i.t.s.
TCR 4	HSA 7pter-7qter	like in HSA 7	- end of HSA 7p
			- 7q11.1
TCR 5	HSA 15q11.2-15qter, HSA 14q11.2-14qter	HSA 15q26.1 ~ 26.2	- fus HSA 14q11.2 / 15q26.3
TCR 6	HSA 1p22-1qter, HSA 19pter-19p13.2	fus HSA 1q22 / 1p14	- fus HSA 1q22 / 1q41;
			- fus HSA 1q41 / 1p22;
			- 1q24
TCR 7	HSA 8pter-8qter	like in HSA 8	n.d.i.t.s.
TCR 8	HSA 1pter-1p22, HSA 19p13.2-19qter	like in HSA 19	- end of HSA 19q
TCR 9	HSA 6pter-6q15, HSA 16p13.1-16qter	like in HSA 16	- end of HSA 6p;
			- 6p21
TCR 10	HSA 12pter-12qter	like in HSA 12	- end of HSA 12p
TCR 11	HSA 2q14.1-2qter	HSA 2q24.2	- distal from HSA 2q14.1;
			- 2q21;
			- 2q31
TCR 12	HSA 10pter-10qter	like in HSA 10	- end of HSA 10p;
			- fus HSA 10q21.1 / 10q22.3
			- HSA 10p11.1
			- HSA 10q11.1
TCR 13	HSA 11pter-11qter	HSA 11p15.3	n.d.i.t.s.
TCR 14	HSA 9pter-9qter	HSA 9q33 ~ 34.1	- end of HSA 9q
			- end of HSA 9p
TCR 15	HSA 21q11.2-21qter, HSA 22q11.21-22qter	fus 21q11.2 / 22q11.21	n.d.i.t.s.
TCR 16	HSA 6q15-6qter, 16pter-16p13.1	HSA 6q21	- HSA 6q21
TCR 17	HSA 2pter-2q14.1	like in HSA 2	- end of HSA 2p
TCR 18	HSA 17pter-17qter	like in HSA 17	- HSA 17p11.1
TCR 19	HSA 13q12.1-13qter	HSA 13q14	- HSA 13q32 ~ 33
TCR 20	HSA 18pter-18qter	HSA 18q21	n.d.i.t.s.
TCR 21	HSA 20pter-20qter	HSA 20p12	- HSA 20p11.1
			- HSA 20q11.1
TCR X	HSA Xpter-Xqter	like in HSA X	n.d.i.t.s.
TCR Y_1	HSA 5p12-5q31.2, HSA Ypter-Yp11.2	like in HSA 5	- HSA 5p11
			- HSA 5q11.1
TCR Y_2	HSA 5pter-5p12, HSA 5q31.2-5qter,HSA Yp11.2-Yq11.23	like in HSA Y	- distal from HSA Yp11.23

Abbreviations: fus = fusion of; n.d.i.t.s. = none detected in this study.

positions were the same as in HSA: TCR 1 (= HSA 5), TCR 3 (= HSA 4), TCR 4 (= HSA 7), TCR 7 (= HSA 8), TCR 8 (= HSA 19), TCR 9 (= HSA 16), TCR 10 (= HSA 12), TCR 12 (= HSA 10), TCR 17 (= HSA 2), TCR 18 (= HSA 17), TCR X (= HSA X), TCR Y1 (= HSA 5), and TCR Y2 (= HSA Y). Centromere positions changed compared to HSA in TCR 2 (HSA 3q26), TCR 5 (HSA 15q26.1 ~ 26.2), TCR 6 (HSA 1q22/ 1p14), TCR 11 (HSA 2q24.2), TCR 13 (HSA 11p15.3), TCR 14 (HSA 9q33 ~ 34.1), TCR 15 (HSA 21q11.2/ 22q11.2), TCR 6 (HSA 6q21), TCR 19 (HSA 13q14), TCR 20 (HSA 18q21) and TCR 21 (HSA 20p12).

None of the aforementioned TCR centromeric regions that kept their position during evolution compared to

Table 2 Evolutionary conserved breakpoints in TCR chromosomes compared to HSA; the positions are analyzed concerning their location in GTG-light bands, colocalization with human fragile sites and breakpoints observed in HLA and GGO using MCB-approach

HSA chr.	Evolutionary conserved breakpoints including neo-centromere and heterochromatin positions	GTG- light band	Fragile site in same band	Same breakpoint in HLA [Mrasek et al., 2003 [13]]	Same breakpoint in GGO [Mrasek et al., 2001 [12]]
1	1p22	+	FRA1D	-	-
	1q22	-	-	-	-
	1q24	-	-	+	-
	1q41	-	FRA1R	-	-
2	2p25.3	-	FRA2M	-	-
	2q14.1	-	FRA2	-	+
	2q21	+	FRA2F	-	?+
	2q24.2	+	FRA2T	+	-
	2q31	+	FRA2G	-	-
3	3p26.3	-	FRA3E	-	-
	3p25	+	FRA3F	-	-
	3p23	+	-	-	-
	3p21.3	+	FRA3H	?+	-
	3p14	-	FRA3B	?+	-
	3q22	-	FRA3N	?+	-
	3q25	+	FRA3D	+	-
	3q26	-	FRA3O	-	-
	3q28	-	FRA3P	-	-
4	4p12	+	FRA4H	-	+
	4q22	-	FRA4F	-	-
5	5p15.2	-	FRA5H	-	-
	5q11.2	+	FRA5I	?+	-
	5q21	-	FRA5F	-	-
	5q31.2	-	FRA5C	-	-
	5q35.3 (a)	+	FRA5G	-	+
	5q35.3 (b)	+	FRA5G	-	+
6	6p25.3	+	-	-	-
	6p21	+	FRA6H	-	-
	6q15	+	FRA6G	+	-
	6q21	+	FRA6F	-	-
7	7p22.3	+	FRA7B	+	-
	7p15.3	+	-	-	-
	7q11.1	-	FRA7A	-	-
	7q11.23	+	FRA7J	-	+
9	9p34.2	-	-	-	-
	9q24.3	+	-	-	-
	9q33 ~ 34.1	-	FRA9M	-	-
10	10p15.3	+	FRA10H	-	-
	10p11.2	+	FRA10J	-	?+
	10p11.1	-	-	-	-
	10q11.1	-	FRA10G	-	-
	10q21.1	-	FRA10C	+	-

Table 2 Evolutionary conserved breakpoints in TCR chromosomes compared to HSA; the positions are analyzed concerning their location in GTG-light bands, colocalization with human fragile sites and breakpoints observed in HLA and GGO using MCB-approach *(Continued)*

	10q22.3	+	FRA10D	?+	+
11	11p15.4	-	-	-	-
	11p15.3	+	FRA11J	-	-
	11q12	-	-	+	-
12	12p13.33	+	FRA12F	-	-
13	13q12.1	+	-	-	-
	13q14	+	FRA13G	?+	-
	13q32 ~ 33	+	FRA13D	+	-
14	14q11.2	+	FRA14D	?+	+
15	15q11.2	+	FRA15C	?+	-
	15q26.1 ~ 26.2	+	FRA15G	?+	-
16	16p13.1	+	FRA16H	+	-
17	17p11.1	-	FRA17C	?+	-
	17q21.3	+	FRA17D	?+	-
	17q24	-	FRA17E	+	-
18	18q21	+	FRA18B	-	-
19	19p13.2	-	-	?+	-
	19q13.2	-	-	+	-
	19q13.43	-	-	?+	-
20	20p12	-	FRA20B	-	-
	20p11.1	-	-	-	-
	20q11.1	-	FRA20D	-	-
21	21q11.2	+	FRA21	?+	-
22	22q11.21	+	-	?+	-
Y	Yp11.31	-	-	-	-
	Yp11.2	+	-	-	-
	Yq11.23	+	-	-	-

Abbreviations: - = no; + = yes; ?+ = most likely yes; a and b in 5q35.3 = break within subtelomere region.

human showed positive FISH-signals with any of the used HSA centromere specific probes (data not shown). Also, none of the other human heterochromatin specific probes from HCM probe set gave any specific signals in TCR, with 2 exceptions: NOR-specific signals were observed in TCR 5 (at fusion of HSA 14q11.2 and 15q26.3) (Figure 1) and the probes midi54 (Figure 1) and midi 36 (data not shown); the latter two located on the distal end of the long arm of TCR 14.

In the literature there were 81 TCR specific heterochromatic insertions and/ or additions to chromosomes reported (Figure 2). In this study only 25 of them were confirmed and mapped (Figure 2 and Table 1, last column).

Table 2 summarizes the 69 evolutionary conserved breakpoints observed in TCR in this study; they are given according to the homologous regions in HSA. Only HSA chromosomes X (TCR X) and 8 (TCR 7) are completely unaltered during evolution from a common ancestor of HSA and TCR. All other homologous of TCR chromosomes have undergone one (HSA 12, 14, 16, 18, 21 and 22), two (HSA 4 and 15), three (HSA Y, 11, 13, 17, 19, and 20), four (HSA 1 and 6), five (HSA 2), six (HSA 5, and 10), or nine (HSA 3) evolutionary conserved break events during speciation in respect to the human karyotype.

Besides, the characterized breakpoints of TCR are compared with such previously mapped in *Hylobates lar* (HLA) and *Gorilla gorilla* (GGO) using MCB approach (Table 2). Again, an alignment of the breakpoint and their positioning in GTG-light bands and their spatial proximity to human fragile sites was done.

Discussion

The present study represents the first one that comprehensively characterizes the karyotype of TCR. In general,

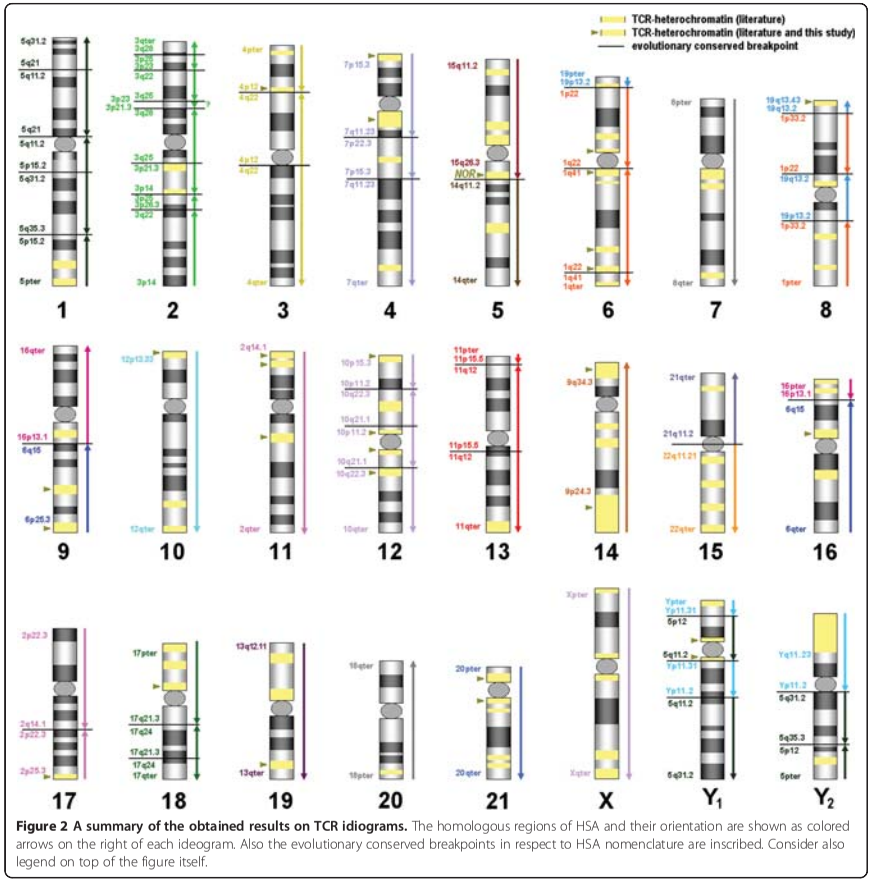

Figure 2 A summary of the obtained results on TCR idiograms. The homologous regions of HSA and their orientation are shown as colored arrows on the right of each ideogram. Also the evolutionary conserved breakpoints in respect to HSA nomenclature are inscribed. Consider also legend on top of the figure itself.

previous homologies of HSA and TCR chromosomes could be confirmed [10]. However, in this study, homologous regions for TCR chromosomes 4, 10, 11, 14, 17, 18 and 21 (that were not studied before) [10] were specifically aligned to their HSA-homologous. In contrast to [10] NOR was mapped here to the fusion points of HSA 14 and HSA 15, i.e. TCR 5 and not TCR 15. In our two studied individuals derived from Thailand, no differences in TCR 1 banding pattern were seen, which is in accordance with the literature [10].

For the first time, the exact breakpoints could be determined for the extremely rearranged karyotype of TCR, in comparison to HSA. In fact, 69 evolutionary conserved breakpoints were determined in a male TCR and confirmed in a female individual, excluding Y_1 and Y_2 chromosomes, obviously.

In this study no special attention was given to the centromeric regions of TCR, i.e. they were not detailed characterized as in other studies e.g. by [15] or [16]. However, a first impression is provided in which centromeres kept their positions during evolution from common ancestors to HSA and TCR and were neo-centromeres (Table 1), i.e. ~50% of them stayed at the same positions and ~50% moved either in one of the two species or in

both. As expected from the literature [17], even the centromeric regions that kept their positions did not have the identical alphoid sequences in HSA and TCR.

Previous studies in human chromosomal rearrangements revealed that the majority of them (70-88%) are found in G-light sub-bands [18]. In contrast only 37 (45.5%) of the 69 evolutionary conserved breakpoints of TCR were located in GTG-light bands (Table 2). However, 70% of the here observed TCR breakpoints colocalized with human fragile sites [19] supporting their potential role in the "Fragile Breakage Model" [20] and in the formation of evolutionary chromosomal rearrangements [21-26] (Table 2).

Concerning evolution it is interesting to report that in TCR and in HLA 11 evolutionary conserved breakpoints are identical and 15 more are most likely in concordance to each other. Even more interesting, 6 identical and 2 most likely identical evolutionary conserved breakpoints were identified in TCR and in GGO (Table 2). These findings need to be confirmed in further studies by locus-specific probes, and if confirmed, they will be very useful for the reconstruction of a common ancestral karyotype. Compared to the postulated Hominidea ancestral karyotype proposed by [25], only four chromosomes remained unchanged in TCR, i.e. chromosomes 4, 7, 11 and X, eleven chromosomes underwent only intrachromosomal changes like inversions (TCR 2, 3, 10, 12, 13, 14, 17, 18, 19, 20, 21) and two TCR chromosomes resulted from a fusion of ancestral chromosomes (TCR 5 and 15).

Interestingly, the regions between TCR 1 and TCR Y_1 and TCR Y_2 being homologous to HSA 5 were shown to be subject to different evolutionary conserved rearrangements. Broadly speaking, TCR Y1 is homologous to TCR 1p and TCR Y2 to TCR 1q. However, each arm of chromosome TCR 1 underwent a further paracentric inversion, most likely being important to separate the sex chromosomes from the chromosome 1 during meiosis. Thus, a XY_1Y_2 sex chromosome system is present in TCR, and not an $X_1X_2Y_1Y_2$ system as initially suggested [10]. However, as in TCR from Indonesia, two other forms of TCR 1 chromosome could be found [10]. Therefore, the existence of an $X_1X_2Y_1Y_2$ system cannot be completely excluded by this study.

The sex determination system in mammals is usually highly conserved as XY-system. However, multiple sex chromosome systems, like the one present in TCR and few other apes [27,28] are exceptionally found in some species of e.g. the orders Insectivora, Chiroptera, Artiodactyla, Rodentia [29], and in marsupials [30]. In general, constitutional Y-chromosome / autosome translocations in human appear de novo and have a deleterious effect and, although the infertility is the only common feature, other clinical symptoms can also be observed depending on the involved breakpoints [31]. In such cases, the infertility is thought to be a result of disruption of the sex vesicle during meiosis [32]. From this point of view it is hard to imagine conditions which are in favor of developing a multiple sex- from an XY-chromosome system. On the other hand, in population genetic models of Y-autosome and X-autosome rearrangements the population can gain a selective advantage under a wide range of conditions. If they can invade the population, Y-autosome rearrangements always spread to fixation, whereas X-autosome rearrangements may be maintained as stable polymorphisms" [33]. The XY_1Y_2 sex chromosome system observed in TCR fits well into the suggestions of [34] that (i) female meiotic drive is the major contribution to the evolution of neo-sex chromosomes and (ii) that "in mammals, the XY_1Y_2 sex chromosome system is more prevalent in species with karyotypes of more biarmed chromosomes" rather than in species with acrocentric chromosomes. Research on meiotic behavior of such sex systems is scarce; however, one study on Bolivian owl monkey (*Aotus spec.*) showed that no XY pairing was observable but the Y-chromosomes formed trivalents with an autosome during gametogenesis [27].

Conclusions

In conclusion, the presented comparative map of TCR karyotype gives new insights into primate evolution and can be used as a starting point for further detailed analyses. Evolutionary conserved breakpoints, TCR-specific heterochromatic regions, centromeric sequences as well as the sex chromosome system can be fruitful fields of research in near future.

Methods

Cell culture and chromosomal preparation

Immortalized lymphoblast cell lines derived from a male and female TCR, were provided by the Khon Kaen University, Thailand. Culture techniques and chromosome preparation followed standard protocols.

Fluorescence in situ hybridization

General considerations for MCB labeling schemes and details regarding probe preparation and labeling have been described before [12,35,36]. Single and dual-color FISH techniques were performed for the applied bacterial artificial chromosome (BAC-) probes [37]. Locus-specific BAC clones were purchased at BAC/PAC Chori and DNA was isolated, PCR-amplified and labeled as described before [37]; and probes RP11-475I16 and RP11-395 L14 (both in 2q14.1), RP11-110A24 (in 19p13.3), RP-11457 M7 (in Yp11.2) and RP11-122 L9 (in Yp11.31) were applied in this study. Besides, commercially available human derived probes for the SRY gene on the Y-chromosome, HSA probes for subtelomeric regions 3pter, 3qter, 5pter, 5qter, 6pter, 6qter, 7pter, 7qter, 9pter, 9qter, 10pter, 10qter, 18pter, 18qter, 19pter, 19qter, XYpter and XYqter, and centromeric probes cep 2, cep4, cep 7, cep 8, cep 10, cep 12, cep 16, cep 17, cep X cep Y (Abbott/ Vysis, Wiesbaden, Germany) and SE 1/5/19, SE 13/21 and SE 14/22 (Kreatech, Amsterdam, The Netherlands) were also applied.

Additionally, the following homemade HSA derived microdissection probes were used: a probe specific for the short arm of all human acrocentric chromosomes (midi54) [12,13], and partial chromosome paints for 3p, 3q, 5p, 5q, 6p, 6q, 7p, 7q, 9p, 9q, 10p, 10q, 18p, 18q, 19p, 19q, Yp and Yq [35]. Furthermore, the heterochromatin mix (HCM-) probe set [38] covering chromosomal regions 1q12, 16q11.2, 9q12, 9p12/ 9q13 (midi36) 15p11.2-p11.1, 19p12/q12 and Yq12 and subcentromere specific multicolor FISH (subcen-FISH) for chromosomes 3, 6, 7, 9, 11, 13 and 20 were also applied [36].

Microscopic evaluation

Images were captured using an Axioplan II microscope (Carl Zeiss Jena GmbH, Germany) equipped with filter sets for DAPI, FITC, TR, SO, Cy5 and DEAC. Image analysis was done using pseudocolor banding and fluorochrome profiles of the ISIS digital FISH imaging system (Meta Systems Hard & Software GmbH, Altlussheim, Germany). At least 10 up to 20 metaphases were recorded, derived from a male and a female TCR for each applied probe and probe set.

Competing interests

Authors declare that there is no conflict of interest.

Authors' contributions

XF carried out molecular cytogenetic studies and the draft of the manuscript, KP carried out the molecular cytogenetic studies, HM carried out the molecular cytogenetic studies, PS carried out the molecular cytogenetic studies, NK carried out the molecular cytogenetic studies, WS carried out the cell culture, AT carried out the cell culture, AC carried out the cell culture and participated in manuscript discussion, TL participated in the design of the study and the manuscript, MBC participated in the design of the study and the manuscript discussion, AW participated in the design and coordinated the study and the manuscript. All authors read and approved the final manuscript.

Acknowledgments

This work was supported by the China Scholarship Council.

Author details

[1]Institute of Human Genetics, Jena University Hospital, Friedrich Schiller University, Kollegiengasse 10, Jena D-07743, Germany. [2]Faculty of Science and Technology, Surindra Rajabhat University, 186 Moo 1, Surin, Maung District 32000, Thailand. [3]Center of Medical Genetics and Primary Health Care, Abovyan Str 34/3, 001, Yerevan, Armenia. [4]Faculty of Science and Technology, Rajabhat Maha Sarakham University, 80 Nakonsawan Rd, Maha Sarakham, Talad, Maung District 44000, Thailand. [5]Department of Biology, Faculty of Science, Khon Kaen University, 123 Moo 16 Mittapap Rd., Khon Kaen, Muang District 40002, Thailand. [6]Departamento de Genética e Evolução, Universidade Federal de São Carlos, São Carlos, SP, Brazil. [7]Institut für Humangenetik, Postfach, Jena D-07740, Germany.

Received: 15 November 2013 Accepted: 21 November 2013
Published: 17 December 2013

References

1. Raffles TS: **Descriptive catalogue of a zoological collection, made on account of the Honourable East India Company, in the island of Sumatra and its vicinity, under the direction of Sir Thomas Stanford Raffles, Lieutenant-Governor of Fort Marlborough: with additional notices of the natural history of those countries.** *Transact Linn Soc London* 1821, **13**:239–274.
2. Harding LE: **Trachypithecus cristatus (Primates: Cercopithecidae).** *Mamm Species* 2010, **42**:149–165.
3. Fooden J: **Primates obtained in peninsular Thailand June–July, 1973, with notes on the distribution of continental Southeast Asian leaf- monkeys (Presbytis).** *Primates* 1976, **17**:95–118.
4. Roos C, Nadler T, Walter L: **Mitochondrial phylogeny, taxonomy and biogeography of the silvered langur species group (Trachypithecus cristatus).** *Mol Phylogenet Evol* 2008, **47**:629–636.
5. Hsu TC, Benirschke K: In *An atlas of mammalian chromosomes.* Edited by Hsu TC, Benirschke K. NewYork: Springer-Verlag, Folio 199; 1970.
6. Dutrillaux B, Couturier J, Muleris M, Lombard M, Chauvier G: **Chromosomal phylogeny of forty-two species or subspecies of cercopithecoids (Primates Catarrhini).** *Ann Genet* 1982, **25**:96–109.
7. Ponsa M, de Boer LEM, Egozcue J: **Banding patterns of the chromosomes of Presbytis cristatus pyrrhus and P. obscurus.** *Am J Primatol* 1983, **4**:165–169.
8. Muleris M, Couturier J, Dutrillaux B: **Phylogénie chromosomique des Cercopithecoidea.** *Mammalia* 1986, **50**:38–52.
9. Dutrillaux B, Webb G, Muleris M, Couturier J, Butler R: **Chromosome study of Presbytis cristatus: presence of a complex Y-autosome rearrangement in the male.** *Ann Genet* 1984, **27**:148–153.
10. Bigoni F, Koehler U, Stanyon R, Ishida T, Wienberg J: **Fluorescene in situ hybridization establishes homology between human and silvered leaf monkey chromosomes, reveals reciprocal translocations between chromosomes homologous to human Y/5, 1/9, and 6/16, and delineates an X1X2Y1Y2/X1X1X2X2 sex-chromosome system.** *Am J Phys Anthropol* 1997, **102**:315–327.
11. Graphodatsky AS, Trifonov VA, Stanyon R: **The genome diversity and karyotype evolution of mammals.** *Mol Cytogenet* 2011, **4**:22.
12. Mrasek K, Heller A, Rubtsov N, Trifonov V, Starke H, Rocchi M, Claussen U, Liehr T: **Reconstruction of the female Gorilla gorilla karyotype using 25-color FISH and multicolor banding (MCB).** *Cytogenet Cell Genet* 2001, **93**:242–248.
13. Mrasek K, Heller A, Rubtsov N, Trifonov V, Starke H, Claussen U, Liehr T: **Detailed Hylobates lar karyotype defined by 25-color FISH and multicolor banding.** *Int J Mol Med* 2003, **12**:139–146.
14. Weise A, Heller A, Starke H, Mrasek K, Kuechler A, Pool-Zobel BL, Claussen U, Liehr T: **Multitude multicolor chromosome banding (mMCB) - a comprehensive one-step multicolor FISH banding method.** *Cytogenet Genome Res* 2003, **103**:34–39.
15. Stanyon R, Rocchi M, Capozzi O, Roberto R, Misceo D, Ventura M, Cardone MF, Bigoni F, Archidiacono N: **Primate chromosome evolution: ancestral karyotypes, marker order and neocentromeres.** *Chromosome Res* 2008, **16**:17–39.
16. Ventura M, Antonacci F, Cardone MF, Stanyon R, D'Addabbo P, Cellamare A, Sprague LJ, Eichler EE, Archidiacono N, Rocchi M: **Evolutionary formation of new centromeres in macaque.** *Science* 2007, **316**:243–246.
17. Rocchi M, Archidiacono N, Schempp W, Capozzi O, Stanyon R: **Centromere repositioning in mammals.** *Heredity* 2012, **108**:59–67.
18. Manvelyan M, Schreyer I, Höls-Herpertz I, Köhler S, Niemann R, Hehr U, Belitz B, Bartels I, Götz J, Huhle D, Kossakiewicz M, Tittelbach H, Neubauer S, Polityko A, Mazauric ML, Wegner R, Stumm M, Küpferling P, Süss F, Kunze H, Weise A, Liehr T, Mrasek K: **Forty-eight new cases with infertility due to balanced chromosomal rearrangements: detailed molecular cytogenetic analysis of the 90 involved breakpoints.** *Int J Mol Med* 2007, **19**:855–864.
19. Mrasek K, Schoder C, Teichmann AC, Behr K, Franze B, Wilhelm K, Blaurock N, Claussen U, Liehr T, Weise A: **Global screening and extended nomenclature for 230 aphidicolin-inducible fragile sites, including 61 yet unreported ones.** *Int J Oncol* 2010, **36**:929–940.
20. Pevzner P, Tesler G: **Human and mouse genomic sequences reveal extensive breakpoint reuse in mammalian evolution.** *Proc Natl Acad Sci U S A* 2003, **100**:7672–7677.
21. Bailey JA, Baertsch R, Kent WJ, Haussler D, Eichler EE: **Hotspots of mammalian chromosomal evolution.** *Genome Biol* 2004, **5**:R23.
22. Murphy WJ, Larkin DM, Everts-van der Wind A, Bourque G, Tesler G, Auvil L, Beever JE, Chowdhary BP, Galibert F, Gatzke L, Hitte C, Meyers SN, Milan D, Ostrander EA, Pape G, Parker HG, Raudsepp T, Rogatcheva MB, Schook LB, Skow LC, Welge M, Womack JE, O'brien SJ, Pevzner PA, Lewin HA:

Dynamics of mammalian chromosome evolution inferred from multispecies comparative maps. *Science* 2005, **309**:613–617.
23. Ruiz-Herrera A, Castresana J, Robinson TJ: **Is mammalian chromosomal evolution driven by regions of genome fragility?** *Genome Biol* 2006, **7**:R115.
24. Ruiz-Herrera A, Robinson TJ: **Chromosomal instability in Afrotheria: fragile sites, evolutionary breakpoints and phylogenetic inference from genome sequence assemblies.** *BMC Evol Biol* 2007, **7**:199.
25. Misceo D, Capozzi O, Roberto R, Dell'oglio MP, Rocchi M, Stanyon R, Archidiacono N: **Tracking the complex flow of chromosome rearrangements from the Hominoidea Ancestor to extant Hylobates and Nomascus Gibbons by high-resolution synteny mapping.** *Genome Res* 2008, **18**:1530–1537.
26. Alekseyev MA, Pevzner PA: **Comparative genomics reveals birth and death of fragile regions in mammalian evolution.** *Genome Biol* 2010, **11**:R117.
27. Ma NS, Elliott MW, Morgan L, Miller A, Jones TC: **Translocation of Y chromosome to an autosome in the Bolivian owl monkey, Aotus.** *Am J Phys Anthropol* 1976, **45**:191–202.
28. Solari AJ, Rahn MI: **Fine structure and meiotic behaviour of the male multiple sex chromosomes in the genus Alouatta.** *Cytogenet Genome Res* 2005, **108**:262–267.
29. Fredga K: **Unusual sex chromosome inheritance in mammals.** *Philos Trans R Soc Lond B Biol Sci* 1970, **259**:15–36.
30. Toder R, O'Neill RJ, Wienberg J, O'Brien PC, Voullaire L, Marshall-Graves JA: **Comparative chromosome painting between two marsupials: origins of an XX/XY1Y2 sex chromosome system.** *Mamm Genome* 1997, **8**:418–422.
31. Conte RA, Kleyman SM, Klein V, Bialer MG, Verma RS: **Characterization of a de novo t(Y;9) (q11.2;q22) by FISH technique.** *Ann Genet* 1996, **39**:10–15.
32. Pinho MJ, Neves R, Costa P, Ferrás C, Sousa M, Alves C, Almeida C, Fernandes S, Silva J, Ferrás L, Barros A: **Unique t(Y;1)(q12;q12) reciprocal translocation with loss of the heterochromatic region of chromosome 1 in a male with azoospermia due to meiotic arrest: a case report.** *Hum Reprod* 2005, **20**:689–696.
33. Charlesworth B, Wall JD: **Inbreeding, heterozygote advantage and the evolution of neo-X and neo-Y sex chromosomes.** *Proceedings: Biological Sciences* 1999, **266**:51–56.
34. Yoshida K, Kitano J: **The contribution of female meiotic drive to the evolution of neo-sex chromosomes.** *Evolution* 2012, **66**:3198–3208.
35. Liehr T, Claussen U: **Current developments in human molecular cytogenetic techniques.** *Curr Mol Med* 2002, **2**:283–297.
36. Weise A, Mrasek K, Fickelscher I, Claussen U, Cheung SW, Cai WW, Liehr T, Kosyakova N: **Molecular definition of high-resolution multicolor banding probes: first within the human DNA sequence anchored FISH banding probe set.** *J Histochem Cytochem* 2008, **56**:487–493.
37. Liehr T, Heller A, Starke H, Rubtsov N, Trifonov V, Mrasek K, Weise A, Kuechler A, Claussen U: **Microdissection based high resolution multicolor banding for all 24 human chromosomes.** *Int J Mol Med* 2002, **9**:335–339.
38. Bucksch M, Ziegler M, Kosayakova N, Mulatinho MV, Llerena JC Jr, Morlot S, Fischer W, Polityko AD, Kulpanovich AI, Petersen MB, Belitz B, Trifonov V, Weise A, Liehr T, Hamid AB: **A new multicolor fluorescence in situ hybridization probe set directed against human heterochromatin: HCM-FISH.** *J Histochem Cytochem* 2012, **60**:530–536.

doi:10.1186/1755-8166-6-58
Cite this article as: Xiaobo *et al.*: First detailed reconstruction of the karyotype of Trachypithecus cristatus (Mammalia: Cercopithecidae). *Molecular Cytogenetics* 2013 **6**:58.

2.3 Article No. 3

X Fan, W Sangpakdee, A Tanomtong, A Chaveerach, K Pinthong, S Pornnarong, W Supiwong, VA Trifonov, GG Hovhannisyan, RM Aroutouinian, T Liehr, A Weise. 2014. **Molecular cytogenetic analysis of Thai southern pig-tailed macaque (*Macaca nemestrina*) by multicolor banding**. Proceedings of Yerevan State University, 2014:46-50.

Abstract: In previous studies origin of human and ape chromosomes have been analyzed by comparative chromosome banding analysis and/or by fluorescence in situ hybridization (FISH). In the present study FISH-banding, i.e. multicolor banding using probes derived from *Homo sapiens* was applied to reanalyze the chromosomes of Thai southern pig-tailed macaque (*Macaca nemestrina*). The results agreed with those of previous studies in other macaques, e.g. *Macaca sylvanus*. Thus, genetic differences leading to the observed large morphological differences within the Ceropithecoidae must be in the subchromosomal or even epigenetic level and have to be discovered yet.

PROCEEDINGS OF THE YEREVAN STATE UNIVERSITY

Chemistry and Biology 2014, № 1, p. 46–50

Biology

MOLECULAR CYTOGENETIC ANALYSIS OF THAI SOUTHERN PIG-TAILED MACAQUE (*MACACA NEMESTRINA*) BY MULTICOLOR BANDING

X. FAN [1], W. SANGPAKDEE[2], A. TANOMTONG [2], A. CHAVEERACH [2], K. PINTHONG [1,2,3], S. PORNNARONG [1,2], W. SUPIWONG [1,2], V. A. TRIFONOV[1,4], G. G. HOVHANNISYAN [5], R. M. AROUTIOUNIAN [*5], T. LIEHR [**1], A. WEISE [1]

[1] *Jena University Hospital, Friedrich Schiller University, Institute of Human Genetics, Germany*
[2] *Department of Biology Faculty of Science, Khon Kaen University, Thailand*
[3] *Faculty of Science and Technology, Surindra Rajabhat University, Thailand*
[4] *Institute of Molecular and Cellular Biology, Russia*
[5] *Chair of Genetics and Cytology YSU, Armenia*

In previous studies origin of human and ape chromosomes have been analyzed by comparative chromosome banding analysis and/or by fluorescence *in situ* hybridization (FISH). In the present study FISH-banding, i.e. multicolor banding using probes derived from *Homo sapiens* was applied to reanalyze the chromosomes of Thai southern pig-tailed macaque (*Macaca nemestrina*). The results agree with those of previous studies in other macaques, e.g. *Macaca sylvanus*. Thus, genetic differences leading to the observed large morphological differences within the *Ceropithecoidae* must be in the subchromosomal or even epigenetic level and have to be discovered yet.

Keywords: FISH analysis, pig-tailed macaque, multicolor banding.

Introduction. Since the early 1980s the idea is pursued that cytogenetic studies in ape species could provide substantial contributions to better understandding of evolutionary history of primate and human phylogeny [1, 2]. After introduction of molecular cytogenetics, especially multicolor-fluorescence *in situ* hybridization (FISH), FISH studies using whole chromosome painting probes and FISH-banding approaches [3] were yet applied. However, the latter was not used systematically to study the question of karyotype evolution in primates; only occasionally studies were performed [4–6]. The most common applied FISH-banding approach is the so-called multicolor banding (MCB), which in contrast to other FISH-banding techniques is anchored in the human DNA-sequence [7]. MCB was already successfully applied for characterization and comparative molecular cytogenetic mapping of the following primate species before: *Gorilla gorilla* [8],

[*] E-mail: genetik@ysu.am [**] E-mail: Thomas.Liehr@med.uni-jena.de

Hylobates lar [9], *Trachypithecus cristatus* and *Macaca sylvanus* (MSN) [10]. Recently, next generation sequencing was also introduced to answer the question: what are the differences between the species. Interestingly, basic cytogenetic data are needed essentially for exact alignment of these new complex datasets [11].

Here we present the first MCB-based study for characterization of the Thai southern pig-tailed macaque (*Macaca nemestrina,* MNE). Macaques (*Catarrhini*, *Ceropithecoidae*, *Cercopithecinae*, *Papionini*) underwent a radiation in Pliocene or Pleistocene, i.e. during the last 3–5 million years [12]. Macaques can be found from Western Africa to far Eastern Asia presenting in many morphologically diverse species. Surprisingly, on the chromosomal level this group is kept absolutely constant: 42 chromosomes with no differences on the cytogenetic level [13]. This is also underlined by the fact that different macaque species can form hybrids, even fertile ones, easily [14].

MSN was studied before by banding cytogenetics [13] and FISH using a low resolution FISH-banding approach [5]. Here we provide the first MCB-based FISH-banding study in MSN.

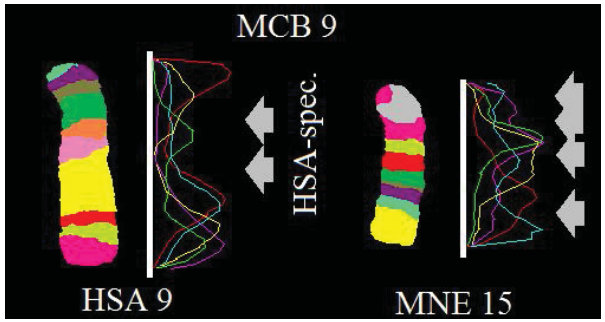

Representative example for MCB-result obtained in MNE. Result of MCB 9 probe set applied on a human chromosome 9 (HSA) compared to the result obtained on homologous MNE chromosome 15. For each chromosome pseudocolor depiction and underlying fluorochrome profiles are shown. The human chromosome has HSA specific amplification in 9q12 (arrows). The MNE chromosome 15 has compared to HAS insertion of an unknown DNA in 9q34 (gray) and several rearrangements (arrows) – see Table.

Material and Methods. Peripheral blood of MSN (1 male) was acquired in Thailand. Blood lymphocytes from heparinzed blood were subjected to short term culture and cytogenetic work-up using standard procedures.

24 MCB probes derived from human chromosomes *Homo sapiens* (HSA) were applied in 24 independent FISH-experiments in MSN-chromosome-preparations as previously was reported [8]. Evolutionary conserved chromosomal breakpoints were characterized with respect to the human chromosome complement (see Table).

Results and Discussion. In comparison with human karyotype the present MCB study was revealed in MSN 43 evolutionary break-events (see Table). The nomenclature of macaque chromosomes used here was adapted from [2]. As there

are different nomenclatures around these points have to be stressed – e.g. MSN chromosomes 12 and 13 have the designations 9 and 15 elsewhere [15]. Here reported breakpoints were identical to those known from other macaque species, living in Western Africa, while MSN is situated thousands of kilometers away from Thailand [10, 16] (see Table).

Less surprisingly HSA amplifications present in 1q12, 9q12, 16q11.2 and Yq12 were not present in MSN of the corresponding regions (see Fig.). On the other hand, species of specific amplifications of unknown genetic material was present in MSN in regions homologous to HSA 9q34, 17p10 and 17q24. For the latter 17q24 complex regions of segmental duplication were reported [17]. Also species of specific amplifications are suggested to play a major role in speciation [8].

Breakpoints of MNE according to MCB (Abbreviations: cen = centromeric position)

MSN	MSN chromosomes given as derivatives of human chromosomes	cen
1	inv(1) (q23.3q42.13), dim(1) (q12)	1q42.13
2	der(3) (qter−>q27.3::p22.3−>p24::q22.1−>q27.3::p22.3−> −>p12.3::p26.3 −>p24::q22.1−>p12.3:)	3q26.1
3	der(7) (21qter−>21q11.2::7p22.3−>7p22.1::7q21.3−> −> 7q22.1::7q11.23 −>7p21.3::7p21.3−>7q11.23::7q22.1−>7qter)	like HSA 7
4	inv(6) (p24q25.2) and inv(6) (q21q25.2)	6q24.3
5	inv(4) (p15.3q10)	like HSA 4
6	no change to HSA 5	like HSA 5
7	der(15)t(14; 15) (q11.2; q26.3)	15q25
8	no change to HSA 8	like HSA 8
9	inv(10) (q11.23q22.3)	like HSA 10
10	der(20) (22qter−>22p13::20p11.21−>20p13::20q11.21−>20qter)	like HSA 22
11	no change to HSA 12	like HSA 12
12	inv(2) (q14.1q21.1)	2q22.1
13	inv(2) (q11.1q14.1)	2p11.2
14	inv(11) (p15.4q13.4)	11p15.4
15	der(9) (9qter−>9q34::?::9q34−>9p24.3::9q21.11−>9q22.33:), dim(9)(q12)	9q33.2
16	der(17) (pter−>p10::?::p10−>q12::q23.3−>q21.32::q12−> −>q21.32::q23.3−>q24::?::q24−>qter)	like HSA 17
17	no change to HSA 13	13q21.31
18	no change to HSA 18	18q21.2
19	no change to HSA 19	like HSA 19
20	inv(16) (q22.1q22.3), dim(16) (q11.2)	like HSA 16
X	no change to HSA X	like HSA X
Y	del(Y) (q12q12)	like HSA Y

Centromeric regions in MSN 3, 5, 6, 8–11, 16, 19, 20, X and Y were identical to human centromeric positions (see Table). As the centromeric regions, even if being intraspecifically stable, do not contain identical alphoid DNA stretches [18] it is suggested that these chromosomal region evolve faster than other genomic regions. Centromere repositioning as discussed elsewhere [19] was observed for MSN 1, 2, 4, 7, 12–15, 17 and 18 (see Table).

Conclusion. Recently we studied *Macaca sylvanus* (MSY) [10] by MCB. Interestingly, neither at cytogenetic, nor at FISH-banding level differences between MSY and MNE were found. Altogether, the present study is confirmed in details for another macaque species and the general chromosomal composition cannot be the reason for specification in this genus.

Supported in parts by the China Scholarship Council (support for FX), a "Thai Government Science and Technology Scholarship" for KP, a "Strategic scholarship fellowships frontier research network for SP, the DLR/BMBF RUS 09/008 (AW) and 01DK13005 (TL).

Received 26.12.2013

REFERENCES

1. **Yunis J.J., Prakash O.** The Origin of Man: A Chromosomal Pictorial Legacy. // Science, 1982, v. 215, p. 1525–1530.
2. **Morescalchi A.M., Camperio C.A., Stanyon R.** Chromosome Banding and Molecular Cytogenetics of the *Barbary Macaque, Macaca Sylvanus*. // It. J. Zool., 1998, v. 65, p. 101–107.
3. **Liehr T., Starke H., Heller A., Kosyakova N., Mrasek K., Gross M., Karst C., Steinhaeuser U., Hunstig F., Fickelscher I., Kuechler A., Trifonov V., Romanenko S.A., Weise A.** Multicolor Fluorescence *in situ* Hybridization (FISH) Applied to FISH-Banding. // Cytogenet Genome Res., 2006, v. 114, p. 240–244.
4. **de Oliveira E.H., Neusser M., Figueiredo W.B., Nagamachi C., Pieczarka J.C., Sbalqueiro I.J., Wienberg J., Müller S.** The Phylogeny of Howler Monkeys (*Alouatta*, *Platyrrhini*): Reconstruction by Multicolor Cross-Species Chromosome Painting. // Chromosome Res., 2002, v. 10, p. 669–683.
5. **Müller S., Wienberg J.** "Bar-Coding" Primate Chromosomes: Molecular Cytogenetic Screening for the Ancestral Hominoid Karyotype. // Hum. Genet., 2001, v. 109, p. 85–94.
6. **Müller S., O'Brien P.C., Ferguson-Smith M.A., Wienberg J.** Cross-Species Colour Segmenting: a Novel Tool in Human Karyotype Analysis. // Cytometry, 1998, v. 33, p. 445–452.
7. **Weise A., Mrasek K., Fickelscher I., Claussen U., Cheung S.W., Cai W.W., Liehr T., Kosyakova N.** Molecular Definition of High-Resolution Multicolor Banding Pprobes: First Within the Human DNA Sequence Anchored FISH Banding Probe Set. // J. Histochem. Cytochem., 2008, v. 56, p. 487–493.
8. **Mrasek K., Heller A., Rubtsov N., Trifonov V., Starke H., Rocchi M., Claussen U., Liehr T.** Reconstruction of the Female Gorilla Karyotype Using 25-Color FISH and Multicolor Banding (MCB). // Cytogenet. Cell Genet., 2001, v. 93, p. 242–248.
9. **Mrasek K., Heller A., Rubtsov N., Trifonov V., Starke H., Claussen U., Liehr T.** Detailed Hylobates Lar Karyotype Defined by 25-Color FISH and Multicolor Banding. // Int. J. Mol. Med., 2013, v. 12, p. 139–146.
10. **Fan X., Pinthong K., Mkrtchyan H., Siripiyasing P., Kosyakova N., Supiwong W., Tanomtong A., Chaveerach A., Liehr T., de Bello Cioffi M., Weise A.** First Detailed Reconstruction of the Karyotype of *Trachypithecus Cristatus* (Mammalia : *Cercopithecidae*). // Mol. Cytogenet., 2013, v. 6, p. 58.
11. **Zhang X., Goodsell J., Norgren R.B.** Jr. Limitations of the Rhesus Macaque Draft Genome Assembly and Annotation. // BMC Genomics, 2012, v. 13, p. 206.
12. **Camperio C.A., Stanyon R., Scheffrahn W., Sampurno B.** Evidence of Gene Flow Between Sulawesi Macaques. // Am. J. Primatol., 1989, v. 17, p. 257–270.
13. **Brown C.J., Dunbar V.G., Shafer D.A.** A Comparison of the Karyotypes of Six Species of the Genus Macaca and a Species of the Genus Cercocebus. // Folia Primatol. (Basel), 1986, v. 46, p. 164–172.

14. **Moore C.M., Janish C., Eddy C.A., Hubbard G.B., Leland M.M., Rogers J.** Cytogenetic and Fertility Studies of a Rheboon, Rhesus Macaque (*Macaca Mulatta*) × Baboon (*Papio Hamadryas*) Cross: Further Support for a Single Karyotype Nomenclature. // Am. J. Phys. Anthropol., 1999, v. 110, p. 119–127.
15. **Ruiz-Herrera A., Ponsà M., García F., Egozcue J., García M.** Fragile Sites in Human and *Macaca Fascicularis* Chromosomes are Breakpoints in Chromosome Evolution. // Chromosome Res., 2002, v. 10, p. 33–44.
16. **Ventura M., Antonacci F., Cardone M.F., Stanyon R., D'Addabbo P., Cellamare A., Sprague L.J., Eichler E.E., Archidiacono N., Rocchi M.** Evolutionary Formation of New Centromeres in Macaque. // Science, 2007, v. 316, p. 243–246.
17. **Cardone M.F., Jiang Z., D'Addabbo P., Archidiacono N., Rocchi M., Eichler E.E., Ventura M.** Hominoid Chromosomal Rearrangements on 17q Map to Complex Regions of Segmental Duplication. // Genome Biol., 2008, v. 9, R28.
18. **Archidiacono N., Antonacci R., Marzella R., Finelli P., Lonoce A., Rocchi M.** Comparative Mapping of Human Alphoid Sequences in Great Apes Using Fluorescence *in situ* Hybridization. // Genomics, 1995, v. 25, p. 477–484.
19. **Rocchi M., Archidiacono N., Schempp W., Capozzi O., Stanyon R.** Centromere Repositioning in Mammals. // Heredity (Edinb.), 2012, v. 108, p. 59–67.

2.4 Article No. 4

X Fan, W Sangpakdee, A Tanomtong, A Chaveerach, K Pinthong, S Pornnarong, W Supiwong, V Trifonov, G Hovhannisyan, K Loth, C Hensel, T Liehr, A Weise. 2014. **Comprehensive molecular cytogenetic analysis of Barbary macaque (*Macaca sylvanus*)**.Biol J Arm, 66:98-102.

Abstract: Comparative chromosome banding analysis and/or fluorescence in situ hybridization (FISH) studies are established approaches to compare human and ape chromosomes. FISH-banding is a relatively new and not routinely applied method suited very well to provide to a better understanding of the evolutionary history of primate and human phylogeny. Here multicolor banding (MCB) applying probes derived from *Homo sapiens* was used to analyze the chromosomes of Thai crab-eating macaque (*Macaca fascicularis*). The results agreed with those of previous studies in other macaques, e.g. *Macaca sylvanus* or *Macaca nemestrina*. This result pinpoints, that morphological differences within the Ceropithecoidae must be founded rather in subchromosomal changes or even in epigenetics than in gross structural alterations.

Հայաստանի Գիտությունների Ազգային Ակադեմիա
Национальная Академия Наук Армении
National Academy of Sciences of Armenia

Հայաստանի Կենսաբանական Հանդես
Биологический Журнал Армении
Biological Journal of Armenia

• Փորձարարական և տեսական հոդվածներ • Экспериментальные и теоретические статьи •
• Experimental and theoretical articles •

Biolog. Journal of Armenia, 1 (66), 2014

COMPREHENSIVE MOLECULAR CYTOGENETIC ANALYSIS OF BARBARY MACAQUE (*MACACA SYLVANUS*)

X. FAN[1], W.SANGPAKDEE[2], A. TANOMTONG[2], A. CHAVEERACH[2], K. PINTHONG[1,2,3], S. PORNNARONG[1,2], W. SUPIWONG[1,2], V. TRIFONOV[1,4], G. HOVHANNISYAN[5], K. LOTH[6], CH. HENSEL[7], TH. LIEHR[1], A. WEISE[1]

[1]Jena University Hospital, Friedrich Schiller University, Institute of Human Genetics, Kollegiengasse 10, D-07743 Jena, Germany
[2]Department of Biology Faculty of Science, Khon Kaen University, 123 Moo 16 Mittapap Rd., Muang District, Khon Kaen 40002, Thailand
[3]Faculty of Science and Technology, Surindra Rajabhat University, 186 Moo 1, Maung District, Surin 32000, Thailand
[4]Institute of Molecular and Cellular Biology, Lavrentev Str. 8/2, Novosibirsk 630090, Russia
[5]Department of Genetics and Cytology, State University, Biological Faculty, Yerevan, Armenia
[6]Serengeti-Park Hodenhagen, Am Safaripark 1, D-29693 Hodenhagen, Germany Thüringer Zoopark Erfurt, Am Zoopark 1, D-99087 Erfurt, Germany

Origin of human and ape chromosomes has been studied by comparative chromosome banding analysis and by fluorescence in situ hybridization (FISH). As it is not always possible to determine exact breakpoints and distribution or orientation of specific DNA stretches by these approaches FISH-banding was applied in the present study to reanalyze the chromosomes of Barbary macaque (*Macaca sylvanus*). Interestingly, the results agree with those of previous studies in other macaques, supporting the idea that the genetic differences leading to the observed large morphological differences within the Ceropithecoidae still have to be discovered.

Barbary macaque – FISH – multicolor banding (MCB) – chromosomal breakpoints

Մարդու և կապիկների քրոմոսոմների ծագումը ուսումնասիրվել է քրոմոսոմների համեմատական դիֆերենցիալ գունավորման և ֆլյուորեսցենտային in situ հիբրիդացման (FISH) միջոցով:

Քանի որ նշված մոտեցումները միշտ չէ, որ թույլ են տալիս հստակ որոշել կտրվածքների կետերը և ԴՆԹ-ի սպեցիֆիկ հատվածների բաշխումն ու տեղակայումը, տվյալ հետազոտության մեջ Մագրիբյան մակակ (*Macaca sylvanus*) քրոմոսոմների կրկնակի վերլուծության համար կիրառվել է դիֆերենցիալ FISH-ներկում: Հետաքրքրական է, որ արդյունքները համընկնում են այլ մակակների նախորդ հետազոտությունների արդյունքներին՝ հաստատելով Ceropithecoidae ներսում խոշոր ձևաբանական փոփոխություններին հանգեցնող գենետիկական տարբերությունների հետագա ուսումնասիրության անհրաժեշտությունը:

Մագրիբյան մակակ – FISH – քրոմոսոմների բազմագույն հերտավոր ներկում – քրոմոսոմների կտրվածքներ

Было изучено происхождение хромосом человека и обезьяны с применением сравнительной дифференциальной окраски хромосом и флюоресцентной in situ гибридизации (FISH).Так как указанные подходы не всегда позволяют точно определять точки разрывов и

распределение или ориентацию специфических участков ДНК, в данном исследовании для повторного анализа хромосом магрибского макака (*Macaca sylvanus*) была применена дифференциальная FISH-окраска. Интересно, что полученные данные согласуются с результатами предыдущих исследований других макак и подтверждают необходимость дальнейших исследований генетических различий, обуславливающих крупные морфологические различия, внутри Ceropithecoidae.

Магрибский макак – FISH – Многоцветная дифференциальная окраска хромосом – хромосомные разрывы

Cytogenetic studies in ape species were done to great extent in the 1970s to 1980s [18] as "comparative cytogenetic studies of non-human primates can provide a substantial contribution to investigations on the evolutionary history of chromosomes and a better understanding of primate and human phylogeny" [9]. Later on the invent of molecular cytogenetics, especially multicolor-fluorescence in situ hybridization (FISH) studies using whole chromosome painting probes gave another boost for studies on chromosomal changes during primate evolution (for review see [10]). Still the FISH-banding approaches available since end of the 1990s [7] were yet applied neither in many species (see below), nor in systematic studies for the question of karyotype evolution, with a few exceptions [5; 12-13]. The nowadays most frequently applied FISH-banding approach is the so-called multicolor banding (MCB) approach, which is anchored in the human DNA-sequence [17]. MCB was already successfully applied for the characterization and comparative molecular cytogenetic mapping of the following primate species before: Gorilla gorilla [10], Hylobates lar [11] and Trachypithecus cristatus [6].

Here we provide the first MCB-based study for the characterization of the North-African Barbary macaque (Macaca sylvanus = MSY). Macaques belong to the Old World monkeys (Catarrhini), family Ceropithecoidae, subfamily Cercopithecinae and tribe Papionini. It is thought that the genus Macaca underwent a radiation in Pliocene or Pleistocene, i.e. during the last 3-5 million years [3]. While morphologically the genus Macaca underwent multiple changes, on the chromosomal level this group kept surprisingly constant – all of them have 42 chromosomes and on cytogenetic level they do not differ at all [2]. This fact is also supported that different macaque species can form hybrids, even fertile ones, easily [8].

The MSY was studied yet only by banding cytogenetics and FISH using whole chromosome paints [9]. As even in times of next generation sequencing basic cytogenetic data is needed for exact alignment of the new complex datasets [19] here we provide the first MCB-based FISH-banding study in MSY. The hereby obtained data is crucial for further comparative cytogenetic studies in non-human primates and their evolutionary history.

Materials and methods. Peripheral blood of MSY (1 male and 1 female) was acquired in the zoological gardens of Erfurt and Hodenhagen (both Germany), respectively. The corresponding veterinaries acquired blood for the present study only if blood collection was necessary anyway for other medical reasons during routine checkups of the animals. Blood lymphocytes from heparinzed blood were subjected to short term culture and cytogenetic work-up using standard procedures.

24 chromosome-specific MCB probes were applied in 24 independent FISH-experiments in MSY-chromosome-preparations as previously reported [10]. Evolutionary conserved chromosomal breakpoints were characterized with respect to the human chromosome complement (see tab. 1). Nomenclature of MSY chromosomes was adapted from [9].

Results and Discussion. Applying MCB in MSY overall 43 evolutionary breakevents in comparison to human karyotype were recorded (tab. 1). The observed break-

points were observed to be identical to those known from other macaque species before [16]. Still it has to be admitted that the nomenclature of macaque chromosomes is not uniform – e.g. MSY chromosomes 12 and 13 have the designations 9 and 15 in [15], which may confuse.

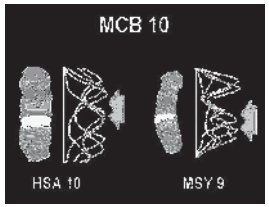

Fig. 1. Representative example for MCB-result obtained in MSY. Result of MCB 10 probe set applied on a human chromosome 10 (HSA) compared to the result obtained on homologous MSY chromosome 9. A paracentric inversion with evolutionary conserved breakpoints in 10q11.23 and 10q22.3 was observed (arrows). For each chromosome pseudocolor depiction and underlying fluorochrome profiles are shown.

Tab. 1. Breakpoints of Macaca sylvanus (MSY) according to MCB. Abbreviations: cen = centromeric position; HSA = Homo sapiens

MSY	MSY chromosomes given as derivatives of human chromosomes	cen
1	inv(1)(q23.3q42.13),dim(1)(q12)	1q42.13
2	der(3)(qter->q27.3::p22.3->p24::q22.1->q27.3::p22.3->p12.3::p26.3->p24::q22.1->p12.3:)	3q26.1
3	der(7)(21qter->21q11.2::7p22.3->7p22.1::7q21.3->7q22.1::7q11.23->7p21.3::7p21.3->7q11.23::7q22.1->7qter)	like HSA 7
4	inv(6)(p24q25.2) and inv(6)(q21q25.2)	6q24.3
5	inv(4)(p15.3q10)	like HSA 4
6	no change to HSA 5	like HSA 5
7	der(15)t(14;15)(q11.2;q26.3)	15q25
8	no change to HSA 8	like HSA 8
9	inv(10)(q11.23q22.3)	like HSA 10
10	der(20)(22qter->22p13::20p11.21->20p13::20q11.21->20qter)	like HSA 22
11	no change to HSA 12	like HSA 12
12	inv(2)(q14.1q21.1)	2q22.1
13	inv(2)(q11.1q14.1)	2p11.2
14	inv(11)(p15.4q13.4)	11p15.4
15	der(9)(9qter->9q34::?::9q34->9p24.3::9q21.11->9q22.33:),dim(9)(q12)	9q33.2
16	der(17)(pter->p10::?::p10->q12::q23.3->q21.32::q12->q21.32::q23.3->q24::?::q24->qter)	like HSA 17
17	no change to HSA 13	13q21.31
18	no change to HSA 18	18q21.2
19	no change to HSA 19	like HSA 19
20	inv(16)(q22.1q22.3),dim(16)(q11.2)	like HSA 16
X	no change to HSA X	like HSA X
Y	del(Y)(q12q12)	like HSA Y

Apart from that, species specific amplifications present in human in 1q12, 9q12, 16q11.2 and Yq12 were not present in MSY at the corresponding regions. Still unknown material was amplified in MSY in regions homologous to 17p10, 17q24 and 9q34. At least for 17q24 complex regions of segmental duplication were reported [4]. Such species specific amplifications are suggested to play major roles in speciation [10].

Centromeric regions present in MSY were identical to human centromeric positions in MSY 3, 5, 6, 8-11, 16, 19, 20, X and Y (tab. 1). It is well known that the centromeric regions, even if being intraspecifically stable do not contain identical alphoid DNA stretches [1]; this is thought to be a hint on faster evolution of these genomic regions compared to other, euchromatic ones.

Different centromeric positions than in human were observed in the MSY chromosomes 1, 2, 4, 7, 12-15, 17 and 18 (tab. 1). The latter was denominated a centromere repositioning and was thoroughly discussed in [14].

Overall, the present study confirmed for another macaque species that the general chromosomal composition cannot be the reason for specification in this genus.

The present study in MSY using high resolution FISH-banding underlined the conclusion already drawn in [9] that "the karyotype has not played a fundamental role in the diversification and speciation in this group, because apparently there is no necessary causal link between chromosomal changes and morphological diversification or speciation". In other words: the genetic differences leading to large morphological differences within the Ceropithecoidae still have to be identified. At the same time it needs to be revised if the family Hylobatidae really is as morphological inconsistent due to its extremely chromosomal diversity [11] or due to other, subchromosomal changes.

Acknowledgments

Supported in parts by the China Scholarship Council (support for FX), a "Thai Government Science and Technology Scholarship" for KP, a "Strategic scholarship fellowships frontier research network for SP and the DLR/BMBF RUS 09/008 (AW).

REFERENCES

1. *Archidiacono N., Antonacci R., Marzella R., Finelli P., Lonoce A., Rocchi M.* Comparative mapping of human alphoid sequences in great apes using fluorescence in situ hybridization. Genomics, *25*, 477-484, 1995.
2. *Brown C.J., Dunbar V.G., Shafer D.A.* A comparison of the karyotypes of six species of the genus Macaca and a species of the genus Cercocebus. Folia Primatol (Basel), *46*, 164-172, 1986.
3. *Camperio Ciani A., Stanyon R., Scheffrahn W., Sampurno B.* Evidence of gene flow between Sulawesi macaques. Am J Primatol, *17*, 257-270, 1989.
4. *Cardone M.F., Jiang Z., D'Addabbo P., Archidiacono N., Rocchi M., Eichler E.E., Ventura M.* Hominoid chromosomal rearrangements on 17q map to complex regions of segmental duplication. Genome Biol, *9*, R28, 2008.
5. *de Oliveira E.H., Neusser M., Figueiredo WB, Nagamachi C., Pieczarka J.C., Sbalqueiro I.J., Wienberg J., Müller S.* The phylogeny of howler monkeys (Alouatta, Platyrrhini): reconstruction by multicolor cross-species chromosome painting. Chromosome Res, *10*, 669-683, 2002.
6. *Fan X., Pinthong K., Mkrtchyan H., Siripiyasing P., Kosyakova N., Supiwong W, Tanomtong A., Chaveerach A., Liehr T., de Bello Cioffi M, Weise A.* First detailed reconstruction of the karyotype of Trachypithecus cristatus. Mol Cytogenet, *in press.*
7. *Liehr T., Starke H., Heller A., Kosyakova N., Mrasek K., Gross M., Karst C., Steinhaeuser U., Hunstig F., Fickelscher I., Kuechler A., Trifonov V., Romanenko S.A., Weise A.* Multicolor fluorescence in situ hybridization (FISH) applied to FISH-banding. Cytogenet Genome Res, 114, 240-244, 2006.
8. *Moore C.M., Janish C., Eddy .CA., Hubbard G.B., Leland M.M., Rogers J.* Cytogenetic and fertility studies of a rheboon, rhesus macaque (Macaca mulatta) x baboon (Papio hamadryas) cross: further support for a single karyotype nomenclature. Am. J. Phys. Anthropol, *110*, 119-127, 1999.

9. *Morescalchi A.M., Camperio Ciani A., Stanyon R.* Chromosome banding and molecular cytogenetics of the Barbary macaque, Macaca sylvanus. It J Zool, *65*, 101-107, 1998.
10. *Mrasek K., Heller A., Rubtsov N., Trifonov V., Starke H., Rocchi M., Claussen U., Liehr T.* Reconstruction of the female Gorilla gorilla karyotype using 25-color FISH and multicolor banding (MCB). Cytogenet Cell Genet, *93*, 242-248, 2001.
11. *Mrasek K., Heller A., Rubtsov N., Trifonov V., Starke H., Claussen U., Liehr T.* Detailed Hylobates lar karyotype defined by 25-color FISH and multicolor banding. Int. J. Mol. Med., *12*, 139-146, 2003.
12. *Müller S., Wienberg J.* "Bar-coding" primate chromosomes: molecular cytogenetic screening for the ancestral hominoid karyotype. Hum Genet, *109*, 85-94, 2001.
13. *Müller S., O'Brien P.C., Ferguson-Smith M.A., Wienberg J.* Cross-species colour segmenting: a novel tool in human karyotype analysis. Cytometry, *33*, 445-452, 1998.
14. *Rocchi M., Archidiacono N., Schempp W., Capozzi O., Stanyon R.* Centromere repositioning in mammals. Heredity (Edinb), *108*, 59-67, 2012.
15. *Ruiz-Herrera A., Ponsà M., García F., Egozcue J., García M.* Fragile sites in human and Macaca fascicularis chromosomes are breakpoints in chromosome evolution. Chromosome Res., *10*, 33-44, 2002.
16. *Ventura M., Antonacci F., Cardone M.F., Stanyon R., D'Addabbo P., Cellamare A., Sprague L.J., Eichler E.E., Archidiacono N., Rocchi M.* Evolutionary formation of new centromeres in macaque. Science, *316*, 243-246, 2007.
17. *Weise A., Mrasek K., Fickelscher I., Claussen U., Cheung S.W., Cai W.W., Liehr T., Kosyakova N.* Molecular definition of high-resolution multicolor banding probes: first within the human DNA sequence anchored FISH banding probe set. J. Histochem. Cytochem., *56,* 487-493, 2008.
18. *Yunis J.J., Prakash O.* The origin of man: a chromosomal pictorial legacy. Science, *215*, 1525-1530, 1982.
19. *Zhang X., Goodsell J., Norgren R.B. Jr.* Limitations of the rhesus macaque draft genome assembly and annotation. BMC Genomics, *13*, 206, 2012.

Received 27.11.2013

2.5 Article No. 5

X Fan, A Tanomtong, A Chaveerach, K Pinthong, S Pornnarong, W Supiwong, T Liehr, A Weise. 2014. **High resolution karyotype of Thai crab-eating macaque (*Macaca fascicularis*)**. Genetika, 46:877-882.

Abstract: Origin of human and ape chromosomes has been studied by comparative chromosome banding analysis and by fluorescence in situ hybridization (FISH). As it is not always possible to determine exact breakpoints and distribution or orientation of specific DNA stretches by these approaches FISH-banding was applied in the present study to reanalyze the chromosomes of Barbary macaque (*Macaca sylvanus*). Interestingly, the results agreed with those of previous studies in other macaques, supporting the idea that the genetic differences leading to the observed large morphological differences within the Ceropithecoidae still have to be discovered.

UDC 575
DOI: 10.2298/GENSR1403877F
Original scientific paper

HIGH RESOLUTION KARYOTYPE OF THAI CRAB-EATING MACAQUE (*Macaca fascicularis*)

Xiaobo FAN[1], Alongkoad TANOMTONG[2], Arunrat CHAVEERACH[2], Krit PINTHONG [1,2 3], Siripiyasing PORNNARONG[1,2], Weerayuth SUPIWONG[1,2], Thomas LIEHR[1], Anja WEISE[1]

[1]Jena University Hospital, Friedrich Schiller University, Institute of Human Genetics, Jena, Germany
[2]Department of Biology Faculty of Science, Khon Kaen University, Muang District, Khon Kaen, Thailand
[3]Faculty of Science and Technology, Surindra Rajabhat University, Maung District, Surin, Thailand

Fan X., A. Tanomtong, A. Chaveerach, K. PInthong,' S. Pornnarong, W. Supiwong, T. Liehr, and Anja Weise (2014*): High resolution karyotype of thai crab-eating macaque* (*Macaca fascicularis*) - Genetika, Vol 46, No. 3, 877-882

Comparative chromosome banding analysis and/or fluorescence in situ hybridization (FISH) studies are established approaches to compare human and ape chromosomes. FISH-banding is a relatively new and not routinely applied method suited very well to provide to a better understanding of the evolutionary history of primate and human phylogeny. Here multicolor banding (MCB) applying probes derived from *Homo sapiens* was used to analyze the chromosomes of Thai crab-eating macaque (*Macaca fascicularis*). The results agree with those of previous studies in other macaques, e.g. *Macaca sylvanus* or *Macaca nemestrina*. This result pinpoints, that morphological differences within the Ceropithecoidae must be founded rather in subchromosomal changes or even in epigenetics than in gross structural alterations.

Key words: fluorescence in situ hybridization (FISH), karyotype, Macaca fascicularis, multicolor banding,

INTRODUCTION

As recently next generation sequencing was introduced to answer the question what are the genetic differences between the species, molecular cytogenetic studies to contribute to a better understand of the evolutionary history of primate and human phylogeny seem to be outdated. However, basic cytogenetic data is needed essentially for exact alignment of these new complex datasets as outlined by ZHANG *et al.* (2012).

Pure banding cytogenetic studies still are the starting point in many species nowadays (e.g. SUPIWONG *et al*., 2013). In primates similar studies were performed in the 1980s and 1990s (MORESCALCHI *et al.,* 1998). After introduction of multicolor-fluorescence in situ hybridization (FISH), FISH studies using whole chromosome painting probes and FISH-banding approaches (LIEHR *et al*., 2006) were done successfully. However, the FISH-banding approaches were not used systematically to study the question of karyotype evolution in primates; only occasionally a few studies were done (DE OLIVEIRA *et al.,* 2002; MÜLLER and WIENBERG, 2001, MÜLLER *et al.*, 1998). The most frequently applied FISH-banding approach is the so-called multicolor banding (MCB), which has the unique feature of being anchored in the human DNA-sequence (WEISE *et al*., 2008). MCB was already used for comparative molecular cytogenetic mapping of the following primate species before: *Gorilla gorilla* (MRASEK *et al*., 2001), *Hylobates lar* (MRASEK *et al.,* 2003), *Trachypithecus cristatus* (FAN *et al*., 2013), *Macaca sylvanus* (FAN et al., 2014a), and *Macaca nemestrina* (FAN *et al.,* 2014b).

Here the first MCB-based study for the characterization the karyotype of crab-eating macaque (*Macaca fascicularis* = MFA) is presented. During Pliocene or Pleistocene, i.e. during the last 3-5 million years Macaques (Catarrhini; Ceropithecoidae; Cercopithecinae; Papionini) underwent a quick radiation in Africa and especially Asia (FAN *et al*., 2014a and b). Macaques are a morphologically highly diverse group. According to the literature, on the chromosomal level this group kept absolutely constant: 42 chromosomes with no differences on the cytogenetic level. Thus, in captivity different macaque species can form hybrids, even fertile ones (MOORE *et al.*, 1999).

MFA was studied before by banding cytogenetics (FERNANDEZ-DONOSO *et al.,* 1970, KANAGAWA *et al.,* 1971); to the best of our knowledge FISH was only applied for single loci (KASAI *et al*., 2000; KOSTOVA *et al*., 2002; RUIZ-HERRERA *et al*., 2004; LIU *et al*., 2007) and not for the whole genome yet, also a new alphoid DNA sequence was isolated from MFA and used in FISH (CROVELLA *et al.,* 1999). Here we provide the first genome wide MCB-based FISH-banding study in MFA.

MATERIALS AND METHODS

Five milliliter of heparinzed peripheral blood of one male MFA was acquired in Thailand. Blood lymphocytes were subjected to short term culture and cytogenetic work-up under standard conditions.

24 multicolor banding (MCB) probes derived from human chromosomes *Homo sapiens* (HSA) were applied in 24 independent FISH-experiments in MFA-chromosome-preparations as previously reported (MRASEK *et al.,* 2001). Evolutionary conserved chromosomal breakpoints were characterized with respect to the human chromosome complement (see Tab. 1).

RESULTS AND DISCUSSION

In MFA 43 evolutionary conserved break-events were identified sing human karyotype as an equation (Tab. 1). It has to be annotated that the nomenclature of macaque chromosomes used here was adapted from MORESCALCHI *et al.* (1998), as there are different nomenclatures around;

Corresponding author: Thomas Liehr, Institut für Humangenetik, Postfach D-07740 Jena, Germany,Tel: ++49-3641-935533, Fax. ++49-3641-935582, email: THOMAS.LIEHR@MED.UNI-JENA.DE

e.g. MFA chromosomes 12 and 13 are designated as 9 and 15, respectively, elsewhere (RUIZ-HERRERA *et al*., 2002). The evolutionary conserved break-events in MFA (Tab. 1) were identical to those known from other macaque species, living in parts in Western Africa (VENTURA *et al.*, 2007; FAN *et al.*, 2014a). They remained stable even though MFA (this study) and *Macaca nemestrina* (FAN *et al.*, 2014b) are living in Thailand, i.e. thousands of kilometers apart.

Table 1. Evolutionary conserved breaks in MFA acc. to MCB

MFA	cen	MFA chromosomes given as derivatives of human chromosomes
1	1q42.13	inv(1)(q23.3q42.13),dim(1)(q12)
2	3q26.1	der(3)(qter->q27.3::p22.3->p24::q22.1->q27.3::p22.3->p12.3::p26.3->p24::q22.1->p12.3:)
3	like HSA 7	der(7)(21qter->21q11.2::7p22.3->7p22.1::7q21.3->7q22.1::7q11.23->7p21.3::7p21.3->7q11.23::7q22.1->7qter)
4	6q24.3	inv(6)(p24q25.2) and inv(6)(q21q25.2)
5	like HSA 4	inv(4)(p15.3q10)
6	like HSA 5	no change to HSA 5
7	15q25	der(15)t(14;15)(q11.2;q26.3)
8	like HSA 8	no change to HSA 8
9	like HSA 10	inv(10)(q11.23q22.3)
10	like HSA 22	der(20)(22qter->22p13::20p11.21->20p13::20q11.21->20qter)
11	like HSA 12	no change to HSA 12
12	2q22.1	inv(2)(q14.1q21.1)
13	2p11.2	inv(2)(q11.1q14.1)
14	11p15.4	inv(11)(p15.4q13.4)
15	9q33.2	der(9)(9qter->9q34::?::9q34->9p24.3::9q21.11->9q22.33:),dim(9)(q12)
16	like HSA 17	der(17)(pter->p10::?::p10->q12::q23.3->q21.32::q12->q21.32::q23.3->q24::?::q24->qter)
17	13q21.31	no change to HSA 13
18	18q21.2	no change to HSA 18
19	like HSA 19	no change to HSA 19
20	like HSA 16	inv(16)(q22.1q22.3),dim(16)(q11.2)
X	like HSA X	no change to HSA X
Y	like HSA Y	del(Y)(q12q12)

Besides, MCB using human probes left unstained some regions in MFA. Those were most likely species specific amplifications of unknown genetic material in regions homologous to HSA 9q34, 17p10 and 17q24. For 17q24 complex regions of segmental duplication were reported previously (CARDONE *et al.*, 2008). On the other hand HSA-specific amplicons present in 1q12, 9q12, 16q11.2 and Yq12 were not present in MFA. These observations go together well with the idea that species specific amplifications are might play a major role in speciation (MRASEK *et al.*, 2001). Further studies of the macaque specific amplicons might mead to interesting results in future.

Finally the centromeric regions in MFA 3, 5, 6, 8-11, 16, 19, 20, X and Y were identical to human centromeric positions (Tab. 1). However, the centromeric regions, even if being intraspecifically stable do not contain sequence identical alphoid DNA stretches. Also these regions are fascinating from the evolutionary point of view, as it is suggested that these chromosomal region evolve faster than other genomic regions. For centromeric positions of MFA 1, 2, 4, 7, 12-15, 17 and 18 so-called centromere repositioning was observed (Tab. 1), as discussed elsewhere (ROCCHI *et al.*, 2012).

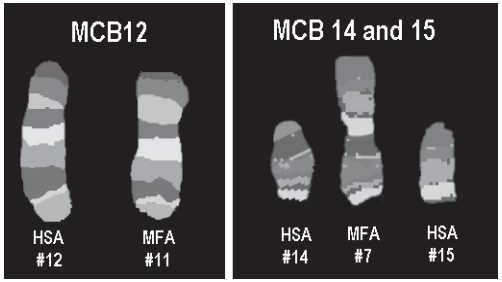

Figure 1.Representative examples for MCB-result obtained in MFA.

A) Result of MCB 12 probe set applied on a human chromosome 12 (HSA) compared to the result obtained on homologous MFA chromosome 12. No differences were observed.

B) MCB 14 and 15 applied on corresponding human chromosomes and on homologous MFA chromosome 7 –a fusion of both chromosomes is observable. The acrocentric short arms of both chromosomes present in HSA are absent in MFA.

CONCLUSION

Based on MCB in MFA the identical karyotype was determined as in our previous studies in *Macaca sylvanus* (FAN et al., 2014a) and *Macaca nemestrina* (FAN et al., 2014b). Thus, at (molecular) cytogenetic level no differences between these three macaques were found, even though differences in macaque-specific amplicons cannot be excluded yet. Still, our studies confirmed that the general chromosomal composition cannot be the underlying biological basis for the radiation and specification in Ceropithecoidae.

ACKNOWLEDGMENTS

Supported in parts by the China Scholarship Council (support for FX), a "Thai Government Science and Technology Scholarship" for KP, a "Strategic scholarship fellowships frontier research network for SP, the DLR/BMBF RUS 09/008 (AW) and 01DK13005 (TL).

Received July 17th, 2014
Accepted Octoberr 12th, 2014

REFERENCES

CARDONE , MF, Z JIANG, P D'ADDABBO, N ARCHIDIACONO, M ROCCHI, EE EICHLER, M VENTURA (2008): Hominoid chromosomal rearrangements on 17q map to complex regions of segmental duplication. Genome Biol *9*:R28.

CROVELLA, S, M DEL PERO, N MARZILIANO, S GARAGNA, V PECILE, M MORGUTTI, M BONIOTTO, A AMOROSO, D MONTAGNON, CC CAMPA, L LAMBERTI, MP BIGATTI, G ARDITO (1999: MFASAT: a new alphoid DNA sequence isolated from *Macaca fascicularis* (Cercopithecidae, Primates). Genome *42*:1066-1070.

DE OLIVEIRA, EH, M NEUSSER, WB FIGUEIREDO, C NAGAMACHI, JC PIECZARKA, IJ SBALQUEIRO, J WIENBERG, S MÜLLER (2002): The phylogeny of howler monkeys (Alouatta, Platyrrhini): reconstruction by multicolor cross-species chromosome painting. Chromosome Res *10*:669-683.

FAN, X, K PINTHONG, H MKRTCHYAN, P SIRIPIYASING, N KOSYAKOVA, W SUPIWONG, A TANOMTONG, A CHAVEERACH, T LIEHR, M DE BELLO CIOFFI, A WEISE (2013):First detailed reconstruction of the karyotype of Trachypithecus cristatus. Mol Cytogenet *6*:58.

FAN, X, A TANOMTONG, A CHAVEERACH, K PINTHONG, S PORNNARONG, W SUPIWONG, V TRIFONOV, G HOVHANNISYAN, K LOTH, C HENSEL, T LIEHR, A WEISE (2014a). Comprehensive molecular cytogenetic analysis of Barbary macaque (*Macaca sylvanus*). Biol J Arm *66*:98-102.

FAN, X, A TANOMTONG, A CHAVEERACH, K PINTHONG, S PORNNARONG, W SUPIWONG, V TRIFONOV, G HOVHANNISYAN, R AROUTOUINIAN, T LIEHR, A WEISE (2014b):Molecular cytogenetic analysis of Thai southern pig-tailed macaque (*Macaca nemestrina*) by multicolor banding. Proc Yerevan State Univ *2014*:46-50.

FERNANDEZ-DONOSO, R, J LINDSTEN, E NORRBY (1970): The chromosomes of the Cynomolgus macaque (*Macaca fascicularis*). Hereditas *65*:269-275.

KANAGAWA, H, ES HAFEZ, M NAWAR (1971): The chromosomes of the crab-eating macaque (Macaca fascicularis). Folia Primatol (Basel) *16*:270-275.

KASAI, F, E TAKAHASHI, K KOYAMA, K TERAO, Z SUTO, K TOKUNAGA, Z NAKAMURA, M HIRAI (2000): Comparative FISH mapping of the ancestral fusion point of human chromosome 2. Chromosome Res *8*:727-735.

KOSTOVA, E, S RÖTTGER, W SCHEMPP, J GROMOLL (2002): Identification and characterization of the cynomolgus monkey chromodomain gene cynCDY, an orthologue of the human CDY gene family. Mol Hum Reprod *8*:702-709.

LIEHR, T, H STARKE, A HELLER, N KOSYAKOVA, K MRASEK, M GROSS, C KARST, U STEINHAEUSER, F HUNSTIG, I FICKELSCHER, A KUECHLER, V TRIFONOV, SA ROMANENKO, A WEISE (2006): Multicolor fluorescence in situ hybridization (FISH) applied to FISH-banding. Cytogenet Genome Res *114*:240-244.

LIU, QY, XX WANG, JY ZHANG, WH CHEN, XW HE, Y LIN, JF WANG, Y ZHU, SN HU, XN WANG (2007): Mapping cynomolgus monkey MHC class I district on chromosome 6p13 using pooled cDNAs. Biotech Histochem *82*:267-272.

MOORE, CM, C JANISH, CA EDDY, GB HUBBARD, MM LELAND, J ROGERS (1999): Cytogenetic and fertility studies of a rheboon, rhesus macaque (*Macaca mulatta*) x baboon (*Papio hamadryas*) cross: further support for a single karyotype nomenclature. Am J Phys Anthropol *110*:119-127.

MORESCALCHI,,AM A CAMPERIO CIANI, R STANYON (1998): Chromosome banding and molecular cytogenetics of the Barbary macaque, *Macaca sylvanus*. It J Zool *65*:101-107.

MRASEK, K., A. HELLER, N. RUBTSOV, V. TRIFONOV, H. STARKE, M. ROCCHI, U.CLAUSSEN, T.LIEHR (2001): Reconstruction of the female *Gorilla gorilla* karyotype using 25-color FISH and multicolor banding (MCB). Cytogenet. Cell Genet *93*:242-248.

MRASEK, K, A HELLER, N RUBTSOV, V TRIFONOV, H STARKE, U CLAUSSEN, T LIEHR (2003): Detailed *Hylobates lar* karyotype defined by 25-color FISH and multicolor banding. Int J Mol Med *12*:139-146.

MÜLLER, S, J WIENBERG (2001): "Bar-coding" primate chromosomes: molecular cytogenetic screening for the ancestral hominoid karyotype. Hum Genet *109*:85-94.

MÜLLER, S, PC O'BRIEN, MA FERGUSON-SMITH, J WIENBERG (1998): Cross-species colour segmenting: a novel tool in human karyotype analysis. Cytometry *33*:445-452.

ROCCHI, M, N ARCHIDIACONO, W SCHEMPP, O CAPOZZI, R STANYON (2012): Centromere repositioning in mammals. Heredity (Edinb.) *108*:59-67.

RUIZ-HERRERA, A, M PONSÀ, F GARCÍA, J EGOZCUE, M GARCÍA (2002): Fragile sites in human and Macaca fascicularis chromosomes are breakpoints in chromosome evolution. Chromosome Res *10*:33-44.

RUIZ-HERRERA ,A, F GARCIA, L FRÖNICKE, M PONSÀ, J EGOZCUE, MG CALDÉS, R STANYON (2004): Conservation of aphidicolin-induced fragile sites in Papionini (Primates) species and humans. Chromosome Res *12*:683-690.

SUPIWONG, W, T LIEHR, MB CIOFFI, A CHAVEERACH, N KOSYAKOVA, K PINTHONG, T TANEE, A TANOMTONG (2013): Karyotype and cytogenetic mapping of 9 classes of repetitive DNAs in the genome of the naked catfish *Mystus bocourti* (*Siluriformes, Bagridae*). Mol Cytogenet. 6:51.

VENTURA, M, F ANTONACCI, MF CARDONE., R STANYON, P D'ADDABBO, A CELLAMARE, LJ SPRAGUE., EE EICHLER, N ARCHIDIACONO, M ROCCHI (2007): Evolutionary formation of new centromeres in macaque. Science *316*:243-246.

WEISE, A, K MRASEK, I FICKELSCHER, U CLAUSSEN, SW CHEUNG, WW CAI, T LIEHR, N KOSYAKOVA (2008): Molecular definition of high-resolution multicolor banding probes: first within the human DNA sequence anchored FISH banding probe set. J Histochem Cytochem 56:487-493.

ZHANG, X, J GOODSELL, RB JR NORGREN (2012): Limitations of the rhesus macaque draft genome assembly and annotation. BMC Genomics *13*:206.

KARIOTIP VISOKE REZOLUCIJE MAKAK RAKOJEDA (*Macaca fascicularis*)

Xiaobo FAN[1], Alongkoad TANOMTONG[2], Arunrat CHAVEERACH[2], Krit PINTHONG [1,2 3], Siripiyasing PORNNARONG[1,2], Weerayuth SUPIWONG[1,2], Thomas LIEHR[1], Anja WEISE[1]

[1]Jena Univerzitetska Bolnica, Friedrich Schiller Univerzitet, Institut za humanu genetiku, Nemačka
[2]odeljenje biologije Fakulteta nauke, Khon Kaen Univerzitet, Muang District, Khon Kaen, Tajland
[3]Fakultet nauke i tehnologije, Surindra Rajabhat Univerzitet, Maung District, Surin, Tajland

Izvod

komparativna hromozomska analiza i/ili in situ fluoroscentna hibridizacija (FISH) se koriste za poređenje ljudske i hromozome majmuna. FISH-tehnologija je relativno nova I ne koristi se rutinski is a relatively new and not routinely applied method koja može da obezbedi veću razumevanje evolucije primata i ljudsku filogeniju. Višebojne trakaste probe derivati iz *Homo sapiens* su korišćeni za analizu Thai makak rakojeda (*Macaca fascicularis*). dobijeni rezultati su u saglasnosti sa ranijim ispitivanjima drugih makaki, *Macaca sylvanus* ili *Macaca nemestrina*. ovi rezultati ukazuju da morfološke razlike unutar Ceropithecoidaemorjau biti zasnovane pre na subhromozomskim promenamili čak epigenetici nego u velikim strukturalnim promenama.

Primljeno 17. VII. 2014.
Odobreno 12. X. 2014.

2.6 Article No. 6

A Weise, N Kosyakova, M Voigt, N Aust, K Mrasek, S Löhmer, N Rubtsov, T Karamysheva, V Trifonov, D Hardekopf, T Jancuková, S Pekova, K Wilhelm, T Liehr, **X Fan**. 2015. **Comprehensive analyses of white handed gibbon chromosomes enables access to 92 evolutionary conserved breakpoints compared to the human genome**. Cytogenet Genome Res, 145:42-49.

Abstract: Gibbon species (Hylobatidae) impress with an unusually high number of numerical and structural chromosomal changes within the family itself as well as compared to other Hominoidea including humans. In former studies applying molecular cytogenetic methods, 86 evolutionary conserved breakpoints (ECBs) were reported in the white-handed gibbon (*Hylobates lar*, HLA) with respect to the human genome. To analyze those ECBs in more detail and also to achieve a better understanding of the fast karyotype evolution in Hylobatidae, molecular data for these regions are indispensably necessary. In the present study, we obtained whole chromosome-specific probes by microdissection of all 21 HLA autosomes and prepared them for aCGH. Locus-specific DNA probes were also used for further molecular cytogenetic characterization of selected regions. Thus, we could map 6 yet unreported ECBs in HLA with respect to the human genome. Additionally, in 26 of the 86 previously reported ECBs, the present approach enabled a more precise breakpoint mapping. Interestingly, a preferred localization of ECBs within segmental duplications, copy number variant regions, and fragile sites was observed.

Original Article

Cytogenetic and Genome Research

Cytogenet Genome Res 2015;145:42–49
DOI: 10.1159/000381764

Accepted: February 25, 2015
by M. Schmid
Published online: April 24, 2015

Comprehensive Analyses of White-Handed Gibbon Chromosomes Enables Access to 92 Evolutionary Conserved Breakpoints Compared to the Human Genome

Anja Weise[a] Nadezda Kosyakova[a] Martin Voigt[a] Nadine Aust[a]
Kristin Mrasek[a] Sharon Löhmer[a] Nikolai Rubtsov[b] Tatyana V. Karamysheva[b]
Vladimir A. Trifonov[c, d] David Hardekopf[e] Tereza Jančušková[e] Sona Pekova[e]
Kathleen Wilhelm[a] Thomas Liehr[a] Xiaobo Fan[a]

[a] Institute of Human Genetics, Jena University Hospital, Friedrich Schiller University, Jena, Germany;
[b] Institute of Cytology and Genetics, [c] Institute of Molecular and Cellular Biology SB RAS, and
[d] Novosibirsk State University, Novosibirsk, Russia; [e] Chambon Laboratory for Molecular Diagnostics
(member of the Synlab Czech Laboratory Group), Prague, Czech Republic

Key Words
Comparative genomics · Evolutionary conserved breakpoints · *Hylobates lar* · Molecular cytogenetics

Abstract
Gibbon species (Hylobatidae) impress with an unusually high number of numerical and structural chromosomal changes within the family itself as well as compared to other Hominoidea including humans. In former studies applying molecular cytogenetic methods, 86 evolutionary conserved breakpoints (ECBs) were reported in the white-handed gibbon (*Hylobates lar*, HLA) with respect to the human genome. To analyze those ECBs in more detail and also to achieve a better understanding of the fast karyotype evolution in Hylobatidae, molecular data for these regions are indispensably necessary. In the present study, we obtained whole chromosome-specific probes by microdissection of all 21 HLA autosomes and prepared them for aCGH. Locus-specific DNA probes were also used for further molecular cytogenetic characterization of selected regions. Thus, we could map 6 yet unreported ECBs in HLA with respect to the human genome. Additionally, in 26 of the 86 previously reported ECBs, the present approach enabled a more precise breakpoint mapping. Interestingly, a preferred localization of ECBs within segmental duplications, copy number variant regions, and fragile sites was observed.

The superfamily Hominoidea consists of great (orangutans, gorillas, chimpanzees, and humans) and lesser (gibbons) apes. The evolutionary paths of human (*Homo sapiens sapiens*, HSA) and gibbon are closely linked by a common ancestor living between 15 and 20 million years ago [Müller et al., 2003; Perelman et al., 2011]. In contrast to the family of great apes, gibbons demonstrate a high number of chromosomal rearrangements including inversions, translocations, fissions, and fusions [Brown and O'Neill, 2009]. Overall, gibbon species differ greatly in their chromosomal constitution, even between the 4 extant genera: *Hoolock* (2n = 38), *Hylobates* (2n = 44), *Symphalangus* (2n = 50), and *Nomascus* (2n = 52) [Müller et al., 2003]. There are also profound differences among the *Hylobates* group. For example, since the separation of *H. lar* and *H. syndactylus*, these 2 subspecies have independently accumulated 14 and 16 translocations within their group, respectively [O'Brien et al., 2006].

Despite the close relation to humans and the great apes, the classical banding pattern of gibbon chromosomes showed only few homologies between great and lesser apes, except for the X chromosome which is well conserved. On the other hand, the karyotypes of Old World monkeys, such as macaques and baboons, are very close to the ancestral primate karyotype and thus share most of their karyotype structure with the great apes [Stanyon et al., 2008].

The white-handed gibbon (*H. lar*, HLA) has 44 chromosomes, remarkably without a single acrocentric pair [Mrasek et al., 2003]. However, compared to human and most other primates, HLA shows an exceptionally high rate of chromosomal rearrangements. Several studies were previously done to investigate the chromosomal organization of HLA. In 1975, Tantravahi and colleagues carried out a cytogenetic study based on quinacrine, trypsin-Giemsa, and centromeric heterochromatin stains. Yet, they could only show how different HLA was in comparison to human and some other great apes. Jauch et al. [1992] used chromosome painting to detect the homologies between gibbon, great apes, and human and demonstrated a high degree of karyotype reshuffling in gibbon. Müller et al. [2003] applied human chromosome-specific probes to study homologous regions in all 4 hylobatid genera and to reconstruct the chromosomal evolution within the family. Multicolor banding was applied by Mrasek et al. [2003], revealing 71 breakpoints present in HLA compared to human. Recently, Misceo et al. [2008] performed a vast study using over 1,000 human BAC clones to determine the extension, reciprocal arrangement, and orientation of chromosomal segments of HLA compared to HSA. They ended up with a total number of 86 evolutionary conserved breakpoints (ECBs). More molecular data on ECBs were published recently by Carbone et al. [2014] from total sequencing of *H. pileatus* and *H. moloch*.

Since the chromosome rearrangement rate of gibbons is at least an order higher in magnitude compared to the average rearrangement rate in mammals [Zhao et al., 2004; Misceo et al., 2008], investigating the HLA genome could provide a better understanding of the mechanisms of genome plasticity in terms of species evolution. In fact, ECBs in HLA might correspond to human regions encompassing large amounts of duplicated genes [Carbone et al., 2009]. Moreover, physical clustering of gene families may be explained, or further insights might be obtained why some genes remain conserved over millions of years while others evolved more quickly [O'Brien and Yuhki, 1999]. So far, no excessive analysis of HLA samples using aCGH has been accomplished. The higher resolution of this method should generate a more complete picture than cytogenetics or molecular cytogenetics alone and is also able to detect submicroscopic, previously hidden, rearrangements [Gribble et al., 2009; Capozzi et al., 2012; Liehr et al., 2013].

Methods

Material
A female HLA cell line, provided by Prof. M. Rocchi (Bari, Italy) [Mrasek et al., 2003], was used in this study. As far as applicable, we state that (a) the research complied with protocols approved by the appropriate Institutional Animal Care Committee of the University of Jena, who declared that they are not responsible for cell line studies; (b) the research adhered to the legal requirements of Germany; and (c) the research adhered to the American Society of Primatologists (ASP) Principles for the Ethical Treatment of Non-Human Primates.

Microdissection
Chromosomes of the HLA cell line were subjected to glass-needle-based microdissection as described previously [Yang et al., 2009]. A total of 10–15 copies of each HLA autosome were microdissected, DOP-PCR amplified, labeled, and used for reverse FISH to prove the specificity and quality before aCGH was applied. Apart from HLA chromosomes 1 and 7, FISH-based microdissection was used for HLA probe preparation as previously reported [Kosyakova et al., 2013].

aCGH
DOP-PCR-amplified and labeled HLA-derived DNA was applied in aCGH as previously reported for human partial chromosome paints [Weise et al., 2008]. aCGH analysis was performed using 4 × 180 K SurePrint G3 Human CGH microarray slides (Agilent Technologies, Santa Clara, Calif., USA). These slides were produced via the Agilent 60-mer SurePrint technology containing 170,334 60-mer oligonucleotide probes that cover the entire human genome with a 13-kb overall median probe spacing. Probes were processed following Agilent's 'Oligonucleotide Array-Based CGH for Genomic DNA Analysis' protocol (v.6.2). Two fluorescence dyes were used to label references and samples. The arrays were scanned after hybridization using a dual-color laser scanner. Images were subsequently processed by Agilent's Feature Extraction v10.5 and analyzed using Agilent Workbench 5.0 (NCBI36/hg18).

Molecular Cytogenetics
FISH was performed using commercially available probes according to the manufacturer's instructions. The following specific subtelomeric probes were applied: 1pter, 4pter, 4qter, 5qter, 6qter, 7qter, 8pter, 8qter, 9pter, 10pter, 10qter, 12pter, 12qter, 14qter, 15qter, 16pter, 16qter, 17qter, 19pter,20pter, 20qter, Xpter, Xqter (Kreatech, Amsterdam, The Netherlands); and 1qter, 2pter, 2qter,

1424–8581/15/1451–0042$39.50/0

E-Mail karger@karger.com
www.karger.com/cgr

Anja Weise
Institute of Human Genetics
Jena University Hospital, Friedrich Schiller University
Postfach, D–07740 Jena (Germany)
E-Mail Anja.Weise@med.uni-jena.de

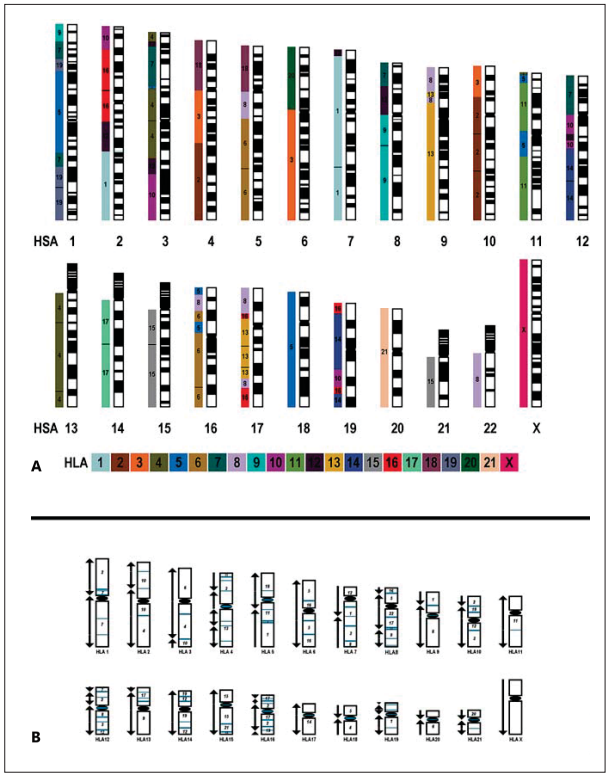

Fig. 1. A Schematic drawing of HLA array results with respect to the human karyotype. **B** Schematic HLA karyogram showing the orientation of the chromosomal blocks being syntenic to HSA. The scheme is drawn according to data presented in this work together with data from Marsek et al. [2003] and Misceo et al. [2008].

3pter, 3qter, 5pter, 6pter, 7pter, 9pter, 9qter, 11pter, 11qter, 13qter, 15qter, 17pter, 18pter, 18qter, 19qter, 21qter, 22qter (Abbott/Vysis, Wiesbaden, Germany). BACs from BACPAC Chori were used for further characterization of the following regions: 1p36, 1p36.21, 3q29, 9p21, 9q34.3, 11q13, 16p11.2, 16p13, 17p11.2, 17q23, and 20q13. FISH was done according to standard procedures [Mrasek et al., 2003]. The evaluation was done using a Zeiss Axioplan fluorescence microscope (Zeiss, Jena, Germany) with MetaSystems (Isis) software (Altlussheim, Germany). A total of 10–20 metaphases per probe were analyzed.

Databases

All human genome mapping calculations, assignments to cytogenetic bands, and sequence analyses were done according to the UCSC database version March 2006 (NCBI36/hg18, http://genome.ucsc.edu/cgi-bin/hgGateway). Each ECB determined by aCGH was analyzed for copy number variant regions (CNVs) and/or segmental duplications (SDs) and known disease causing regions. As the mean resolution of the used aCGH approach was 26 kb, ±25 kb was the minimum size of the region analyzed in the databases for each of the ECBs analyzed.

Results and Discussion

In the present study, for the first time the combined microdissection/aCGH approach [Backx et al., 2007; Weise et al., 2008; Villa et al., 2011; Jancuskova et al., 2013] was successfully applied to narrow down 43 euchromatic autosomal ECBs in HLA (fig. 1). Additionally,

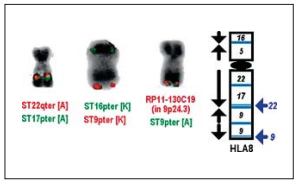

Fig. 2. Application of human subtelomeric probes identified 3 new rearrangements not reported before (FISH pictures and blue arrows) for HLA chromosome 8. Black arrows along the karyogram represent the orientation of the corresponding chromosome fragments with homologous HSA fragments. [A] = Vysis/Abbott probe; [K] = Kreatech probe; ST = subtelomeric probe.

human subtelomeric probes were applied to confirm and/or refine the aCGH data (fig. 2; online suppl. tables 1, 2; see www.karger.com/doi/10.1159/000381764 for all online suppl. material). The data obtained here (original data of aCGH is exemplarily depicted in figure 3) were evaluated together with previously published own data [Mrasek et al., 2003] and with results of other authors [Misceo et al., 2008]. Thus, in online suppl. tables 3 and 4, the best presently available approximation to 92 ECBs in HLA is presented. In figure 1, these data are summarized comparing syntenic blocks between HSA and HLA. Even though meanwhile newer versions than NCBI36/hg18 are available, this version had to be used for this work as numerous BAC probes are no longer listed in current versions like GRCh37/hg19 or GRCh38/hg38.

Novel Submicroscopic Chromosomal Changes and Previously Undetected Breakpoints

As aCGH is not suited to detect balanced translocations in a whole genomic setting, we combined glass-needle-based microdissection with aCGH to refine ECB mapping in HLA with respect to the human karyotype. The combined microdissection/aCGH approach was applied previously for the exact sizing of partial chromosome paints [Weise et al., 2008] or the precise determination of chromosomal breakpoints [Backx et al., 2007; Villa et al., 2011; Jancuskova et al., 2013]. HLA chromosomes of interest were painted by specifically labeled human DNA probes, and FISH microdissection of the labeled chromosomes was done. The obtained DNA libraries were amplified by DOP-PCR and applied in aCGH. To verify suspect and weakly covered aCGH regions like subtelomeric regions, we applied all available 41 human subtelomeric probes and additional locus-specific human BAC probes in 2- to 3-color-FISH settings to HLA chromosomes derived from a female HLA cell line.

As shown in online suppl. tables 3 and 5, this combined approach was able to detect the following yet unreported breakpoints: 3–4, 9–5 (fig. 2), 16–1, 16–3, 16–4, and 22–4 (figs. 2, 4). On the other hand, BAC-FISH, being able to resolve ECBs involved in balanced as well as in unbalanced rearrangements as applied by Misceo et al. [2008], could identify the following 37 breakpoints not detectable by aCGH: 1–3, 1–4, 1–8, 2–2, 2–3, 3–6, 5–3, 6–1, 6–3, 7–2, 7–3, 7–4, 7–5, 7–6, 8–3, 10–2, 10–3, 12–5, 13–2, 13–3, 13–4, 14–2, 15–2, 15–3, 16–5, 17–4, 17–5, 17–8, 17–9, 18–1, 18–2, 19–5, 20–1, 20–2, 20–3, 22–3, and 22–4.

For breakpoints 3–1, 9–3, 9–4, and 11–1 another problem of aCGH has to be considered. Those ECBs where not resolved in aCGH due to a low coverage of the corresponding regions in the assay itself. This shows that different approaches need to be performed and combined to obtain most comprehensive information on ECBs. Even in the age of next-generation-sequencing, balanced and complex rearrangements as well as repetitive heterochromatic regions and CNVs cannot unambiguously be resolved by an exclusive use of these modern approaches. Therefore, comparative chromosome painting of HSA and HLA provides a necessary overview on the extensive diversity within this group, such as chromosome numbers, composition of syntenic blocks, and type of translocations [Capozzi et al., 2012]. CNVs and fast mapping of euchromatic breakpoints is accomplished by the here applied approach of array painting. As a further step, next-generation whole-genome sequencing may provide additional insights into specific genetic information and functional mechanisms linked with large-scale changes during speciation [Carbone et al., 2014].

Evolutionary Conserved Breakpoints and Copy Number Variant Regions

Detailed breakpoint analyses of the results summarized in online suppl. table 4 revealed that the majority of ECBs (77/92; 83.7%) has already been reported to be involved in deleterious but viable deletions or duplications (which in most cases are larger than the analyzed breakpoint region) in human genetic diseases. Additionally, ~98.9% of the breakpoints are localized in CNVs, while only 50% of them are colocalized with SDs. This finding is in concordance with Carbone et al. [2006] who analyzed 100 ECBs in gibbons with a resolution of 200 kb and found that 46% of these breakpoints correspond to SDs with respect to the

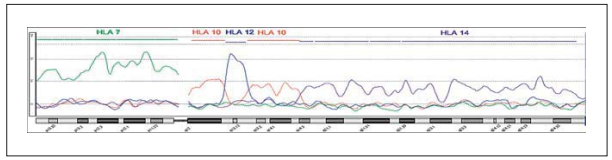

Fig. 3. Combined aCGH results for homologues regions of microdissected HLA chromosomes 7, 10, 12, and 14 on human chromosome 12 (180k Agilent array).

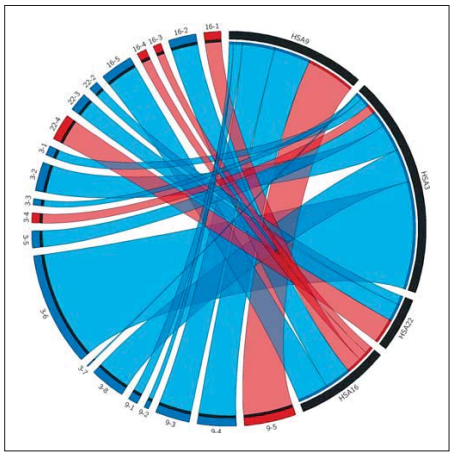

Fig. 4. Human chromosomes 3, 9, 16, and 22 with new identified ECBs in HLA are visualized by a circular diagram (created by http://mkweb.bcgsc.ca/circos/). Previously unreported breakpoints: 3–4, 9–5 (see also figure 2), 16–1, 16–3, 16–4, and 22–4 (fig. 2; online suppl. tables 3, 4) are depicted in red, known ones in blue. The size of the region to which the ECBs were narrowed down are depicted as width of the interlink between HLA and HSA.

human sequence [Carbone et al., 2009; Capozzi et al., 2012]. Recent molecular data by Wilson et al. [2015] further underline the correlation and colocalization of CNVs, common fragile sites (CFSs), as well as ECBs. CFSs represent a special kind of genomic instability under replication stress. It is suggested that the latter may induce CNV formation. Thus, CNVs and CFSs may also be seen as different manifestations of perturbed replication dynamics in the corresponding loci. The observed SDs in ECBs could also be explained as a result of break-induced replication repair leading to enrichment of genomic duplications in these break-prone regions [Costantino et al., 2014]. Another interesting feature that underlines the reuse of ECBs as break-prone regions is their involvement in sequence rearrangements, like inversions, insertions, and sequence/homology gaps being identified in other primates compared to the human genome (here analyzed for chimpanzee, orangutan, gorilla, rhesus monkey, and marmoset (online suppl. table 4)). Overall, ECBs may be interpreted as evolutionary highly active maybe due to a complex (epi)genetic architecture of those regions. The latter again stresses the necessity to combine various approaches for ECB mapping and studying genomic and karyotype evolution in as many species as possible.

Evolutionary Conserved Breakpoints and OMIM Genes

In all analyzed ECBs, the gene density in only 3/92 cases (3.3%) is larger than 0.5 genes per 10 kb, indicating that ECBs in HLA appear in more or less gene poor regions. When analyzing the closer surroundings of all identified autosomal ECBs (minimum ±25 kb around each ECB, detailed results are shown in online suppl. tables 4 and 6), then 59% of the analyzed regions included overall 157 known OMIM genes. Furthermore, only 47 of those genes in ECB regions are known as disease causing.

In general, the influence of ECBs on the phenotype could be direct, i.e. due to interruption of genes, or indirect, due to position effects influencing the expression/regulation of corresponding genes. Therefore, we analyzed the 154 identified OMIM genes in more detail for their function (online suppl. table 6) and found that 25% of them are highly expressed in the brain or are involved in neuronal function, 19% are somehow connected with cancer, 17% play a role for the function of the immune system, 10% are linked with intracellular trafficking, 8% each regulate/interact with DNA or are involved in metabolic processes, 5% influence the gestalt, 3% each are part of mitochondrial networks or are highly expressed in testis, and 2% are involved in cell cycle traits. The high degree

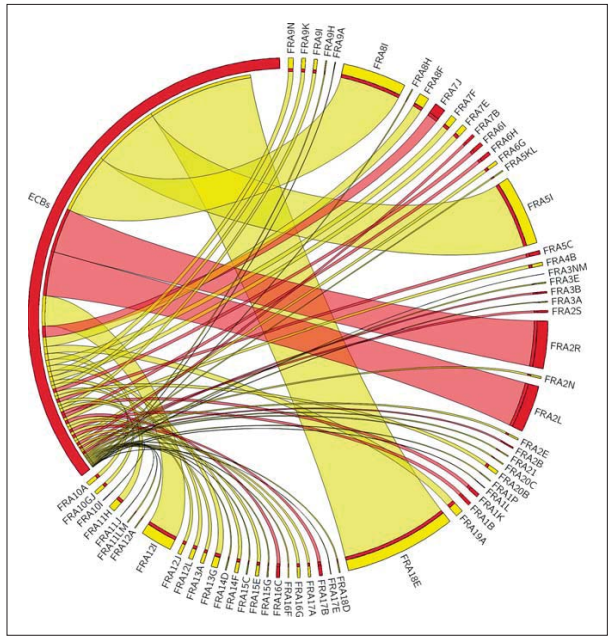

Fig. 5. ECBs and FSs are interlinked by a circular diagram (see also figure 4). Cytogenetically mapped FSs are depicted in yellow, molecular mapped FSs in red. The size of the region to which the FSs were narrowed down is depicted as width of the interlink between ECBs and FSs.

of association with brain-related genes and genes involved in the immune system are well documented and were previously discussed in the literature as a target for selection [Kehrer-Sawatzki and Cooper, 2007]. The identified OMIM genes which might have an influence concerning the differences in the gestalt are associated with growth (OMIM: 614145), obesity (OMIM: 606803), have skeletal (OMIM: 604032) and muscular functions (OMIM: 6009000), and affect hair keratin (OMIM: 602153) and skin physiology (OMIM: 607397 and 612121).

Concerning the lineage-specific high rate of chromosomal rearrangements in HLA, a well-controlled border between deleterious effects of chromosomal rearrangements (like in cancer) and well-controlled speciation must have taken place. Therefore, genes involved in cell cycle, DNA repair, and cancer development may be potential targets for this lineage-specific chromosome instability.

Interestingly, some of these genes play multiple roles like *RBBP8* (RetinoBlastoma-Binding Protein 8, OMIM: 604124) which is involved in DNA regulation, cell cycle, DNA repair, and, therefore, also in cancer development. RBBP8 is found among several proteins that bind directly to the retinoblastoma protein which regulates cell proliferation. It is also associated with BRCA1 and is thought to modulate its functions in transcriptional regulation, DNA repair, and/or cell cycle checkpoint control. It is suggested that *RBBP8* may itself be a tumor suppressor acting in the same pathway as *BRCA1*. Mutations of *RBBP8* are found in patients with Seckel syndrome 2, Jawad syndrome, and patients with pancreatic carcinoma.

Evolutionary Conserved Breakpoints and Common Fragile Sites

CFSs can be induced in every individual and represent an intrinsic feature of human chromosome biology [Mrasek et al., 2010]. Furthermore, they are reported for several species like *Drosophila* [von Grotthuss et al.,

2010], mammals [Alekseyev and Pevzner, 2010], yeast [Rosen et al., 2013], or birds [Gordon et al., 2007]. We compared ~230 common known human CFSs and rare FSs [Mrasek et al., 2010] together with 47 recently molecularly defined fragile site (online suppl. table 7) to underscore their role in evolutionary breakpoint reuse as suggested in a 'fragile breakage model of chromosome evolution' [Peng et al., 2006]. In the present as well as in other studies [Fan et al., 2013], a high rate of coincidence between ECBs and FSs [Mrasek et al., 2010] was observed: 65/92 (70.6%) ECBs between HLA and HSA could be correlated with cytogenetic localization of FSs. For 12 of these 65 FSs, molecular data of their localization was available (online suppl. table 7), and all of them were in line with the suggestion of a colocalization of ECBs and FS (fig. 5). These data further support the hypothesis that chromosome rearrangements have not occurred randomly over the course of evolution but are focused preferentially within fragile regions.

Genomic Sequence and Karyotype Evolution

While ECBs share some common features (FSs, CNVs, SDs), the comparison of available molecular breakpoint data in different gibbon species shows a high diversity, suggesting a more or less independent origin of ECBs within the gibbon family [Carbone et al., 2006, 2009, 2014; Roberto et al., 2007; Giririjan et al., 2009]. Still, this is investigated in more detail currently by high-resolution molecular and cytogenetic studies [Carbone et al., 2014]. Yet, in Hylobatidae, 10–20 fold faster chromosome rearrangement rates compared to most mammals [Misceo et al., 2008] were revealed, and similar rates were detected in muroid rodents [Romanenko et al., 2012] and equids [Trifonov et al., 2012]. The possible mechanisms responsible for such an increased genome evolution might be due to LAVA (gibbon specific retrotransposon)-induced premature transcription termination of chromosome segregation genes [Carbone et al., 2014]. Pericentric inversions are considered to be the most common euchromatic chromosomal differences between humans and the great apes [Nickerson and Nelson, 1998; Locke et al., 2003, Kehrer-Sawatzki et al., 2005]. According to fig. 1B, para- and pericentric inversions may be considered for HLA evolution for all but chromosome 18 and the X chromosome. Besides the recent thoughts published by Reinhard Stindl [2014] on altered chromosome fusion, inversion and separation during evolution might also be considered to explain specification events.

Conclusion

Overall, the currently available data did not change the suggestion that all hylobatid-specific rearrangements have a derived state and that these genomic changes have occurred after a common gibbon-ancestor split from the last common hominoid ancestor between 15 and 20 million years ago [Goodman, 1999; Perelman et al., 2011]. In more detail, half of the rearrangements that distinguish the hylobatid karyotypes from the human karyotype are shared by all 4 small ape genera and therefore occurred in their common ancestor. However, the breakpoint regions were narrowed down more precisely, which is necessary for further comparative studies in evolution research in Hominoidea and within gibbon subspecies.

Acknowledgments

This work was supported in part by DLR RUS 09/008 and the China Scholarship Council.

References

Alekseyev MA, Pevzner PA: Comparative genomics reveals birth and death of fragile regions in mammalian evolution. Genome Biol 11:R117 (2010).

Backx L, Van Esch H, Melotte C, Kosyakova N, Starke H, et al: Array painting using microdissected chromosomes to map chromosomal breakpoints. Cytogenet Genome Res 116: 158–166 (2007).

Brown JD, O'Neill RJ: The mysteries of chromosome evolution in gibbons: methylation is a prime suspect. PLoS Genet 5:e1000501 (2009).

Capozzi O, Carbone L, Stanyon RR, Marra A, Yang F, et al: A comprehensive molecular cytogenetic analysis of chromosome rearrangements in gibbons. Genome Res 22:2520–2528 (2012).

Carbone L, Vessere GM, ten Hallers BF, Zhu B, Osoegawa K, et al: A high-resolution map of synteny disruptions in gibbon and human genomes. PLoS Genet 2:e223 (2006).

Carbone L, Harris RA, Vessere GM, Mootnick AR, Humphray S, et al: Evolutionary breakpoints in the gibbon suggest association between cytosine methylation and karyotype evolution. PLoS Genet 5:e1000538 (2009).

Carbone L, Harris RA, Gnerre S, Veeramah KR, Lorente-Galdos B, et al: Gibbon genome and the fast karyotype evolution of small apes. Nature 513:195–201 (2014).

Costantino L, Sotiriou SK, Rantala JK, Magin S, Mladenov E, et al: Break-induced replication repair of damaged forks induces genomic duplications in human cells. Science 343:88–91 (2014).

Fan X, Pinthong K, Mkrtchyan H, Siripiyasing P, Kosyakova N, et al: First detailed reconstruction of the karyotype of *Trachypithecus cristatus* (Mammalia: *Cercopithecidae*). Mol Cytogenet 6:58 (2013).

Giririjan S, Chen L, Graves T, Marques-Bonet T, Ventura M, et al: Sequencing human-gibbon breakpoints of synteny reveals mosaic new insertions at rearrangement sites. Genome Res 19:178–190 (2009).

Gribble SM, Ng BL, Prigmore E, Fitzgerald T, Carter NP: Array painting: a protocol for the rapid analysis of aberrant chromosomes using DNA microarrays. Nat Protoc 4:1722–1736 (2009).

Goodman M: The genomic record of humankind's evolutionary roots. Am J Hum Genet 64:31–39 (1999).

Gordon L, Yang S, Tran-Gyamfi M, Baggott D, Christensen M, et al: Comparative analysis of chicken chromosome 28 provides new clues to the evolutionary fragility of gene-rich vertebrate regions. Genome Res 17:1603–1613 (2007).

Jancuskova T, Plachy R, Stika J, Zemankova L, Hardekopf DW, et al: A method to identify new molecular markers for assessing minimal residual disease in acute leukemia patients. Leuk Res 37:1363–1373 (2013).

Jauch A, Wienberg J, Stanyon R, Arnold N, Tofanelli S, et al: Reconstruction of genomic rearrangements in great apes and gibbons by chromosome painting. Proc Natl Acad Sci USA 89:8611–8615 (1992).

Kehrer-Sawatzki H, Cooper DN: Understanding the recent evolution of the human genome: insights from human-chimpanzee genome comparisons. Hum Mutat 28:99–130 (2007).

Kehrer-Sawatzki H, Sandig CA, Goidts V, Hameister H: Breakpoint analysis of the pericentric inversion between chimpanzee chromosome 10 and the homologous chromosome 12 in humans. Cytogenet Genome Res 108:91–97 (2005).

Kosyakova N, Hamid AB, Chaveerach A, Pinthong K, Siripiyasing P, et al: Generation of multicolor banding probes for chromosomes of different species. Mol Cytogenet 6:6 (2013).

Liehr T, Weise A, Hamid AB, Fan X, Klein E, et al: Multicolor FISH methods in current clinical diagnostics. Exp Rev Mol Diagn 13:251–255 (2013).

Locke DP, Archidiacono N, Misceo D, Cardone MF, Deschamps S, et al: Refinement of a chimpanzee pericentric inversion breakpoint to a segmental duplication cluster. Genome Biol 4:R50 (2003).

Misceo D, Capozzi O, Roberto R, Dell'oglio MP, Rocchi M, et al: Tracking the complex flow of chromosome rearrangements from the *Hominoidea* ancestor to extant *Hylobates* and *Nomascus* gibbons by high-resolution synteny mapping. Genome Res 18:1530–1537 (2008).

Mrasek K, Heller A, Rubtsov N, Trifonov V, Starke H, et al: Detailed *Hylobates lar* karyotype defined by 25-color FISH and multicolor banding. Int J Mol Med 12:139–146 (2003).

Mrasek K, Schoder C, Teichmann AC, Behr K, Franze B, et al: Global screening and extended nomenclature for 230 aphidicolin-inducible fragile sites, including 61 yet unreported ones. Int J Onc 36:929–940 (2010).

Müller S, Hollatz M, Wienberg J: Chromosomal phylogeny and evolution of gibbons (Hylobatidae). Hum Genet 113:493–501 (2003).

Nickerson E, Nelson DL: Molecular definition of pericentric inversion breakpoints occurring during the evolution of humans and chimpanzees. Genomics 50:368–372 (1998).

O'Brien SJ, Menninger JC, Nash WG: Atlas of Mammalian Chromosomes. John Wiley & Sons, Danvers (2006).

O'Brien SJ, Yuhki N: Comparative genome organization of the major histocompatibility complex: lessons from the Felidae. Immunol Rev 167:133–144 (1999).

Perelman P, Johnson WE, Roos C, Seuánez HN, Horvath JE, et al: A molecular phylogeny of living primates. PLoS Genet 7:e1001342 (2011).

Peng Q, Pevzner PA, Tesler G: The fragile breakage versus random breakage models of chromosome evolution. PLoS Comput Biol 2:e14 (2006).

Roberto R, Capozzi O, Wilson RK, Mardis ER, Lomiento M, et al: Molecular refinement of gibbon genome rearrangements. Genome Res 17:249–257 (2007).

Romanenko SA, Perelman PL, Trifonov VA, Graphodatsky AS: Chromosomal evolution in Rodentia. Heredity (Edinburg) 108:4–16 (2012).

Rosen DM, Younkin EM, Miller SD, Casper AM: Fragile site instability in *Saccharomyces cerevisiae* causes loss of heterozygosity by mitotic crossovers and break-induced replication. PLoS Genet 9:e1003817 (2013).

Stanyon R, Rocchi M, Capozzi O, Roberto R, Misceo D, et al: Primate chromosome evolution: ancestral karyotypes, marker order and neocentromeres. Chromosome Res 16:17–39 (2008).

Stindl R: The telomeric sync model of speciation: species-wide telomere erosion triggers cycles of transposon-mediated genomic rearrangements, which underlie the saltatory appearance of nonadaptive characters. Naturwissenschaften 101:163–186 (2014).

Tantravahi R, Dev VG, Firschein IL, Miller DA, Miller OJ: Karyotype of the gibbons *Hylobates lar* and *H. moloch* inversion in chromosome 7. Cytogenet Cell Genet 15:92–102 (1975).

Trifonov VA, Musilova P, Kulemsina AI: Chromosome evolution in Perissodactyla. Cytogenet Genome Res 137:208–217 (2012).

Villa O, Mallo M, Kosyakova N, Salido M, Liehr T, et al: Deletion of *TET2* gene in an acute myeloid leukemia case with a t(4;15)(q24;q26) characterized by glass needle based chromosome microdissection and oligonucleotide array. Leuk Res 35:e161–163 (2011).

von Grotthuss M, Ashburner M, Ranz JM: Fragile regions and not functional constraints predominate in shaping gene organization in the genus *Drosophila*. Genome Res 20:1084–1096 (2010).

Weise A, Starke H, Mrasek K, Claussen U, Liehr T: New insights into the evolution of chromosome 1. Cytogenet Genome Res 108:217–222 (2005).

Weise A, Mrasek K, Fickelscher I, Claussen U, Cheung SW, et al: Molecular definition of high-resolution multicolor banding probes: first within the human DNA sequence anchored FISH banding probe set. J Histochem Cytochem 56:487–493 (2008).

Wilson TE, Arlt MF, Park SH, Rajendran S, Paulsen M, et al: Large transcription units unify copy number variants and common fragile sites arising under replication stress. Genome Res. 25:189–200 (2015).

Yang F, Trifonov V, Ng BL, Kosyakova N, Carter NP: Generation of paint probes by flow-sorted and microdissected chromosomes, In Liehr T (ed): Fluorescence In Situ Hybridization (FISH) – Application Guide, pp 35–52 (Springer, Berlin 2009).

Zhao S, Shetty J, Hou L, Delcher A, Zhu B, et al: Human, mouse, and rat genome large-scale rearrangements: stability versus speciation. Genome Res 14:1851–1860 (2004).

2.7 Article No. 7

X Fan, W Supiwong, A Weise, K Mrasek, N Kosyakova, A Tanomtong, K Pinthong, VA Trifonov, M de Bello Cioffi, P Grothmann, T Liehr, EHC de Oliveira. 2015. **Comprehensive characterization of evolutionary conserved breakpoints in four New World Monkey karyotypes compared to *Chlorocebus aethiops* and *Homo sapiens***. Helyon, Article No ~ e00042.

Abstract: Comparative cytogenetic analysis in new world monkeys (NWMs) using human multicolor banding (MCB) probe sets were not previously done. Here we report on an MCB study complemented with selected locus-specific and heterochromatin specific probes in four NWMs and one old world monkey (OWMs) species, i.e. in *Alouatta caraya* (ACA), *Callithrix jacchus* (CJA), *Cebus apella* (CAP), *Saimiri sciureus* (SSC), and *Chlorocebus aethiops* (CAE), respectively. Thus 363 evolutionary conserved breakpoints (ECBs) among those species were identified and compared with those of other species in previous reports. Especially for chromosomal regions being syntenic to human chromosomes 6, 8, 9, 10, 11, 12 and 16 previously cryptic rearrangements could be observed. 50.4% (54/107) NWM ECBs were colocalized with those of OWM, 62.6% (62/99) NWM-ECBs were related with those of HLA and 66.3% (71/107) NWM-ECBs corresponded with those known from other mammalians. Furthermore, human fragile sites were aligned with the ECBs found in the five studied species and interestingly 66.3% ECBs colocalized with those fragile sites (FSs). Overall, this study presents detailed chromosomal maps of one OWM and four NWM species. Our data will be helpful to further investigation on chromosome evolution in NWM and hominoids in general.

Heliyon

ELSEVIER

Received:
15 September 2015
Revised:
20 October 2015
Accepted:
23 October 2015

Heliyon (2015) e00042

CrossMark

Comprehensive characterization of evolutionary conserved breakpoints in four New World Monkey karyotypes compared to *Chlorocebus aethiops* and *Homo sapiens*

Xiaobo Fan[a], **Weerayuth Supiwong**[b], **Anja Weise**[a], **Kristin Mrasek**[a], **Nadezda Kosyakova**[a], **Alongkoad Tanomtong**[b], **Krit Pinthong**[b], **Vladimir A. Trifonov**[c], **Marcelo de Bello Cioffi**[d], **Pierre Grothmann**[e], **Thomas Liehr**[a,*], **Edivaldo H.C.de Oliveira**[f]

[a] *Jena University Hospital, Friedrich Schiller University, Institute of Human Genetics, Kollegiengasse 10, D-07743 Jena, Germany*

[b] *Department of Biology Faculty of Science, KhonKaen University, 123 Moo 16 Mittapap Rd., Muang District, KhonKaen 40002, Thailand*

[c] *Institute of Molecular and Cellular Biology SB RAS, Novosibirsk, Russia*

[d] *Departamento de Genética e Evolução, Universidade Federal de São Carlos, São Carlos, SP, Brazil*

[e] *Serengeti-Park Hodenhagen GmbH, Am Safaripark 1, 29693, Hodenhagen, Germany*

[f] *Faculdade de Ciências Naturais, ICEN, Universidade Federal do Pará, Campus Universitário do Guamá, 66075-110 Belém-PA, Brazil*

*Corresponding author at: Institut für Humangenetik, Postfach, D-07740 Jena, Germany. Tel.: +49 3641 935533; fax: +49 3641 935582.

E-mail address: Thomas.Liehr@med.uni-jena.de (T. Liehr).

Abstract

Comparative cytogenetic analysis in New World Monkeys (NWMs) using human multicolor banding (MCB) probe sets were not previously done. Here we report on an MCB based FISH-banding study complemented with selected locus-specific and heterochromatin specific probes in four NWMs and one Old World Monkey (OWM) species, i.e. in *Alouatta caraya* (ACA), *Callithrix jacchus* (CJA), *Cebus apella* (CAP), *Saimiri sciureus* (SSC), and *Chlorocebus aethiops* (CAE), respectively. 107 individual evolutionary conserved breakpoints (ECBs) among those species were identified and compared with those of other species in previous reports. Especially for chromosomal regions being syntenic to human chromosomes 6, 8, 9, 10, 11, 12 and 16 previously cryptic rearrangements could be observed. 50.4% (54/107) NWM-ECBs were colocalized with those of OWMs, 62.6% (62/99) NWM-ECBs were related with those of *Hylobates lar* (HLA) and 66.3% (71/107) NWM-ECBs corresponded with those known from other mammalians. Furthermore, human fragile sites were aligned with the ECBs found in the five studied species and interestingly 66.3% ECBs colocalized with those fragile sites (FS). Overall, this study presents detailed chromosomal maps of one OWM and four NWM species. This data will be helpful to further investigation on chromosome evolution in NWM and hominoids in general and is prerequisite for correct interpretation of future sequencing based genomic studies in those species.

Keywords: Genetics, Evolutionary genetics, Evolutionary conserved breakpoints, Multicolor banding, New World Monkeys, Old World Monkeys, Fragile sites, Atelidae, Cebidae

Abbreviations: ACA: *Alouatta caraya*, BACs: bacterial artificial chromosomes, CAE: *Chlorocebus aethiops*, CJA: *Callithrix jacchus*, CAP: *Cebus apella*, EC: evolutionary conserved, ECBs: evolutionary conserved breakpoints, FISH: fluorescence in situ hybridization, FS: fragile site, HCM: heterochromatin mix, HLA: *Hylobates lar*, HSA: *Homo sapiens*, HSBs: homologous syntenic blocks, MCB: multicolor banding, NGS: Next-generation sequencing, NOR: nucleolus organizer region, NWMs: New World Monkeys, OWMs: Old World Monkeys, SSC: *Saimiri sciureus*, subCTM: sub-centromere/subtelomere-specific multicolor (FISH), wcp: whole human chromosome painting

1. Introduction

New World Monkeys (NWMs) inhabit tropical forests of Southern Mexico, central and South America, but especially the Amazon rainforests. Nowadays, there are over 120 recognized species that comprise of over 16 genera, commonly classified in 3 families. It is known from cytogenetic studies that NWMs have high interchromosomal and intrachromosomal karyotypic diversity in terms of chromosome structure and numbers, the latter ranging from 2n = 16 to 2n = 62 (Groves, 2001).

Four NWM species from two families are included in this study: *Alouatta caraya* (ACA) from the family Atelidae, and *Callithrix jacchus* (CJA), *Cebus apella* (CAP), *Saimiri sciureus* (SSC) from the family Cebidae. These species

have been previously investigated for their chromosomal organization, however primarily just by application of cytogenetic techniques, such as G-banding analyses in CAP (Freitas and Seuánez 1982), CJA (Ardito et al., 1987), ACA (Rahn et al., 1996) and SSC (Srivastava et al., 1969), C-banding in CAP (Freitas and Seuánez 1982), CJA (Bedard et al., 1978), ACA (Mudry et al., 1994) and SSC (Jones and Ma 1975), and Ag-NOR staining in CAP (Freitas and Seuánez 1982), CJA (Bedard et al., 1978), ACA (Mudry et al., 1994) and SSC (Goodpasture and Bloom, 1975). Since the 1990s, fluorescence in situ hybridization (FISH) applying whole human chromosome painting (wcp) probes and/or monkeys chromosome-specific probes have been successively utilized for comparative cytogenetics studies in NWMs, like CAP (Richard et al., 1996; Garcia et al., 2000), CJA (Sherlock et al., 1996; Neusser et al., 2001), ACA (de Oliveira et al., 2002) and SSC (Stanyon et al., 2000).

Apart from NWMs, Old World Monkeys (OWMs) and apes also were subject of research before using cytogenetics and FISH; examples are chimpanzees, gorillas, orangutans, lesser apes, African green monkey (*Chlorocebus aethiops* = CAE), macaques and langurs (Stanyon et al., 1992; Wienberg et al., 1990, 1992; Luke and Verma, 1992; Ried et al., 1992; Koehler et al., 1995; Bigoni et al., 1997; Finelli et al., 1999). While chromosomal diploid numbers and evolutionary conserved rearrangements could be determined or at least suggested already based on cytogenetics, FISH painting using wcp probes made it possible to investigate a wide range of interchromosomal translocations which took place during hominoid-evolution. However, the relatively limited resolution of wcp probes hampered detection of smaller rearrangements and intrachromosomal changes, like inversions. This could be overcome by FISH-banding approaches (Liehr et al., 2006) like multicolor banding (MCB) (Liehr et al., 2002; Weise et al., 2008). MCB was successfully applied for comparative mapping of the following primate species before: *Gorilla gorilla* (Mrasek et al., 2001), *Hylobates lar* (Mrasek et al., 2003), *Trachypithecus cristatus* (Fan et al., 2013), *Macaca nemestrina* (Fan et al., 2014a), *Macaca sylvanus* (Fan et al., 2014b) and *Macaca fascicularis* (Fan et al., 2014c).

In this study, we determined the chromosomal structure of the following 4 NWM species: CAP (2n = 54), CJA (2n = 46), ACA (2n = 50) and SSC (2n = 44), as well as of one species OWM-species CAE (2n = 60). Besides MCB, bacterial artificial chromosomes (BACs) have been used for identification of centromeric positions and possible cryptic aberrations. Furthermore, positions of evolutionary conserved breakpoints (ECBs) among the studied OWM and NWM species were compared to data from the literature. Finally, a new phylogenetic tree was suggested based on the ECBs and EC rearrangements found in this study.

2. Material and methods

2.1. Cell culture and chromosomal preparation

Immortalized lymphoblast cell lines derived from tufted capuchin monkey (*Cebus apella*, CAP; female), common marmoset (*Callithrix jacchus*, CJA; female), howler monkey (*Alouatta caraya*, ACA; female), squirrel monkey (*Saimiri sciureus*, SSC; female) and the African green monkey (*Chlorocebus aethiops*, CAE; female) were cultivated according to standard techniques. Chromosomes were prepared following standard protocols (Mrasek et al., 2001).

2.2. Fluorescence in situ hybridization (FISH)

FISH was done as previously reported using locus-specific bacterial artificial chromosomes (BAC) probes and/or multicolor banding (MCB) probe sets (Fan et al., 2013). Also all chromosome-specific sub-centromere/subtelomere-specific multicolor (subCTM-)FISH probe sets were applied (Gross et al., 2006) apart the Y-chromosome specific one, as only female cell lines were available. Additionally, the following homemade *Homo sapiens* (HSA) derived microdissection probes were utilized: a probe specific for the short arm of all human acrocentric chromosomes (midi54) (Mrasek et al., 2003), and partial chromosome paints for some selected chromosome-arms (Liehr and Claussen, 2002). Furthermore, a probe specific for the nucleolus organizer region (NOR) and a probe set directed against all heterochromatic regions present in the human genome (1q12, 16q11.2, 9q12, 9p12/ 9q13, 15p11.2-p11.1, 19p12/q12 and Yq12), the so-called heterochromatin mix (HCM) probe set (Bucksch et al., 2012) were utilized.

Images were captured by an Axioplan II microscope (Carl Zeiss Jena GmbH, Germany) equipped with filter sets for DAPI, FITC, TR, SO, Cy5 and DEAC. Image analysis was performed via pseudocolor banding and fluorochrome profiles of the ISIS digital FISH imaging system (Meta Systems Hard & Software GmbH, Altlussheim, Germany). A total of 10 up to 20 metaphases per species and probe were analyzed.

3. Results

Multicolor banding (MCB) using human chromosome-specific probe sets was successfully applied in all five here studied species. Results were obtained for all chromosomes excluding Y-chromosome, as only female individuals were available for this study. ECBs and centromeric positions could be estimated at the sub-band level. Fig. 1 and Supplementary Table S1 summarizes the obtained results.

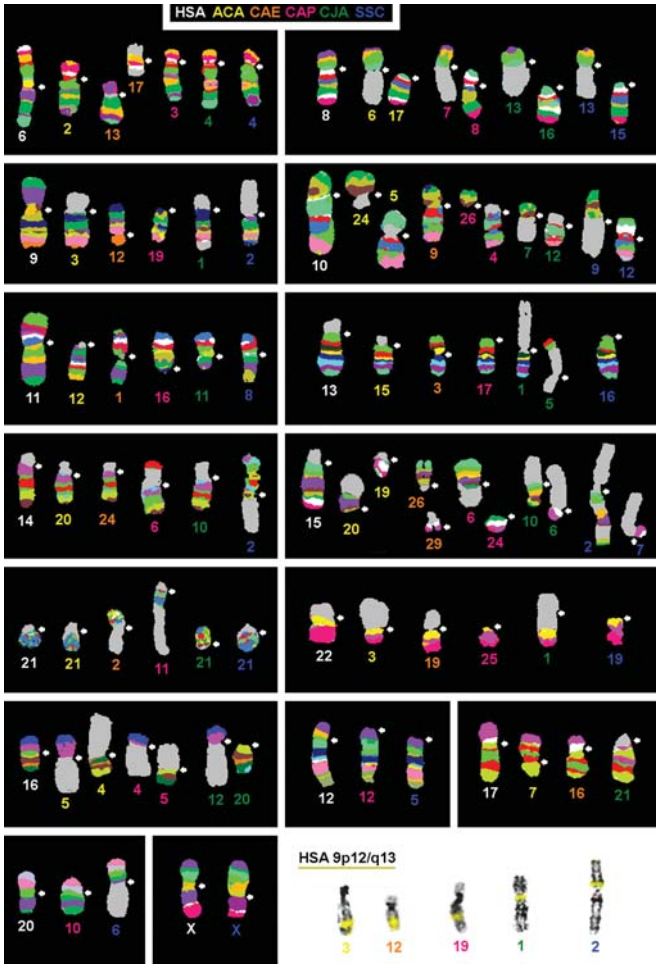

Fig. 1. Representative MCB pseudo-color results using human probes on the five species studied here; depicted are only new, not including confirmatory results of previously published findings from others. HSA chromosomes are numbered by white figures, monkey chromosomes in other colors. Also FISH-results using HSA 9p12/9q13 probes in the five studies species are depicted in the bottom right corner. Arrows show the location of monkey centromere.
Abbreviations: ACA = *Alouatta caraya*, CAE = *Chlorocebus aethiops*, CAP = *Cebus apella*, CJA = *Callithrix jacchus*, HSA = *Homo sapiens*, SSC = *Saimiri sciureus*.

Besides MCB probes specific for all sub-centromeric and sub-telomeric regions in HSA were also applied (results not shown). Some of centromeric positions were flanked by sub-centromeric probes and exactly mapped; remaining centromeric positions could be narrowed down by MCB (Supplementary Table S1). None of the sub-telomeric regions were involved in, compared to human, cryptic rearrangements during evolution of the five studied species (results not shown). Also, apart from 3 exceptions none of the human specific heterochromatic regions covered by the HCM probe-sets could be aligned to the homologous regions in the five studied species: signals for the HSA-specific probe covering 19p12/19q12 were observed on CAP9, ACA8, CJA22, SSC14 and CAE6, respectively; NOR-specific probe and probe specific for HSA 9p12/9q13 corresponded to chromosomes CAP19, ACA3, CJA1, SSC2 and CAE12, respectively (Fig. 1).

In total, in all five studied species, 363 ECBs which cannot be observed in HSA (Supplementary Table S2) and 253 homologous syntenic blocks (HSBs) were identified in this study. Practically all chromosomes studied underwent at least one rearrangement in the studied species compared to human (Supplementary Table S1; Table 1). As substantial parts of the overall observed 363 ECBs were seen in two or all of the studied species overall 107 different ECBs were identified (Supplementary Table S2).

Centromeric regions were either (i) de novo as interstitial ones within evolutionary conserved blocks, (ii) de novo formed in ECBs and/or break/fusion points or (iii) conserved compared to regions homologous to human centromeres. Also (iv) the latter two types could seed two centromeric positions. All four types of centromere positioning were found in all five studied species to different extents (Supplementary Table S1).

An analysis of HSBs based on detected ECBs on the five studied species is shown in Fig. 2. HSB rates were different per homologous HSA-chromosomes and species. E.g. HSA3 had much more HSBs than similar sized HSA1 and HSA2 chromosomes. The overall tendency is that the number of ECBs decreased with the size of the human chromosomes. Overall SSC had the most while CAP had the smallest number of HSBs compared to HSA.

The ECBs of CAP, ACA, CJA, SSC and CAE from Supplementary Table S1 were further compared with ECBs in other species (Supplementary Table S2). 50.4% (54/107) NWM-ECBs were colocalized with those OWM, 62.6% (62/99) NWM-ECBs were related with those of HLA and 66.3% (71/107) NWM-ECBs corresponded with those known from other mammalians, based on Supplementary Table S2. Furthermore, human fragile sites (FS) were aligned with the ECBs found in the five studied species and interestingly 66.3% ECBs colocalized with those FS.

Table 1. Evolutionary conserved breakpoints as found in the present study; those used for designing of Fig. 3 are highlighted by asterisk.

Homologues in HSA	CAP		CJA		SSC		ACA		CAE	
	hom.	abbr.	hom.	abbr.	hom.	abbr.	hom.	abbr.	hom.	abbr.
1	14	der(1) 1*	7	t(1;10)	11	der(1) 1*	1	t(1;5)	20	–
1	22	der(1) 2*	19	der(1) 2*	18	der(1) 2*	23	der(1) 2*	20; 25	–
1	23	–	18	–	14	t(1;19)	22	–	20	–
3	20	–	17	–	6	20 inv t(3;20)*	X2	t(3;15)*	15	–
3; 21	11	t(3;21)*	21	t(3;21) cen*	21	t(3;21)*	21	t(3;21)*	2; 22	–
4	2	–	3	–	3	4 inv	4; 9; 19	4 compl	7; 27	4 fi
7	15	–	8	7 inv1	10	7 inv2	14	–	21	–
8	8	del(8)*	16	del(8) inv*	15	del(8)*	17	del(8)*	8	–
8; 18	7	t(8;18)*	13	t(8;18)*	13	t(8;18)*	6	t(8;18)*	8; 18	–
10	26	–	7	t(1;10)	9	t(3;10)	24	–	9	–
10; 16	4	t(10;16)*	12	t(10;16)*	9; 12	t(10;16)*	5	t(10;16) inv*	5; 9	10 compl
12	12	12 inv*	9	–	5	12 inv	11	–	11	–
13	17	–	5	t(13;17)*	16	–	15	–	3	–
14; 15	6	t(14;15)* inv	10	t(14;15)*	2	t(14;15) compl*	19; 20	t(14;15) fi*	24; 26	–
16	5	t(2;16)*	20	–	1	t(2;16;5)*	4; 16	t(4;16)	5	–
17	21	17 inv2	5	t(17;20)	17	–	7	–	16	17 inv1
19	9	–	22	–	14	t(1;19)	8	–	6	–
20	10	20 inv*	5	t(17;20)	6	20 inv t(3;20)*	10	t(2;20)	2	t(2;21)
22	25	–	1	t(9;22)*	19	–	3	t(9;22)*	19	–
X	X	–	X	–	X	X neo	X1	–	X	–

Abbreviations: abbr. = abbreviation as used in Fig. 3; hom. = homologous chromosome(s); ACA = *Alouatta caraya*; CAE = *Chlorocebus aethiops*; CAP = *Cebus apella*; CJA = *Callithrix jacchus*; SSC = *Saimiri sciureus*; HSA = *Homo sapiens*; NWM = New World Monkey; OWM = Old World Monkey; t = translocation, del = deletion, der = derivative chromosome, inv = inversions, fi = fission; neo = neo-centromere.

For Capuchin monkey (*Cebus apella*, CAP) 43 ECBs were identified by FISH-banding (Supplementary Table S1). Additionally there are eight conserved centromeric regions compared with human (i.e. HSA1, HSA13, HSA16, HSA19, HSA20, HSA22, HSAX). Twenty-three regions were identified as de novo centromeres: twenty presented at break/fusion points (details see the Supplementary Table S1), three in the middle of conserved chromosomal block (i.e. 4q32.1, 5q31.3, 8q21.13). The regions homologous to 15q24.1 as well as centromeric region homologous to HSA1 were used for seeding of two centromeric positions, each (Supplementary Table S1).

Howler monkey (*Alouatta caraya*, ACA) had 51 ECBs and interestingly, ACAX2 chromosome was delineated as der(3)

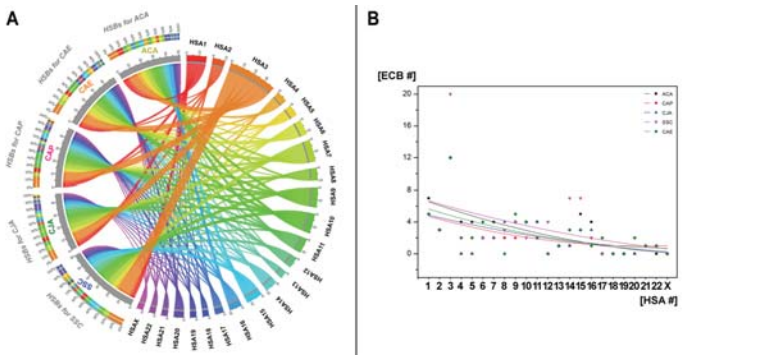

Fig. 2. Analysis of homologous syntenic block and evolutionary conserved breakpoints (ECBs) on the five studied species. A: The linkage map shows homologous syntenic blocks (HSB) of HSA chromosomes 1-22 and X compared to ACA = *Alouatta caraya*, CAE = *Chlorocebus aethiops*, CAP = *Cebus apella*, CJA = *Callithrix jacchus*, HSA = *Homo sapiens*, SSC = *Saimiri sciureus*. HSB rates per chromosome and species are shown. B: The graph shows the distribution of breakpoints in five studied monkeys with respect to the human chromosomes (colored dots), and the calculated breakpoints tendency curve (lines). As expected the number of breakpoints decreased with the size of the human chromosomes. SSC had in this study compared to HSA the most ECBs, CAP the smallest number of ECBs.

(15qter→15q24.3::3q27.1→3q22.1::3p25.3→3p21.31:). Five centromeric regions remained conserved compared to human (HSA1, HSA8, HSA13, HSA19, HSAX). Twenty-seven regions were identified as de novo centromeres: twenty-three formed at break/fusion points (details see the Supplementary Table S1), four were again in the middle of conserved blocks (i.e. 4q34.1, 10p11.21, 12p13.3 and 17q23.2); the regions homologous to 2q14.3 and 15q24.1 seeded two centromeric positions (Supplementary Table S1).

Common Marmoset (*Callithrix jacchus*, CJA) had 48 ECBs in a chromosome set of 46. Also there are ten centromeric regions conserved compared to human (HSA1, HSA3, HSA9, HSA12, HSA14, HSA15, HSA16, HSA19 and HSAX). Neocentromeres formed in twenty regions; seventeen are present at break/fusion points, three are interstitial in conserved blocks (i.e. 4q32.1, 5q31.3 and 7p21.1), and two regions (2q14.3 and HSA 16) seeded again two centromeric positions, each (Supplementary Table S1).

FISH-results for Squirrel monkey (*Saimiri sciureus*, SSC) are summarized in Supplementary Table S1: there are 67 ECBs in this species compared to HSA. Six centromeres were conserved compared to human (HSA1, HSA13, HSA15, HSA16 and HSA22). Twenty-three regions were identified as de novo centromeres of which nineteen are located at break/fusion points, the remainder

centromeres are interstitial in conserved blocks (i.e. 4q32.1, 10q26.3, 11q12.1 and Xq25). Finally, HSA 1 was used for seeding of two centromeric positions (Supplementary Table S1).

Results for African green monkey (*Chlorocebus aethiops*, CAE) and its 60 CAE chromosomes 39 ECBs can be found in Supplementary Table S1. In CAE there are eleven conserved centromeric regions compared to human (HSA2, HSA5, HSA8, HSA10, HSA12, HSA14, HSA16, HSA17, HSA19, HSA20, HSAX). De novo centromeres formed in 21 regions: fourteen are present at break/fusion points, there are seven interstitial ones in conserved blocks (i.e. 2q14.3, 3q26.33, 4q13.1, 6p11.2, 9q34.13, 13q21.31, 18q21.1), and two regions (7q11.21 and 15q24.1) seeded two centromeric positions, each (Supplementary Table S1).

4. Discussion

This study comprehensively characterized by high resolution molecular cytogenetics four species from NWMs derived from family Atelidae and Cebidae. Also one OWM species from the Cercopithecini was selected for the present study. This combination of species was done considering the assumption that NWM ancestors came from Africa. This idea was based on basis of morphological resemblance between NWM and the African anthropoid fossils (Schrago and Russo, 2003) and the African rafting source theory (Kay 2015). However, the present study did not find gross similarities between CAE from OWMs and the studied NMW species. Thus, CAE may have common ancestors with the studied NWMs but is no relative with many EC rearrangements in

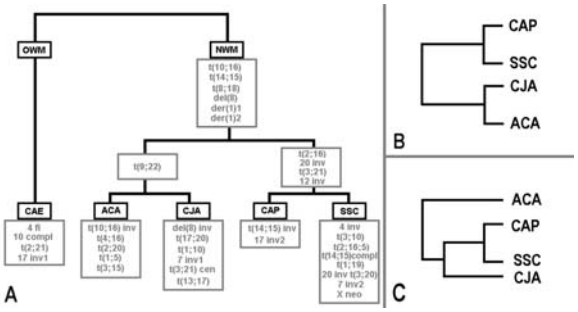

Fig. 3. A) Based on the here described evolutionary conserved changes a putative pedigree for the 4 NMM and one OWM is provided. B) The same putative pedigree according to Ford (1986) and C) Perelman et al. (2011) suggesting the same as Finstermeier et al. (2013).
Abbreviations: ACA = *Alouatta caraya*; CAE = *Chlorocebus aethiops*; CAP = *Cebus apella*; CJA = *Callithrix jacchus*; SSC = *Saimiri sciureus*; NWM = New World Monkey; OWM = Old World Monkey; t= translocation, del = deletion, der= derivative chromosome, inv= inversions, fi= fission; neo= neo-centromere.

http://dx.doi.org/10.1016/j.heliyon.2015.e00042

common (Table 1 and Fig. 3) Also available previously published own data on karyotypes of Macaques (tribe Papionini) (Fan et al., 2014a,b,c) *Trachypithecus cristatus* (TCR) (Fan et al., 2013), and *Hylobates lar* (HLA) (Mrasek et al., 2003) revealed by identical approaches as used here were included in the present study (Supplementary Table S2).

In general, our results confirmed previous data on homologous regions of the here studied five species and HSA (Garcia et al., 2000; Stanyon et al., 2000; Neusser et al., 2001; de Oliveira et al., 2002), but also we found that homologous regions for HSA chromosomes 6, 8, 10, 11, 12, 16 and 17 underwent at least one rearrangement, each, compared to ACA, CJA, CAP, SSC and CAE, respectively. In fact, 107 evolutionary conserved breakpoints (ECBs) and 253 homologous syntenic blocks (HSB) were determined. Besides multicolor banding (MCB), specific human sub-centromeric and sub-telomeric probes were also applied to identify the distribution of centromeres and telomeres in five species. Some of chromosome centromeric positions were neo-centromeres that were not characterized in previous studies (Garcia et al., 2000; Neusser et al., 2001). Remaining centromeres kept their positions during evolution from common ancestors to HSA. In contrast to previous report in HLA (Weise et al., 2015), none cryptic rearrangements were detected in the sub-telomeric regions during evolution of the five studied species.

Compared to reciprocal chromosome painting or multicolor chromosome bar coding in previous NWM studies (Neusser et al., 2001; Finelli et al., 1999; Müller and Wienberg 2001), MCB technique can be applied for the detailed identification of balanced and unbalanced chromosome rearrangements, even detected intrachromosomal rearrangements, to provide a genome-wide overview of sub-regional organization of syntenic segments and position of breakpoints, changes which are difficult if not impossible to be visualized by chromosome banding (Wienberg 2005). However, mostly sub-telomeric rearrangements and the high plasticity of sub-telomeric regions, in contrast to BAC mapping in HLA study (Misceo et al., 2008) escape the detection by MCB. To overcome this problem, sub-centromere/sub-telomere as locus specific probes also were utilized to check for cryptic rearrangements during evolution of the five studied species. Array-comparative genomic hybridization can only detect precisely map unbalanced rearrangements. Thus it can only be applied in evolutionary studies when combining with glass needle based microdissection like previously shown by us (Weise et al., 2015). Even though possible it is a very laborious approach which was not chosen for the present study.

Next-generation sequencing (NGS) technology was applied in some evolutionary studies (Li et al., 2010; Carbone et al., 2014), however, it is difficult to correctly align sequence and assemble genomes which are extremely reshuffled; thus

http://dx.doi.org/10.1016/j.heliyon.2015.e00042

karyotypic data is essentially necessary to correctly understand the NGS-data. Also NGS is not able to annotate information on position of repetitive elements. Therefore the human heterochromatin oriented heterochromatin mix (HCM) FISH set was applied in this study and localized some homologous regions like NOR or regions homologous to 9p12/9q13. Despite monkey specific repetitive elements were failed to be detected, they may be also of importance of evolution. Here also microdissection can be applied, even though this was not used in the present study (own unpublished data).

Overall, MCB combined with sub-centromeric/sub-telomeric probes and HCM-FISH set effectively detected detailed ECBs and orientation of newly arranged chromosomal regions in NWM. In present study, HSA 12, 18, 19, 20 and X were found as most conserved syntenic blocks during evolution. Chromosomes ACA11 and CJA9 were completely homologous to HSA 12. This finding is different from previous reports in other NWM which demonstrated a pericentric inversion (e.g. in *Lagothrix lagotricha*,*Callicebus moloch*, *Saimiri boliviensis*) (Stanyon et al., 2008). In concordance with the literature HSA18 is well conserved throughout mammals (Stanyon et al., 2008), here it was homologous to ACA6, CAP7, CJA13 and SSC13, respectively. Also our data in all five species HSA19 is conserved as syntenic block supports the hypothesis that this block is highly conserved after fusing of 19p and 19q in the anthropoid ancestor including NWM, OWM apes and human (Stanyon et al., 2008). Chromosomes homologous to HSA20 have structural changes due to neocentromere formation, translocations or inversions in ACA10, CAE2, CJA5 and other species (Stanyon et al., 2008). Additionally, we confirmed previous reports that X-chromosome has a centromeric shift in SSC (Rocchi et al., 2012). This finding supported that there are only a few exceptions from an X-chromosome being stable in most NWMs (Stanyon et al., 2008).

Centromere repositioning is a widespread phenomenon in genome evolution and a clustering of segmental duplications around the centromere is a common feature of primate sub-centromeric regions (Eder et al., 2003; Ventura et al., 2007). In this study, sub-telomeric and sub-centromeric probes were selected, which located very close to the telomere or centromere, respectively. Totally, of the centromeres in the studied five species (ACA, CAE, CAP, CJA and SSC), 43% of the centromeres were conserved and mapped between human sub-centromeric probes that flanked the centromeres. It is well known that the centromeric regions do not contain identical alphoid DNA stretches; this is understood as a hint on faster evolution of these genomic regions compared to others, euchromatic ones (Archidiacono et al., 1995). Besides, neocentromeres distinct from HSA centromere position were identified (see details in Supplementary Table S1). Noteworthy, other authors suggested that blocks of segmental duplication locate in close proximity to centromeric satellite DNA;

these neocentromeres could be thus rapidly stabilized by acquiring alpha satellite DNA (Ventura et al., 2007; She et al., 2004). As previously discussed for HLA (Mrasek et al., 2003) identical regions can be used twice for centromere-seeding and regions being telomeric in HSA can be centromeric positions in other species (Supplementary Table S1). Also Ventura et al. 2004 reported that the centromere of human chromosome 15 occurred in the telomeric region of the short arm of the ancestral chromosome 15/14 association. Possible explanations are that duplicon exchanges between sub-centromeric and sub-telomeric duplications are relatively frequent (Bailey et al., 2002) and that evolutionary new centromere appearance in telomeric regions may be affected by the spread of sub-centromeric duplications (Ventura et al., 2004).

For numbers of identified ECBs and HSBs, as expected the number of both decreased with the size of the human chromosome compared to as a reference (Fig. 2B). In this study CAP had the smallest number of ECBs, compared to HSA. This finding is in concordance with previous reports that the subfamily Cebidae among NWM occupies a more basal position and CAP has conserved chromosomal composition in the ancestral NWM karyotype (Amaral et al., 2008).

50.4% NWM ECBs colocalized with those of OWM and 62.6% NWM ECBs related with those of HLA (Supplementary Table S2). Our data show a higher percentage of ECBs colocalization between NWM and HLA, even though they are distantly related species. One possible explanation is that HLA experienced a high degree of chromosomal rearrangements by rapid derived karyotype evolution, although human and HLA are closely linked by a common ancestor (Weise et al., 2015). Furthermore, 66.3% (71/107) NWM ECBs were identified to correspond with those of mammalians in general (Supplementary Table S2). This finding is consistent with previous reports that 64% human chromosomal bands that contain evolutionary breakpoints presented in seven mammalian species (Ruiz-Herrera et al., 2006). Thus, there must be some 'breakpoint prone regions' in the mammalian genomes, which may be used by evolution as well as in human diseases (Liehr et al., 2011). These regions seem to correlate by large means especially with human FS (Supplementary Table S2) (Mrasek et al., 2010). Our data showing 66.3% of the here detected ECBs colocalized with FS confirmed previous findings that ECB regions are highly relevant to common FS in the breakage frequency model and that expressed FS have a tendency to concentrate at ECBs (Ruiz-Herrera et al., 2006; Fungtammasan et al., 2012).

In the present study, the karyotype of human was compared with chromosomes of CAP, ACA, SSC and CJA. CAE is an OWM considered to have common ancestors with NWMs studied and was used as an outgroup here. The data presented here enabled to follow up the chromosomal evolution among the

NWMs. Shared chromosomal rearrangements were considered as cladistics markers for linkage. Fig. 3 summarizes a putative pedigree for NWMs analyzed (see also Table 1). The translocation of human 9/22 homologs was observed in both ACA and CJA as a landmark distinct from a sister group of CAP and SSC. And unique translocations of 10/16, 4/16, 2/20, 3/15 and 1/5 in ACA on the sub-chromosomal region level confirmed previous publications (de Oliveira et al., 2012). Furthermore, less number of chromosomal rearrangements was observed in CAP, which proved that CAP at a basal position in NWM depicted before (Neusser et al., 2001; Amaral et al., 2008). Meanwhile, CAP sharing chromosome rearrangements with SSC including two translocations HSA2/16, 3/21 and inversions in HSA20 and HSA12, forming a clade, indicated they have a closer relationship than other two species. This finding is in agreement with previous molecular phylogenetic tree (Finstermeier et al., 2013). The results obtained here are in concordance with previous morphological studies (Ford 1986), however do not fit to recent molecular phylogenetic ones (Perelman et al., 2011; Finstermeier et al., 2013). It is a possible explanation that due to uncoupled molecular and morphological evolution, the likelihood of reconstructing similar phylogenetic relationships was affected. Therefore phylogenetic history merely relied on previous molecular trees need be reevaluate (Perez and Rosenberger, 2014). The controversy of NWM phylogenetic relationship still remains as distinct molecular and morphological datasets, further comparative cytogenetic studies could provide new insights to reach a final conclusion relied on the high resolution of genetic datasets of sufficient species.

5. Conclusion

Overall, the present study provides new insights into chromosomal evolution in NWMs, thus confirming and extending previous observations. Moreover, our results are bases for more detailed characterization of ECBs in future. The latter may then lead to further investigations of genomic features of ECBs, such as tandem repeats, segmental duplications and copy number variant regions. Meanwhile, our molecular cytogenetic data confirms ideas on involvement of FSs in genomic stability during evolution.

Declarations

Author contribution statement

Xiaobo Fan: Conceived and designed the experiments; Performed the experiments; Analyzed and interpreted the data; Wrote the paper.

Weerayuth Supiwong: Performed the experiments.

Anja Weise: Analyzed and interpreted the data; Wrote the paper.

Kristin Mrasek, Nadezda Kosyakova: Analyzed and interpreted the data.

Alongkoad Tanomtong, Krit Pinthong, Vladimir A. Trifonov, Marcelo de Bello Cioffi, Pierre Grothmann, Edivaldo H.C. de Oliveira: Contributed reagents, materials, analysis tools or data.

Thomas Liehr: Conceived and designed the experiments; Contributed reagents, materials, analysis tools or data; Wrote the paper.

Competing interest statement

The authors declare no conflict of interest.

Funding statement

Xiaobo Fan was supported by the China Scholarship Council.

Additional information

Supplementary data associated with this article can be found, in the online version, at http://dx.doi.org/10.1016/j.heliyon.2015.e00042.

References

Amaral, P.J.S., Finotelo, L.F.M., De Oliveira, E.H.C., Pissinatti, A., Nagamachi, C.Y., Pieczarka, J.C., 2008. Phylogenetic studies of the genus Cebus (CebidaePrimates) using chromosome painting and G-banding. BMC Evol. Biol. 8, 169.

Ardito, G., Lamberti, L., Bigatti, P., Stanyon, R., Govone, D., 1987. NOR distribution and satellite association in Callithrix jacchus. Caryologia 40, 185–194.

Archidiacono, N., Antonacci, R., Marzella, R., Finelli, P., Lonoce, A., Rocchi, M., 1995. Comparative mapping of human alphoid sequences in great apes using fluorescence in situ hybridization. Genomics 25, 477–484.

Bailey, J.A., Gu, Z., Clark, R.A., Reinert, K., Samonte, R.V., Schwartz, S., Adams, M.D., Myers, E.W., Li, P.W., Eichler, E.E., 2002. Recent segmental duplications in the human genome. Science 297, 1003–1007.

Bedard, M.T., Ma, N.S.F., Jones, T.C., 1978. Chromosome banding patterns and Nucleolar Organizing Regions in three species of Callithrichidae (Saguinus oedipus, Saguinus fuscicollis and Callithrix jacchus). J Med. Primatol. 7, 82–97.

Bigoni, F., Koehler, U., Stanyon, R., Ishida, T., Wienberg, J., 1997. Fluorescene in situ hybridization establishes homology between human and silvered leaf monkey chromosomes, reveals reciprocal translocations between chromosomes homologous to human Y/5, 1/9, and 6/16, and delineates an X1X2Y1Y2/X1X1X2X2 sex-chromosome system. Am. J Phys. Anthropol. 102, 315–327.

Bucksch, M., Ziegler, M., Kosayakova, N., Mulatinho, M.V., Llerena Jr., J.C., Morlot, S., Fischer, W., Polityko, A.D., Kulpanovich, A.I., Petersen, M.B., Belitz, B., Trifonov, V., Weise, A., Liehr, T., Hamid, A.B., 2012. A new multicolor fluorescence in situ hybridization probe set directed against human heterochromatin: HCM-FISH. J Histochem. Cytochem. 60, 530–536.

Carbone, L., Harris, R.A., Gnerre, S., Veeramah, K.R., Lorente-Galdos, B., Huddleston, J., Meyer, T.J., Herrero, J., Roos, C., Aken, B., Anaclerio, F., Archidiacono, N., Baker, C., Barrell, D., Batzer, M.A., Beal, K., Blancher, A., Bohrson, C.L., Brameier, M., Campbell, M.S., Capozzi, O., Casola, C., Chiatante, G., Cree, A., Damert, A., de Jong, P.J., Dumas, L., Fernandez-Callejo, M., Flicek, P., Fuchs, N.V., Gut, I., Gut, M., Hahn, M.W., Hernandez-Rodriguez, J., Hillier, L.W., Hubley, R., Ianc, B., Izsvák, Z., Jablonski, N.G., Johnstone, L.M., Karimpour-Fard, A., Konkel, M.K., Kostka, D., Lazar, N.H., Lee, S.L., Lewis, L.R., Liu, Y., Locke, D.P., Mallick, S., Mendez, F.L., Muffato, M., Nazareth, L.V., Nevonen, K.A., O'Bleness, M., Ochis, C., Odom, D.T., Pollard, K.S., Quilez, J., Reich, D., Rocchi, M., Schumann, G.G., Searle, S., Sikela, J.M., Skollar, G., Smit, A., Sonmez, K., ten Hallers, B., Terhune, E., Thomas, G.W., Ullmer, B., Ventura, M., Walker, J.A., Wall, J.D., Walter, L., Ward, M.C., Wheelan, S.J., Whelan, C.W., White, S., Wilhelm, L.J., Woerner, A.E., Yandell, M., Zhu, B., Hammer, M.F., Marques-Bonet, T., Eichler, E.E., Fulton, L., Fronick, C., Muzny, D.M., Warren, W.C., Worley, K.C., Rogers, J., Wilson, R.K., Gibbs, R.A., 2014. Gibbon genome and the fast karyotype evolution of small apes. Nature 513, 195–201.

de Oliveira, E.H.C., Neusser, M., Figueiredo, W.B., Nagamachi, C., Pieczarka, J.C., 2002. The phylogeny of howler monkeys (Alouatta, Platyrrhini): reconstruction by multicolor cross-species chromosome painting. Chromosome Res. 10, 669–683.

de Oliveira, E.H.C., Neusser, M., Müller, S., 2012. Chromosome evolution in new world monkeys (Platyrrhini). Cytogenet. Genome Res. 137, 259–272.

Eder, V., Mario, V., Ianigro, M., Teti, M., Rocchi, M., Archidiacono, N., 2003. Chromosome 6 phylogeny in primates and centromere repositioning. Mol. Biol. Evol. 20, 1506–1512.

Fan, X., Pinthong, K., Mkrtchyan, H., Siripiyasing, P., Kosyakova, N., Supiwong, W., Tanomtong, A., Chaveerach, A., Liehr, T., de Bello Cioffi, M.,

Weise, A., 2013. First detailed reconstruction of the karyotype of Trachypithecus cristatus (Mammalia: Cercopithecidae). Mol. Cytogenet. 6, 58.

Fan, X., Sangpakdee, W., Tanomtong, A., Chaveerach, A., Pinthong, K., Pornnarong, S., Supiwong, W., Trifonov, V.A., Hovhannisyan, G.G., Aroutouinian, R.M., Liehr, T., Weise, A., 2014a. Molecular cytogenetic analysis of Thai southern pig-tailed macaque (Macaca nemestrina) by multicolor banding. Proceedings of Yerevan State University 2014 46–50.

Fan, X., Sangpakdee, W., Tanomtong, A., Chaveerach, A., Pinthong, K., Pornnarong, S., Supiwong, W., Trifonov, V., Hovhannisyan, G., Loth, K., Hensel, C., Liehr, T., Weise, A., 2014b. Comprehensive molecular cytogenetic analysis of Barbary macaque (Macaca sylvanus). Biol. J Arm. 66, 98–102.

Fan, X., Tanomtong, A., Chaveerach, A., Pinthong, K., Pornnarong, S., Supiwong, W., Liehr, T., Weise, A., 2014c. High resolution karyotype of Thai crab-eating macaque (Macaca fascicularis). Genetika 46, 877–882.

Finelli, P., Stanyon, R., Plesker, R., Ferguson-Smith, M.A., O'Brien, P.C., Wienberg, J., 1999. Reciprocal chromosome painting shows that the great difference in diploid number between human and African green monkey is mostly due to non-Robertsonian fissions. Mamm. Genome 10, 713–718.

Finstermeier, K., Zinner, D., Brameier, M., Meyer, M., Kreuz, E., Hofreiter, M., Roos, C., 2013. A mitogenomic phylogeny of living primates. PLoS One 8, e69504.

Freitas, L., Seuánez, H., 1982. Chromosome heteromorphisms in Cebus apella. J Hum. Evol. 10, 173–180.

Ford, S.M., 1986. Systematics of the New World monkeys. In: Swindler, D.R., Erwin, J. (Eds.), Comparative primate biology, volume I: systematics, evolution and anatomy. Alan R Liss, New York, pp. 73–135.

Fungtammasan, A., Walsh, E., Chiaromonte, F., Eckert, K.A., Makova, K.D., 2012. A genome-wide analysis of common fragile sites: what features determine chromosomal instability in the human genome. Genome Res. 22, 993–1005.

Garcia, F., Nogues, C., Ponsa, M., Ruiz-Herrera, A., Egozcue, J., Garcia Caldes, M., 2000. Chromosomal homologies between humans and Cebus apella (Primates) revealed by ZOO-FISH. Mamm. Genome 11, 399–401.

Goodpasture, C., Bloom, S.E., 1975. Visualization of nucleolar organizer regions im mammalian chromosomes using silver staining. Chromosoma 53, 37–50.

Gross, M., Starke, H., Trifonov, V., Claussen, U., Liehr, T., Weise, A., 2006. A molecular cytogenetic study of chromosome evolution in chimpanzee. Cytogenet. Genome Res. 112, 67–75.

Groves, C., 2001. Primate Taxonomy (Smithsonian Series in Comparative Evolutionary Biology). Smithsonian Institution Press, Washington, London.

Jones, T.C., Ma, N.S.F., 1975. Cytogenetics of the squirrel monkey (Saimiri sciureus). Fed Proc 34, 1646–1650.

Kay, R.F., 2015. New World monkey origins. Science 347, 1068–1069.

Koehler, U., Arnold, N., Wienberg, J., Tofanelli, S., Stanyon, R., 1995. Genomic reorganization and disrupted chromosomal synteny in the siamang (Hylobates syndactylus) revealed by fluorescence in situ hybridization. Am. J Phys. Anthropol. 97, 37–47.

Li, R., Fan, W., Tian, G., Zhu, H., He, L., Cai, J., Huang, Q., Cai, Q., Li, B., Bai, Y., Zhang, Z., Zhang, Y., Wang, W., Li, J., Wei, F., Li, H., Jian, M., Li, J., Zhang, Z., Nielsen, R., Li, D., Gu, W., Yang, Z., Xuan, Z., Ryder, O.A., Leung, F.C., Zhou, Y., Cao, J., Sun, X., Fu, Y., Fang, X., Guo, X., Wang, B., Hou, R., Shen, F., Mu, B., Ni, P., Lin, R., Qian, W., Wang, G., Yu, C., Nie, W., Wang, J., Wu, Z., Liang, H., Min, J., Wu, Q., Cheng, S., Ruan, J., Wang, M., Shi, Z., Wen, M., Liu, B., Ren, X., Zheng, H., Dong, D., Cook, K., Shan, G., Zhang, H., Kosiol, C., Xie, X., Lu, Z., Zheng, H., Li, Y., Steiner, C.C., Lam, T.T., Lin, S., Zhang, Q., Li, G., Tian, J., Gong, T., Liu, H., Zhang, D., Fang, L., Ye, C., Zhang, J., Hu, W., Xu, A., Ren, Y., Zhang, G., Bruford, M.W., Li, Q., Ma, L., Guo, Y., An, N., Hu, Y., Zheng, Y., Shi, Y., Li, Z., Liu, Q., Chen, Y., Zhao, J., Qu, N., Zhao, S., Tian, F., Wang, X., Wang, H., Xu, L., Liu, X., Vinar, T., Wang, Y., Lam, T.W., Yiu, S.M., Liu, S., Zhang, H., Li, D., Huang, Y., Wang, X., Yang, G., Jiang, Z., Wang, J., Qin, N., Li, L., Li, J., Bolund, L., Kristiansen, K., Wong, G.K., Olson, M., Zhang, X., Li, S., Yang, H., Wang, J., Wang, J., 2010. The sequence and de novo assembly of the giant panda genome. Nature 463, 311–317.

Liehr, T., Claussen, U., 2002. Multicolor-FISH approaches for the characterization of human chromosomes in clinical genetics and tumor cytogenetics. Curr. Genomics 3, 213–235.

Liehr, T., Heller, A., Starke, H., Rubtsov, N., Trifonov, V., Mrasek, K., Weise, A., Kuechler, A., Claussen, U., 2002. Microdissection based high resolution multicolor banding for all 24 human chromosomes. Int. J Mol. Med. 9, 335–339.

Liehr, T., Starke, H., Heller, A., Kosyakova, N., Mrasek, K., Gross, M., Karst, C., Steinhaeuser, U., Hunstig, F., Fickelscher, I., Kuechler, A., Trifonov, V.,

Romanenko, S.A., Weise, A., 2006. Multicolor fluorescence in situ hybridization (FISH) applied to FISH-banding. Cytogenet. Genome Res. 114, 240–244.

Liehr, T., Kosayakova, N., Schröder, J., Ziegler, M., Kreskowski, K., Pohle, B., Bhatt, S., Theuss, L., Wilhelm, K., Weise, A., Mrasek, K., 2011. Evidence for correlation of fragile sites and chromosomal breakpoints in carriers of constitutional balanced chromosomal rearrangements. Balkan J Med. Genet. 14, 13–16.

Luke, S., Verma, R.S., 1992. Origin of human chromosome 2. Nat. Genet. 2, 11–12.

Misceo, D., Capozzi, O., Roberto, R., Dell'oglio, M.P., Rocchi, M., Stanyon, R., Archidiacono, N., 2008. Tracking the complex flow of chromosome rearrangements from the Hominoidea ancestor to extant Hylobates and Nomascus gibbons by high-resolution synteny mapping. Genome Res. 18, 1530–1537.

Mrasek, K., Heller, A., Rubtsov, N., Trifonov, V., Starke, H., Rocchi, M., Claussen, U., Liehr, T., 2001. Reconstruction of the female Gorilla gorilla karyotype using 25-color FISH and multicolor banding (MCB). Cytogenet. Cell Genet. 93, 242–248.

Mrasek, K., Heller, A., Rubtsov, N., Trifonov, V., Starke, H., Claussen, U., Liehr, T., 2003. Detailed Hylobateslar karyotype defined by 25-color FISH and multicolor banding. Int. J Mol. Med. 12, 139–146.

Mrasek, K., Schoder, C., Teichmann, A.C., Behr, K., Franze, B., Wilhelm, K., Blaurock, N., Claussen, U., Liehr, T., Weise, A., 2010. Global screening and extended nomenclature for 230 aphidicolin-inducible fragile sites, including 61 yet unreported ones. Int. J Oncol. 36 (4), 929–940.

Mudry, M., Ponsa, M., Borell, A., Egozcue, J., Garcia, M., 1994. Prometaphase chromosomes of the howler monkey (Alouatta caraya): G, C, NOR and restriction enzyme (Res) banding. Am J Primatol 33, 121–132.

Müller, S., Wienberg, J., 2001. Bar-coding primate chromosomes: Molecular cytogenetic screening for the ancestral hominoid karyotype. Hum. Genet. 109, 85–94.

Neusser, M., Stanyon, R., Bigoni, F., Wienberg, J., Müller, S., 2001. Molecular cytotaxonomy of New World monkeys (Platyrrhini) –comparative analysis of five species by multi-color chromosome painting gives evidence for a classification of Callimico goeldii within the family of Callitrichidae. Cytogenet. Cell Genet. 94, 206–215.

Perelman, P., Johnson, W.E., Roos, C., Seuanez, H.N., Horvath, J.E., Moreira, M.A.M., Kessing, B., Pontius, J., Roelke, M., Rumpler, Y., Schneider, M.P.C., Silva, A., O'Brien, S.J., Pecon-Slattery, J., 2011. A molecular phylogeny of living primates. PLoS Genet. 7, e1001342.

Perez, S.I., Rosenberger, A.L., 2014. The status of platyrrhine phylogeny: a metaanalysis and quantitative appraisal of topological hypotheses. J Hum. Evol. 76, 177–187.

Rahn, I.M., Mudry, M.D., Merani, M.S., Solari, A.J., 1996. Meiotic behavior of the X1X2Y1Y2 quadrivalent of the primate Alouatta caraya. Chromosome Res. 4, 350–356.

Richard, F., Lombard, M., Dutrillaux, B., 1996. ZOO-FISH suggests a complete homology between human and Capucin monkey (Platyrrhini) euchromatin. Genomics 36, 417–423.

Ried, T., Baldini, A., Rand, T.C., Ward, D.C., 1992. Simultaneous visualization of seven different DNA probes by in sltu hybridization using combinatorial fluorescence and digital imaging microscopy. Proc. Natl. Acad. Sci. USA 89, 1388–1392.

Rocchi, M., Archidiacono, N., Schempp, W., Capozzi, O., Stanyon, R., 2012. Centromere repositioning in mammals. Heredity 108, 59–67.

Ruiz-Herrera, A., Castresana, J., Robinson, T.J., 2006. Is mammalian chromosomal evolution driven by regions of genome fragility? Genome Biol. 7, R115.

She, X., Horvath, J.E., Jiang, Z., Liu, G., Furey, T.S., Christ, L., Clark, R., Graves, T., Gulden, C.L., Alkan, C., Bailey, J.A., Sahinalp, C., Rocchi, M., Haussler, D., Wilson, R.K., Miller, W., Schwartz, S., Eichler, E.E., 2004. The structure and evolution of centromeric transition regions within the human genome. Nature 430, 857–864.

Sherlock, J.K., Griffin, D.K., Delhanty, J.D.A., Parrington, J.M., 1996. Homologies in human and marmoset (Callithrix jacchus) chromosomes revealed by comparative chromosome painting. Genomics 33, 214–219.

Schrago, C.G., Russo, C.A., 2003. Timing the origin of New World monkeys. Mol. Biol. Evol. 20, 1620–1625.

Srivastava, P.K., Srivastava, A.K., Lucas, F.V., 1969. Somatic chromosomes of squirrel monkey (Saimiri sciureus). Primates 10, 171–180.

Stanyon, R., Wienberg, J., Romagno, D., Bigoni, F., Jauch, A., Cremer, T., 1992. Molecular and classical cytogenetic analyses demonstrate an apomorphic

reciprocal chromosomal translocation in Gorilla gorilla. Am. J Phys. Anthropol. 88, 245–250.

Stanyon, R., Consigliére, S., Müller, S., Morescalchi, A., Neusser, M., Wienberg, J., 2000. Fluorescence in situ hybridization (FISH) maps chromosomal homologies between the dusky titi and squirrel monkey. Am. J Primatol. 50, 95–107.

Stanyon, R., Rocchi, M., Capozzi, O., Roberto, R., Misceo, D., Ventura, M., Cardone, M.F., Bigoni, F., Archidiacono, N., 2008. Primate chromosome evolution: Ancestral karyotypes, marker order, and neocentromeres. Chromosome Res. 16, 17–39.

Ventura, M., Weigl, S., Carbone, L., Cardone, M.F., Misceo, D., Teti, M., D'Addabbo, P., Wandall, A., Björck, E., de Jong, P.J., She, X., Eichler, E.E., Archidiacono, N., Rocchi, M., 2004. Recurrent sites for new centromere seeding. Genome Res. 14, 1696–1703.

Ventura, M., Antonacci, F., Cardone, M.F., Sprague, L.J., Eichler, E.E., Archidiacono, N., Rocchi, M., 2007. Evolutionary formation of new centromeres in macaque. Science 316, 243–246.

Weise, A., Mrasek, K., Fickelscher, I., Claussen, U., Cheung, S.W., Cai, W.W., Liehr, T., Kosyakova, N., 2008. Molecular definition of high-resolution multicolor banding probes: first within the human DNA sequence anchored FISH banding probe set. J Histochem. Cytochem. 56, 487–493.

Weise, A., Kosyakova, N., Voigt, M., Aust, N., Mrasek, K., Wilhelm, K., Liehr, T., Fan, X., 2015. Comprehensive analyses of white-handed gibbon chromosomes enables access to 92 evolutionary conserved breakpoints compared to the human genome. Cytogenet. Genome Res. 145, 42–49.

Wienberg, J., 2005. Fluorescence in situ hybridization to chromosomes as a tool to understand human and primate genome evolution. Cytogenet. Genome Res 108, 139.

Wienberg, J., Jauch, A., Stanyon, R., Cremer, T., 1990. Molecular cytotaxonomy of primates by chromosomal in situ suppression hybridization. Genomics 8, 347–350.

Wienberg, J., Stanyon, R., Jauch, A., Cremer, T., 1992. Homologies in human and Macaca fuscata chromosomes revealed by in situ suppression hybridization with human chromosome specific DNA libraries. Chromosoma 101, 265–270.

3. Discussion

There is no doubt that nonhuman primates (NHPs) have a high degree of similarity with human at many levels including genetic. However, some researchers argue that NHPs models were unsuccessful when used for preclinical trials, and even increased the risk of disease because of species-specific differences (Shanks and Greek 2008). On the other hand numerous successful involvements of NHPs in preclinical studies can be mentioned. As NWMs, CAPs were used in Leishmania infection studies, CJA in Parkinson's disease, ACA in yellow fever and SSC in testing vaccines against malaria. TCR as an OWM with multiple sex chromosome system served to investigate chromosomal rearrangements leading to reproductive diseases (Yoshida et al. 2012); additionally, CAE (OWM as well) was used in AIDS research, and macaques were widely tested in preclinical studies for Alzheimer's disease, HIV infection and hepatitis (Sibal and Samson 2001).

Taken into account the ethical issues to avoid NHPs suffering or discomfort, in this work only peripheral blood samples and/or cell lines derived from NWMs and OWMs were used to prepare chromosomes, and six macaque species were chosen to exclude the influence of introgression leading to a mosaic genome. With increasing the number of NHPs analyzed, comparative cytogenetic studies can provide new insights into chromosomal evolution and the basics of chromosomal rearrangements, possibly transferable on how chromosomal defects in the human disorders appear. Even though whole-genome sequencing in various NHPs was performed, both, molecular cytogenetic data and high resolution genomic data is necessary to get full insights into what may have happened during primate evolution (Haus et al. 2014; article 7).

As mentioned in result part (article 2-7), there were 73 ECBs in TCR, 53 in MNE, MSY and MFA, 41 in CAE, 51 in ACA, 44 in CAP, 47 in CJA, and 64 in SSC. Besides, for the three macaque species MMU, MAR and MAS the identical 53 ECBs were identified as for MNE, MSY and MFA. As shown in article 6 in HLA 92 ECBs were characterized by aCGH using a combination with microdissection. Totally, 730 ECBs were followed during evolution and aligned with FSs observed in HSA. Overall, this work could provide new evidence of relationship of ECBs and FSs, as well as their relation to breakpoints observed in human disorders. Surely, the detailed

characterization of those ECBs provided new insights into evolution of primates. These issues are discussed in the following paragraphs.

3.1 Comparison and limitations of applied and available approaches

Modern molecular cytogenetic techniques play an important role in human genetic diagnostics, especially the FISH approach is a helpful tool in the decisions of genetic consultation and also therapy to cancer (Bishop 2010). With the wide usage of experimental animals to study the pathogenesis of human disorders a basic understanding of genetic content of those animal models is essential. Thus, among others, also numerous comparative cytogenetic studies in NWMs and OWMs have been applied before, using multicolor chromosome painting and reciprocal chromosome painting to establish an overview on chromosome numbers, composition of syntenic blocks and types of evolutionary conserved rearrangements (Finelli et al. 1999, Neusser et al. 2001, Müller et al. 2001, De Oliveira et al. 2002). However, due to the limitations in resolution of such techniques some ECBs escaped detection. In this work application of multicolor banding (MCB) combined with human locus-specific and heterochromatin oriented probes could overcome these problems. MCB technique has been successfully applied previously for confirmation and detailed characterization of ECBs in interchromosomal and intrachromosomal rearrangements (Mrasek et al. 2001 and 2003). However, subtelomeric and centromere-near rearrangements can be missed by MCB (Karst et al. 2006). Thus locus specific probes directed against sub-centromere and sub-telomere were also applied (articles 2-7, unpublished data see appendix). Array-comparative genomic hybridization (aCGH) is normally performed to detect copy number variations in whole genomic DNA, but it cannot be used for analysis of balanced chromosomal rearrangements. However, it is possible as reported in article 6 to combine aCGH with glass-needle-based microdissection. Thus it could be effectively applied for the characterization of ECBs of HLA. As it is a very laborious approach no further species were studied the same way here.

In this study the main focus was on chromosomal evolution. In the literature, next-generation sequencing (NGS) technology was meanwhile applied for mapping of chromosomal breakpoints at the nucleotide base level (Carbone et al. 2014). As discussed in article 7, it is difficult to correctly annotate sequences and accurately

assemble genomes without knowledge of the exact karyotype. Also repetitive DNA present in heterochromatic regions cannot be analyzed by NGS approaches. Therefore, in this work the human heterochromatin oriented heterochromatin mix (HCM) FISH set was applied to identify the presence and distribution of the corresponding repetitive elements in the studied species (articles 2-7, unpublished data see appendix). Even though some progress is to be expected by forthcoming third-generation sequencing technologies including long-read technologies, high-quality finished long-insert clones and new assembly algorithms (Alkan et al. 2011) it is technically not possible to align repetitive sequences correctly, yet. Thus, FISH will be a key player here in the future as well.

Key points: *Multicolor banding (MCB) combining with locus specific probes was an effective tool to characterize new ECBs for the first time in OWMs and NWMs. The identification and characterization of 730 ECBs in the studied 13 species provided the bases to align them with FSs observed.*

3.2 Relationship between observed ECBs and FSs

As aforementioned, overall 730 ECBs were identified, 524 of them involving in OWMs and 206 in NWMs species. As the ECBs characterized in HLA were re-studied by microdissection and aCGH and are detected by other means than the other 638, those 92 ECBs were omitted from further analyses. Thus, 56.3% (116/206) NWM ECBs colocalized with those of OWM (article 7), which further provided the molecular cytogenetic evidence for "fragile-breakage" hypothesis that ECBs are a non-random distribution event during evolution (Ruiz-Herrera et al. 2005b). Moreover this work revealed that these some chromosomes and/or certain chromosomal bands are more susceptible for break-events than others. For example, chromosomal break events were frequent both in OWMs and NWMs on the homologous human chromosomes #3, #7 and #9. This finding is in line with previous reports in mammalian species and primates (Shan et al. 2000, Ruiz-Herrera et al. 2008). Pevzner and Tesler (2003) also suggested that accumulation of ECBs in certain chromosomal regions in evolution. The possible reasons why ECBs appear in solid chromosomal regions were proposed by Becker and Lenhard (2007) that there is a limited proportion of loci involved in adaptive radiation and these loci remain unchanged since their function is

essential to embryonic development of all vertebrates. Besides ECBs of NWMs were conserved in OWMs, numerous inducible monkey FSs presented colocalization with human FSs (Smeets et al. 1990, Fundia et al. 2000, Ruiz-Herrera et al. 2002 and 2005a), and suggested these FSs were conserved during evolution. Furthermore, in Article 1 we reported that FS associated tumor suppressor (FATS) gene in mouse is also evolutionary conserved. Afterwards, our ECBs were aligned with monkeys FSs in this work (unpublished data see appendix). The results showed that low proportion of ECBs correlated with monkeys FSs. This is different from previous reports which suggested there is a significant correlation between ECBs and monkey FSs in both Papionini and Cebus species based on G-banding comparison and chromosomal painting (Ruiz-Herrera et al. 2005a). The possible explanations are that (i) an inter-individual variability appeared in the expression of FSs (Ruiz-Herrera et al. 2005b). (ii) There might be limitations in resolution of previous applied techniques for characterization of the location of monkey FSs which led to mismatch with position of ECBs in this study. Thus, it is necessary to be re-evaluated previous monkey FSs data by current molecular cytogenetic approaches. In addition, the colocalization of features of DNA fragility are also needed to be assessed in ECBs and FSs, take into account that insertion of some dinucleotide repeats into AT-rich sequences is a feature of FS-induced instability; such regions are susceptible to DNA lesions induced by replication-blocking (Article 1).

In concordance to previously published data (Ruiz-Herrera et al. 2006, Mrasek et al. 2010), human FSs were further aligned with the ECBs in NWMs and OWMs (article 7). Strikingly a high percentage of human FSs correlated with ECBs in OWMs and NWMs (for example 78.1% in TCR, 75.5% in macaques, 58.5% in CAE, 60.8% in ACA, 65.5% in CAP, 72.3% in CJA and 70.3% in SSC, respectively). The results are in line with article 6 that a high rate of coincidence (70.6%) between ECBs of HLA and human FSs. Our results suggested that ECB regions are highly relevant for and connected to FSs formation, possibly according to the FSs breakage frequency model that based on the statistical analysis (the FSs data from previous study by Mrasek) to predict the probability of a given region to be FSs and predict expected breakage frequency. This model suggested that the breakage frequency of FSs appears to increase in ECBs regions (Fungtammasan et al. 2012). Furthermore, article 6 has reported the colocalization of copy number variants (CNVs), FSs and

ECBs in HLA. CNVs were implicated in chromosomal rearrangements with high recombination rates, and FSs under replication stress may induce CNVs formation, which suggests CNVs play a role in chromosomal evolution, either as a cause or a consequence of chromosomal rearrangements. Additionally, some genes located at cFS actively monitor DNA damage response and have an important role in maintaining genomic stability (Article 1). Taken into account the concentration of FSs at ECB regions and evolutionary conserved FATS genes in tumors, the further assessment of relations between ECBs and breakpoints observed in human disorders will serve to illustrate pathological significance of ECBs.

Key points: *ECBs in NWMs were partially conserved from those in OWMs; the chromosomes homologous to human #3, #7 and #9 present a yet unexplained high frequency of break events in OWMs and NWMs. This work provides further evidence of a correlation of human FSs and ECBs that was characterized here for the first time in OWMs and NWMs.*

3.3 Implications of obtained results for understanding of breakpoints observed in human genetic diagnostics

According to our previous publications about constitutional balanced chromosomal rearrangements, 529 break events from 251 patients were exactly identified by multicolor banding (MCB) and/or subcentromeric multicolor fluorescence in situ hybridization (subcenM-FISH). ~71% of the studied break-events showed colocalization with FSs, which provided evidence for correlation of breakpoints involved in constitutional chromosomal rearrangements and FSs (Liehr et al. 2011). A possible relationship between ECBs and breakpoints that was observed in constitutional chromosomal rearrangements was further investigated (see in appendix). This study revealed that there was colocalization in 64.3% of the studied ECBs in TCR, 71.7% in each macaque species, 58.5% in CAE, 74.5% in ACA, 77.3% in CAP, 78.7% in CJA and 81.25% in SSC, respectively (unpublished data see appendix). This results confirm previous reports that ECBs were colocalized with breakpoints detected in human pathologies based on G-banding comparisons and whole chromosome paints (WCP) (Ruiz-Herrera et al. 2005b), and further support the hypothesis that the distribution of pathological chromosomal breakages are

nonrandom but preferably form in chromosomal bands prone to breakage also during evolution.

Interestingly, more than 50% of ECBs colocalizing with human FSs correspond to breakpoints observed in human disorders (unpublished data see appendix). 54.8% correspond to that of TCR, 58.5% in each macaque species, 52.3% in CAP, 57.4% in CJA and 60.9% in SSC, whereas in CAE and ACA species, the percentage of correspondence is less than 50% (34.1% and 49.01%, respectively). These results further suggest that ECB regions could be considered as “hot zones” for FS formation as well as breakpoints detected in human pathologies. Also, intrachromosomal telomeric sequences (ITSs) are genetic marker that integrated into chromosomes due to rearrangement and are mostly located at breakpoints (Ruiz-Herrera et al. 2005a). Thus, the further detection of the distribution of ITSs in NWMs and OWMs to compare with those in human could serve to provide genomic information of chromosomal reorganization.

As aforementioned, there are enhanced rates of chromosomal rearrangements involving homologous human chromosome #3, #7 and #9 in OWMs and NWMs (article 2-5 and 7). This observation is in concordance with our previous report that the distribution of clinical cytogenetic breakpoints was not uniform and unaffected by the size of the chromosomes (Liehr et al. 2011). With further analysis of these three chromosomes, we observed that some ECBs not only co-localized with human FSs but also corresponded to human clinical breakpoints in certain chromosomal bands. In particular, seven chromosomal bands (3p25.3, 3p11.1, 3q12.1, 3p21.31, 7q11.23, 9p24.3 and 9q34) showed higher frequencies present both in OWMs and NWMs. Taking into account that FSs were implicated as regions of chromosomal instability associated with cancer and ECBs had pathological consequences, I searched these chromosomal bands in Mitelman and OMIM database (http://omim.org/ and http://cgap.nci.nih.gov/Chromosomes/Mitelman). The searching results showed that a large number of the cancer cases and the Mendelian disease loci related chromosomal aberrations have most frequently hit by three chromosomal bands where 3p21.31, 7q11.23 and 9q34 (see table 2 in appendix). These three bands including the large number of repetitive elements, CNVs and segmental duplications (Ruiz-Herrera et al. 2006, Yatsenko et al. 2009) that are susceptible to increase the probability of structural fragility in both evolutionary and disease-associated

chromosome rearrangements (Darai et al. 2005), which played a role in known human disorders, such as tumor suppressor genes (TSGs) of the lung and breast cancer in 3p21.31, Williams–Beuren syndrome (WBS) in 7q21.31 and chronic myelogenous leukemia (CML) in 9q34 (Berg et al. 2007). Furthermore our results support the hypothesis of article 6 that ECBs could affect in the phenotype directly or indirectly, either due to interruption of genes or due to position effects influencing the expression/regulation of corresponding genes. Overall, this study provides the potential evidence of ECBs implicated in human disorders.

Key points: *ECBs in this work had a high positive correlation with chromosomal breakpoints in human disorders. Moreover, more than 50% of ECBs colocalizing with human FSs correspond to breakpoints observed in human disorders, involving seven highly frequent homologous chromosomal bands.*

3.4 Impact of the conducted research in evolutionary research

3.4.1 ECBs and phylogeny

In OWMs, firstly we characterized TCR specie with a multiple sex chromosome system by molecular cytogenetic procedures, which provided new insights into chromosomal constitution and evolution (article 2). Secondly, we confirmed that there are no gross cytogenetic differences between macaque species (articles 3-5 and unpublished data see appendix). Thirdly, CAE has higher chromosome numbers as a result of fission mechanisms during evolution. Characterization of CAE chromosomal structures was considered as evolutionary markers to place it as outgroup of NWM phylogeny (article 7). Finally, the chromosomal rearrangements of eight OWM species including TCR, CAE and six macaque species (MAR, MAS, MMU, MFA, MNE and MSY) have been completed to compare with HSA. Our results provided a clue to reveal a relationship of the chromosomal evolution in OWMs based on common chromosomal rearrangements as cladistics markers. For example, the unique translocations homologous to human 1/19, 5/Y and 6/16 homologs were observed in TCR as a landmark distinct from macaques and CAE (subfamily Cercopithecinae). Meanwhile, the homologous associations of 7/21 and 20/22 homologs in macaques that resulted in reduced chromosome number were

confirmed. The reconstruction of relationship in OWMs was consistent with previous molecular phylogenetic tree on the basis of 54 genes (Perelman et al. 2011).
In four NWMs, our results confirmed the previous suggestion that the NWMs are a closely related group of species, and further confirmed previous results on the sub-chromosomal region level (De Oliveira et al. 2002). As mentioned in the article 7, four NWMs shared associations homologous to human 3/21, 14/15, 10/16 and 8/18 as well as several chromosomal segments from fission events. The common translocation of human 9/22 homologs in both ACA and CJA presented a difference from a sister group of CAP and SSC. These observations demonstrated that CJA was to place together with ACA as one clade. Furthermore, CAP and SSC had a closer relationship than other two species, due to two shared translocations and two inversions (article 7). Our results were consistent with previous morphological studies (Ford 1986), however mismatched to recent molecular phylogenetic tree (Finstermeier et al. 2013). It is a constructive suggestion that uncoupled molecular and morphological evolution affected the likelihood of reconstructing similar phylogenetic relationships (Perez et al. 2014). Therefore, phylogenetic history merely relied on previous molecular trees, need be reevaluate. The issue of NWM phylogenetic relationship still is debated on the basis of distinct molecular and morphological datasets, however, chromosomal evolution studies in as many species as possible can also give new insights to reach a final conclusion on primate evolution.

Key points: *Shared chromosomal rearrangements can be used as cladistics markers to reconstruct linkage. Unique translocations in TCR can be as a landmark to separate this species from macaques and CAE (subfamily Cercopithecinae). Additionally, CAP and SSC can now be considered as closer related and being distinct from a sister group consisting of CJA and ACA. However, the phylogenetic relationship in NWMs still remains discussed controversy due to uncoupled molecular data and morphological evolution, affecting the reconstruction similar phylogenetic relationships. Therefore, chromosomal evolution studies of sufficient species will provide to come to clearer conclusions.*

3.4.2 Centromere positioning in OWM and NWM

Centromere repositioning with chromosomal rearrangement process is a widespread phenomenon in genome evolution. It is well known that the centromeric regions do not contain identical alphoid DNA stretches; this is understood as a hint on faster evolution of these genomic regions compared to others, euchromatic ones (Archidiacono et al. 1995). In this work, subcentromeric and subtelomeric probes that located next to centromeres and telomeres were applied besides MCB. In OWMs, twenty-two of all TCR chromosomes (2n = 44) are conserved with those of HSA and in 50% of TCR chromosomes centromeric positions have changed (article 2). This percentage of centromere repositioning is similar to those in six macaque species (article 3-5, unpublished data see table 3 in appendix). Ventura and co-workers suggested neo-centromeres in macaque could be rapidly stabilized by acquiring new alpha satellite DNA (Ventura et al. 2007).

However, more than 60% of centromeric shifts appeared in CAE and four NWMs chromosomes (article 7). It is a possible explanation that centromeres in OWMs and NWMs followed an independent evolutionary path (Montefalcone et al. 1999). Additionally, we confirmed the previous report that the position of centromere can change along the chromosome without any chromosomal rearrangements (Rocchi et al. 2009), for example in ACA#11 and SSC-X (article 7). According previously discussed for HLA (Mrasek et al. 2003) identical regions can be used twice for centromere-seeding, and regions being telomeric in HSA can be centromeric positions in OWMs and NWMs (article 2-5 and 7), for example TCR#1, ACA#1, CAE#12, CAP#7, CJA#13 and SSC#5. Moreover, a similar finding was reported for the centromere of human chromosome 15 that occurred in the telomeric region of the short arm of the ancestral chromosome 15/14 association (Ventura et al. 2004). Evolutionary neo-centromeres appearance in telomeric regions may be affected by the spread of subcentromeric duplications, owing to relatively frequent duplicon exchanges between subcentromeric and subtelomeric duplications (Bailey et al. 2002).

Key points: *Centromere repositioning occurs very often during chromosomal evolution. In present study, the percentages of conserved centromeres in TCR and macaque species are similar to those of centromere shift, however, a slightly higher percentage of centromere repositioning appeared in CAE and four NWMs. Take into*

account the present interspecific differences, centromeres in OWMs and NWMs underwent an independent evolutionary path.

4. Conclusion and Outlook

Evolutionary conserved breakpoints (ECBs) in Old World Monkeys (OWMs) and New World Monkeys (NWMs) were characterized by human multicolor banding (MCB) probe sets complemented with selected locus-specific and heterochromatin specific probes. Thus, in this work numerous new ECBs were characterized for the first time in eight OWMs and four NWMs, such as TCR, MNE, MSY, MFA, MMU, MAR, MAS, CAE, ACA, CJA, CAP and SSC. Based on alignment of obtained ECBs and fragile sites (FSs) observed in *Homo sapiens* (HSA), more precise conclusions can be drawn concerning the relationship of ECBs and FSs as well as their correspondence to breakpoints that observed in human disorders.

Thus the questions raised in 1.4 can be answered as follows:

(1) In this study ECBs and chromosomal rearrangements were detected effectively by multicolor banding (MCB) combining with locus specific probes, which confirmed previous published data in OWMs and NWMs. Importantly, the identification and characterization of numerous new ECBs for the first time in OWMs and NWMs provide the bases to align them with FSs observed in HSA.

(2) In OWMs and NWMs, our results showed a positive correlation of ECBs and human FSs.

(3) A high percentage of human FSs colocalized with ECBs in OWMs and NWMs e.g. 78.1% in TCR, 75.5% in macaques, 58.5% in CAE, 60.8% in ACA, 65.5% in CAP, 72.3% in CJA and 70.3% in SSC, which provides full insights into a relationship of human FSs and ECBs.

(4) In the aspect of human disease, ECBs of the studied species had a high positive correlation with chromosomal breakpoints that can be observed in human disorders. A cancer related breakpoint was studied in more detail.

Overall, for medical field this data is important as FSs now clearly were aligned on molecular level with ECBs. In other words the disease associated chromosomal defects, seem at least in parts be due to breakage prone regions of the mammalian genome. The fact that breakpoint regions are now narrowed down more precisely is important prerequisite for further comparative studies to understand the genomic mechanism of ECBs and FSs. In the future we will

attempt to microdissect whole chromosome-specific probes of the here studied species and prepare them for aCGH. Afterwards, locus-specific DNA probes will be applied for further characterization of regions of interest to resolve ECBs involved in balanced as well as in unbalanced rearrangements. This approach will enable a more precise breakpoint mapping to obtain most comprehensive information on ECBs. At last, next-generation whole genome sequencing may provide additional insights into specific gene information and functional mechanisms linked with large-scale changes during speciation.

5. References

Abeysinghe SS, Chuzhanova N, Krawczak M, Ball EV, Cooper DN. 2003. Translocation and gross deletion breakpoints in human inherited disease and cancer I: Nucleotide composition and recombination-associated motifs. Human mutation, 22(3):229-244.

Alkan C, Sajjadian S, Eichler EE. 2011. Limitations of next-generation genome sequence assembly. Nature methods, 8(1):61-65.

Aqeilan RI. 2014. Role of common fragile sites and corresponding genes in cancer development. Cellular and Molecular Life Sciences, 71(23):4487-4488.

Archidiacono N, Antonacci R, Marzella R, Finelli P, Lonoce A, Rocchi M. 1995. Comparative mapping of human alphoid sequences in great apes using fluorescence in situ hybridization. Genomics, 25(2):477-484.

Arlt MF, Durkin SG, Ragland RL, Glover TW. 2006. Common fragile sites as targets for chromosome rearrangements. DNA repair, 5(9):1126-1135.

Bailey JA, Gu Z, Clark RA, Reinert K, Samonte RV, Schwartz S, Eichler EE. 2002. Recent segmental duplications in the human genome. Science, 297(5583):1003-1007.

Bakker B, van den Bos H, Lansdorp PM, Foijer F. 2015. How to count chromosomes in a cell: An overview of current and novel technologies. BioEssays, 37(5):570-577.

Becker TS, Lenhard B. 2007. The random versus fragile breakage models of chromosome evolution: a matter of resolution. Molecular Genetics and Genomics, 278(5):487-491.

Bedard MT, Ma NS, Jones TC. 1977. Chromosome banding patterns and nucleolar organizing regions in three species of Callithricidae (Saguinus

oedipus, Saguinus fuscicollis, and Callithrix jacchus). Journal of medical primatology, 7(2):82-97.

Bender MA, Mettler LE. 1958. Chromosome Studies of Primates The application of new culture and cytological techniques should help solve some puzzles of evolution. Science, 128(3317):186-190.

Benirschke K, Anderson JM, Brownhill LE. 1962. Marrow chimerism in marmosets. Science, 138(3539):513-515.

Berg JS, Brunetti-Pierri N, Peters SU, et al. Speech delay and autism spectrum behaviors are frequently associated with duplication of the 7q11.23 Williams-Beuren syndrome region. Genet. Med. 2007,9:427–441.

Bigoni F, Koehler U, Stanyon R, Ishida T, Wienberg J. 1997. Fluorescence in situ hybridization establishes homology between human and silvered leaf monkey chromosomes, reveals reciprocal translocations between chromosomes homologous to human Y/5, 1/9, and 6/16, and delineates an X1 X2 Y1 Y2/X1 X1 X2 X2 sex-chromosome system. American journal of physical anthropology, 102(3):315-327.

Bishop R. 2010. Applications of fluorescence in situ hybridization (FISH) in detecting genetic aberrations of medical significance. Bioscience Horizons, 3:85-95.

Bosinger SE, Johnson ZP, Silvestri G. 2011. Primate genomes for biomedicine. Nature biotechnology, 29(11):983-984.

Burrow AA, Williams LE, Pierce LC, Wang YH. 2009. Over half of breakpoints in gene pairs involved in cancer-specific recurrent translocations are mapped to human chromosomal fragile sites. BMC genomics, 10(1):59.

Carbone L, Harris RA, Gnerre S, Veeramah KR, Lorente-Galdos Band others. 2014. Gibbon genome and the fast karyotype evolution of small apes. Nature, 513(7517):195-201.

Caspersson T, Zech L, Modest EJ, Foley GE, Wagh U, Simonsson E. 1969. Chemical differentiation with fluorescent alkylating agents in Vicia faba metaphase chromosomes. Experimental cell research, 58(1):128-140.

Darai E, Kost-Alimova M, Kiss H, Kansoul H, Klein G, Imreh S. 2005. Evolutionarily plastic regions at human 3p21.3 coincide with tumor breakpoints identified by the “elimination test”. Genomics, 86(1):1-12.

Darlington CD, Haque A. 1955. Chromosomes of monkeys and men. Nature, 175(4444):32.

De Oliveira EHC, Neusser M, Figueiredo WB, Nagamachi C, Pieczarka JC, Sbalqueiro IJ, Müller S. 2002. The phylogeny of howler monkeys (Alouatta, Platyrrhini): reconstruction by multicolor cross-species chromosome painting. Chromosome Research, 10(8):669-683.

De Oliveira EHC, Neusser M, Müller S. 2012. Chromosome evolution in new world monkeys (Platyrrhini). Cytogenetic and genome research, 137(2-4):259-272.

Debacker K, Kooy RF. 2007. Fragile sites and human disease. Human molecular genetics, 16(R2):R150-R158.

Durkin SG, Glover TW. 2007. Chromosome fragile sites. Annu. Rev. Genet., 41:169-192.

Dutrillaux B, Couturier J, Muleris M, Lombard M, Chauvier G. 1981. Chromosomal phylogeny of forty-two species or subspecies of cercopithecoids (Primates Catarrhini). In Annales de genetique, 25(2):96-109.

Dutrillaux B, Webb G, Muleris M, Couturier J, Butler R. 1983. Chromosome study of Presbytis cristatus: presence of a complex Y-autosome rearrangement in the male. In Annales de genetique, 27(3):148-153.

Egozcue J, De Egozcue MV. 1966. The chromosome complement of the howler monkey (Alouatta caraya, Humboldt 1812). Cytogenetic and Genome Research, 5(1-2):20-27.

Ehrlich J, Sankoff D, Nadeau JH. 1997. Synteny conservation and chromosome rearrangements during mammalian evolution. Genetics, 147(1):289-296.

Estop A, Garver J, Pearson PL. 1978. Further studies on the comparative karyology of the African Green and Rhesus monkeys. Genetica, 49(2):131-138.

Finelli P, Stanyon R, Plesker R, Ferguson-Smith MA, O'brien P, Wienberg J. 1999. Reciprocal chromosome painting shows that the great difference in diploid number between human and African green monkey is mostly due to non-Robertsonian fissions. Mammalian genome, 10(7):713-718.

Finstermeier K, Zinner D, Brameier M, Meyer M, Kreuz E, Hofreiter M, Roos C. 2013. A mitogenomic phylogeny of living primates. PLoS One, 8(7):e69504.

Fooden J. 1976. Primates obtained in peninsular Thailand June–July, 1973, with notes on the distribution of continental Southeast Asian leaf-monkeys (Presbytis). Primates, 17(1):95-118.

Ford SM. 1986. Systematics of the New World monkeys. In: Swindler DR, Erwin J (eds) Comparative primate biology, volume I: systematics, evolution and anatomy. New York: Alan R Liss, pp.73–135.

Freitas L, Seuánez H. 1982. Chromosome heteromorphisms in Cebus apella. Journal of Human Evolution, 11(2):173-180.

Fundia A, Gorostiaga M, Mudry M. 2000. Expression of common fragile sites in two Ceboidea species: Saimiri boliviensis and Alouatta caraya (Primates: Platyrrhini). Genetics Selection Evolution, 32(1):87-98.

Fungtammasan A, Walsh E, Chiaromonte F, Eckert KA, Makova KD. 2012. A genome-wide analysis of common fragile sites: what features determine chromosomal instability in the human genome? Genome research, 22(6):993-1005.

Garcia F, Nogués C, Ponsà M, Ruiz-Herrera A, Egozcue J, Garcia Caldés M. 2000. Chromosomal homologies between humans and Cebus apella (Primates) revealed by ZOO-FISH. Mammalian Genome, 11(5):399-401.

Gibbs RA, Rogers J, Katze MG, Bumgarner R, Weinstock GM, Mardis ER,Remington KA, Strausberg RL, Venter JCand others. 2007. Evolutionary and biomedical insights from the rhesus macaque genome. science, 316(5822):222-234.

Glover TW, Arlt MF, Casper AM, Durkin SG. 2005. Mechanisms of common fragile site instability. Human molecular genetics, 14(2):R197-R205.

Goodpasture C, Bloom SE. 1975. Visualization of nucleolar organizer regions in mammalian chromosomes using silver staining. Chromosoma, 53(1):37-50.

Graphodatsky A, Ferguson-Smith MA, Stanyon R. 2012. A short introduction to cytogenetic studies in mammals with reference to the present volume. Cytogenetic and genome research, 137(2-4):83-96.

Griffiths AJF, WM Gelbart, JH Miller, RC Lewontin. 1999. Modern genetic analysis, New York: W.H. Freeman and Company, pp. 586–587.

Groves C. 2001 Primate Taxonomy (Smithsonian Series in Comparative Evolutionary Biology), Smithsonian Institution Press, Washington, London.

Guan XY, Meltzer PS, Trent JM. 1994. Rapid generation of whole chromosome painting probes (WCPs) by chromosome microdissection. Genomics, 22(1):101-107.

Hamerton JL, Klinger HP, Mutton DE, Lang EM. 1963. The somatic chromosomes of the Hominoidea. Cytogenetic and Genome Research, 2(4-5):240-263.

Harding LE. 2010. Trachypithecus cristatus (Primates: Cercopithecidae). Mammalian Species, 42(1):149-165.

Haus T, Ferguson B, Rogers J, Doxiadis G, Certa U, Rose NJand others. 2014. Genome typing of nonhuman primate models: implications for biomedical research. Trends in Genetics, 30(11):482-487.

Higashino A, Sakate R, Kameoka Y, Takahashi I, Hirata M, Tanuma Rand others. 2012. Whole-genome sequencing and analysis of the Malaysian cynomolgus macaque (Macaca fascicularis) genome. Genome Biol, 13(7):R58.

Hsu TC, Benirschke K. 1970. In: An atlas of mammalian chromosomes. NewYork: Springer-Verlag, Folio, 199.

Huang HE, Chin SF, Ginestier C, Bardou VJ, Adélaïde J, Iyer NGand others. 2004. A recurrent chromosome breakpoint in breast cancer at the NRG1/neuregulin 1/heregulin gene. Cancer research, 64(19):6840-6844.

Jasinska AJ, Levinson M, Slaten E, Lee O, Sobel E, Fairbanks LAand others. 2007. A genetic linkage map of the vervet monkey (Chlorocebus aethiops sabaeus). Mammalian Genome, 18(5):347-360.

Jauch A, Wienberg J, Stanyon R, Arnold N, Tofanelli S, Ishida T, Cremer T. 1992. Reconstruction of genomic rearrangements in great apes and gibbons by chromosome painting. Proceedings of the National Academy of Sciences, 89(18):8611-8615.

Jones TC, Ma NS. 1975. Cytogenetics of the squirrel monkey (Saimiri sciureus). In Primate Research, Springer US, pp. 13-21.

Jones TC, Thorington RW, Hu MM, Adams E, Cooper RW. 1973. Karyotypes of squirrel monkeys (Saimiri sciureus) from different geographic regions. American journal of physical anthropology, 38(2):269-277.

Kallioniemi A, Kallioniemi OP, Sudar D, Rutovitz D, Gray JW, Waldman F, Pinkel D. 1992. Comparative genomic hybridization for molecular cytogenetic analysis of solid tumors. Science, 258(5083):818-821.

Karst C, Gross M, Haase D, Wedding U, Höffken K, Liehr T, Mkrtchyan H. 2006. Novel cryptic chromosomal rearrangements detected in acute lymphoblastic leukemia detected by application of new multicolor fluorescent in situ hybridization approaches. International journal of oncology, 28(4):891-897.

Kay RF. 2015. New World monkey origins. Science, 347(6226):1067-1068.

Kearney L. 2001. Molecular cytogenetics. Best Practice & Research Clinical Haematology, 14(3):645-668.

Lau YF, Arrighi FE, Chuang CR. 1977. Studies of the squirrel monkey, Saimiri sciureus, genome. Cytogenetic and Genome Research, 19(1):14-25.

Lejeune J, Gautier M, Turpin R. 1959. Les chromosomes somatique des enfants mongoliens. Comptes Rendu Acad Sci Paris 248:1721.

Liehr T, Claussen U. 2002. Current developments in human molecular cytogenetic techniques. Current molecular medicine, 2(3):283-297.

Liehr T, Kosayakova N, Schröder J, Ziegler M, Kreskowski K, Pohle Band others. 2011. Evidence for correlation of fragile sites and chromosomal breakpoints in carriers of constitutional balanced chromosomal rearrangements. Balkan Journal of Medical Genetics, 14(2):13-16.

Lukusa T, Fryns JP. 2008. Human chromosome fragility. Biochimica et Biophysica Acta (BBA)-Gene Regulatory Mechanisms, 1779(1):3-16.

Marmoset Genome Sequencing and Analysis Consortium. 2014. The common marmoset genome provides insight into primate biology and evolution. Nature Genetics, 46(8): 850–857.

Matsudaira K, Ishida T. 2010. Phylogenetic relationships and divergence dates of the whole mitochondrial genome sequences among three gibbon genera. Molecular phylogenetics and evolution, 55(2):454-459.

Misceo D, Capozzi O, Roberto R, Dell'Oglio MP, Rocchi M, Stanyon Rand others. 2008. Tracking the complex flow of chromosome rearrangements from the Hominoidea Ancestor to extant Hylobates and Nomascus Gibbons by high-resolution synteny mapping. Genome research, 18(9):1530-1537.

Montefalcone G, Tempesta S, Rocchi M, Archidiacono N. 1999. Centromere repositioning. Genome research, 9(12):1184-1188.

Mrasek K, Heller A, Rubtsov N, Trifonov V, Starke H, Rocchi M, Liehr, T. 2001. Reconstruction of the female Gorilla gorilla karyotype using 25-color FISH and multicolor banding (MCB). Cytogenetic and Genome Research, 93(3-4):242-248.

Mrasek K, Heller A, Rubtsov N, Trifonov V, Starke H, Claussen U, Liehr, T. 2003. Detailed Hylobates lar karyotype defined by 25-color FISH and multicolor banding. International journal of molecular medicine, 12(2):139-146.

Mrasek K, Schoder C, Teichmann AC, Behr K, Franze B, Wilhelm K, Weise A. 2010. Global screening and extended nomenclature for 230 aphidicolin-inducible fragile sites, including 61 yet unreported ones. International journal of oncology, 36(4):929-940.

Mudry de Pargament MD. Labal de Vinuesa, ML Colillas, OJ Brieux de Salum S. 1984. Banding patterns of Alouatta caraya. Revista Brasileira de Genetica, 7(2):373-379.

Muleris M, Couturier J, Dutrillaux B. 1986. Phylogénie chromosomique des Cercopithecoidea. Mammalia, 50:38-52.

Müller S, Wienberg J. 2001. "Bar-coding" primate chromosomes: molecular cytogenetic screening for the ancestral hominoid karyotype. Human genetics, 109(1):85-94.

Müller S, Neusser M, Wienberg J. 2002. Towards unlimited colors for fluorescence in-situ hybridization (FISH). Chromosome Research, 10(3):223-232.

Neusser M, Stanyon R, Bigoni F, Wienberg J, Müller S. 2001. Molecular cytotaxonomy of New World monkeys (Platyrrhini)–comparative analysis of five species by multi-color chromosome painting gives evidence for a classification of Callimico goeldii within the family of Callitrichidae. Cytogenetic and Genome Research, 94(3-4):206-215.

O'Connor C, Miko I. 2008. Developing the chromosome theory. Nature Education, 1(1):44.

Pardue ML, Gall JG. 1970. Chromosomal localization of mouse satellite DNA. Science, 168(3937):1356-1358.

Perelman P, Johnson WE, Roos C, Seuánez HN, Horvath JE, Moreira MAand others. 2011. A molecular phylogeny of living primates. PLoS Genet, 7(3):e1001342.

Perez SI, Rosenberger AL. 2014. The status of platyrrhine phylogeny: A meta-analysis and quantitative appraisal of topological hypotheses. Journal of human evolution, 76:177-187.

Perrotez C. 1974. Etude du caryotype du marmoset (Callithrix jacchus) avec des bandes R. Experimentation Animale, 7:173–180.

Pevzner P, Tesler G. 2003. Human and mouse genomic sequences reveal extensive breakpoint reuse in mammalian evolution. Proc Natl Acad Sci USA 100:7672–7677.

Picone B, Sineo L. 2010. Reconstructing the phylogeny of the human chromosome 4 synteny using comparative karyology and genomic data analysis. Caryologia, 63(3):314-334.

Pinkel D, Segraves R, Sudar D, Clark S, Poole I, Kowbel D, Dairkee SH, Ljung BM, Gray JW, Albertson DG. 1998. High resolution analysis of DNA copy number variation using comparative genomic hybridization to microarrays. Nature genetics, 20(2):207-211.

Pinkel D, Straume T, Gray JW. 1986. Cytogenetic analysis using quantitative, high-sensitivity, fluorescence hybridization. Proceedings of the National Academy of Sciences, 83(9):2934-2938.

Ponsa M, De Boer LEM, Egozcue J. 1983. Banding patterns of the chromosomes of Presbytis cristatus pyrrhus and P. obscurus. American Journal of Primatology, 4(2):165-169.

Rahn MI, Mudry M, Merani MS, Solari AJ. 1996. Meiotic behavior of the X1X2Y1Y2 quadrivalent of the primateAlouatta caraya. Chromosome Research, 4(5):350-356.

Richard F, Lombard M, Dutrillaux B. 1996. ZOO-FISH suggests a complete homology between human and capuchin monkey (Platyrrhini) euchromatin. Genomics, 36(3):417-423.

Ried T, Arnold N, Ward DC, Wienberg J. 1993. Comparative high-resolution mapping of human and primate chromosomes by fluorescence in situ hybridization. Genomics, 18(2):381-386.

Rieseberg LH. 2001. Chromosomal rearrangements and speciation. Trends in Ecology & Evolution, 16(7):351-358.

Rocchi M, Archidiacono N, Schempp W, Capozzi O, Stanyon R. 2012. Centromere repositioning in mammals. Heredity, 108(1):59-67.

Rocchi M, Stanyon R, Archidiacono N. 2009. Evolutionary new centromeres in primates. In Centromere Springer Berlin Heidelberg, pp. 103-152.

Roos C, Nadler T, Walter L. 2008. Mitochondrial phylogeny, taxonomy and biogeography of the silvered langur species group (Trachypithecus cristatus). Molecular Phylogenetics and Evolution, 47(2):629-636.

Rothfels KH, Siminovitch L. 1957. The chromosome complement of the Rhesus monkey (Macaca mulatta) determined in kidney cells cultivated in vitro. Chromosoma, 9(1):163-175.

Ruiz-Herrera A, Castresana J, Robinson TJ. 2006. Is mammalian chromosomal evolution driven by regions of genome fragility? Genome biology, 7(12):R115.

Ruiz-Herrera A, Garcia F, Azzalin C, Giulotto E, Egozcue J, Ponsa M, Garcia M. 2002. Distribution of intrachromosomal telomeric sequences (ITS) on Macaca fascicularis (Primates) chromosomes and their implication for chromosome evolution. Human genetics, 110(6):578-586.

Ruiz-Herrera A, Garcia F, Giulotto E, Attolini C, Egozcue J, Ponsa M, Garcia M. 2005a. Evolutionary breakpoints are co-localized with fragile sites and intrachromosomal telomeric sequences in primates. Cytogenetic and genome research, 108(1-3):234-247.

Ruiz-Herrera A, Garcia F, Mora L, Egozcue J, Ponsà M, Garcia M. 2005b. Evolutionary conserved chromosomal segments in the human karyotype are bounded by unstable chromosome bands. Cytogenetic and genome research, 108(1-3):161-174.

Ruiz-Herrera A, Ponsà M, Garcia F, Egozcue J, Garcia M. 2002. Fragile sites in human and Macaca fascicularis chromosomes are breakpoints in chromosome evolution. Chromosome Research, 10(1):33-44.

Ruiz-Herrera A, Robinson TJ. 2008. Evolutionary plasticity and cancer breakpoints in human chromosome 3. BioEssays, 30(11-12):1126-1137.

Schrago CG, Russo CA. 2003. Timing the origin of New World monkeys. Molecular Biology and Evolution, 20(10):1620-1625.

Schröck E, Du Manoir S, Veldman T, Schoell B, Wienberg J, Ferguson-Smith MA, Garini Y. 1996. Multicolor spectral karyotyping of human chromosomes. Science, 273(5274):494-497.

Schwartz M, Zlotorynski E, Kerem B. 2006. The molecular basis of common and rare fragile sites. Cancer letters, 232(1):13-26.

Seabright M. 1971. A rapid banding technique for human chromosomes. The Lancet, 298(7731):971-972.

Shan Z, Zabel B, Trautmann U, Hillig U, Ottolenghi C, Wang Y, Haaf T. 2000. FISH mapping of the sex-reversal region on human chromosome 9p in two XY females and in primates. European Journal of Human Genetics, 8(3):167-173.

Shanks N, Greek R. 2008. Experimental use of nonhuman primates is not a simple problem. Nature medicine, 14(10):1012-1012.

Sherlock JK, Griffin DK, Delhanty JDA, Parrington JM. 1996. Homologies between human and marmoset (Callithrix jacchus) chromosomes revealed by comparative chromosome painting. Genomics, 33(2):214-219.

Sibal LR, Samson KJ. 2001. Nonhuman primates: a critical role in current disease research. ILAR Journal, 42(2):74-84.

Small MF, Stanyon R, Smith DG, Sineo L. 1985. High-resolution chromosomes of rhesus macaques (Macaca mulatta). American Journal of Primatology, 9(1):63-67.

Smeets DF, Van de Klundert FA. 1990. Common fragile sites in man and three closely related primate species. Cytogenetic and Genome Research, 53(1):8-14.

Speicher MR, Ballard SG, Ward DC. 1996. Karyotyping human chromosomes by combinatorial multi-fluor FISH. Nature genetics, 12(4):368-375.

Stanyon R, Consigliere S, Müller S, Morescalchi A, Neusser M, Wienberg J. 2000. Fluorescence in situ hybridization (FISH) maps chromosomal homologies between the dusky titi and squirrel monkey. American journal of primatology, 50(2):95-107.

Stock AD, Hsu TC. 1973. Evolutionary conservatism in arrangement of genetic material. Chromosoma, 43(2):211-224.

Supanuam P, Tanomtong A, Khunsook S, Khrueanet W, Pinthong K, Wonkaonoi W. 2015. The First Report on Standardized Karyotype and Idiogram of Indochinese Silvered Langur, Trachypithecus germaini germaini (Primates, Colobinae) in Thailand. Cytologia, 80(2):183-192.

Sutherland GR. 2003. Rare fragile sites. Cytogenetic and genome research, 100(1-4):77-84.

Tanomtong A, Khunsook S, Wonkaonoi W, Supanuam P, Srisamoot N, Jumrusthanasan S. 2014. The First Karyological Study and Natural NOR Polymorphism in Banded Langur, Presbytis femoralis (Primate, Colobinae). Cytologia, 79(1):29-39.

Tantravahi R, Dev VG, Firschein IL, Miller DA, Miller OJ. 1975. Karyotype of the gibbons Hylobates lar and H. moloch: Inversion in chromosome 7. Cytogenetic and Genome Research, 15(2):92-102.

Tantravahi R, Miller DA, Dev VG, Miller OJ. 1976. Detection of nucleolus organizer regions in chromosomes of human, chimpanzee, gorilla, orangutan and gibbon. Chromosoma,56(1):15-27.

Telenius H, Ponder BA, Tunnacliffe A, Pelmear AH, Carter NP, Ferguson-Smith, MA, Pfragner R. 1992. Cytogenetic analysis by chromosome painting using dop-pcr amplified flow‐sorted chromosomes. Genes, Chromosomes and Cancer, 4(3):257-263.

Tjio JH, Levan A. 1956. The chromosome number of man. Hereditas, 42:16.

Vallender EJ, Miller GM. 2013. Nonhuman primate models in the genomic era: a paradigm shift. ILAR Journal, 54(2):154-165.

Ventura M, Antonacci F, Cardone MF, Stanyon R, D'Addabbo P, Cellamare A, Rocchi M. 2007. Evolutionary formation of new centromeres in macaque. Science, 316(5822):243-246.

Ventura M, Weigl S, Carbone L, Cardone MF, Misceo D, Teti M, She X. 2004. Recurrent sites for new centromere seeding. Genome research, 14(9):1696-1703.

Warren WC, Jasinska AJ, García-Pérez R, Svardal H, Tomlinson C, Rocchi M, Kyung K. 2015. The genome of the vervet (Chlorocebus aethiops sabaeus). Genome research, 25(12):1921-1933.

Wienberg J, Stanyon R, Jauch A, Cremer T. 1992. Homologies in human and Macasa fuscata chromosomes revealed by in situ suppression hybridization with human chromosome specific DNA libraries. Chromosoma, 101(5-6):265-270.

Yatsenko SA, Brundage EK, Roney EK, Cheung SW, Chinault AC, Lupski JR. 2009. Molecular mechanisms for subtelomeric rearrangements associated with the 9q34.3 microdeletion syndrome. Human molecular genetics, 18(11):1924-1936.

Yoshida K, Kitano J. 2012. The contribution of female meiotic drive to the evolution of neo-sex chromosomes. Evolution, 66(10):3198-3208.

Yunis JJ, Sanchez O. 1975. The G-banded prophase chromosomes of man. Humangenetik, 27(3):167-172.

Yunis JJ, Soreng AL. 1984. Constitutive fragile sites and cancer. Science, 226(4679):1199-1204.

6. Appendix

The lists of unpublished data

The distribution of ECBs in OWMs and NWMs compared with breakpoints (BP) in human disorders, human Fragile sites (FSs) and monkey FSs (unpublished data are marked in bold).

No.	TCR	BP in human disorders	Human FSs	Monkey FSs
1	1p33.2	**n.a.**	n.a.	**n.a.**
2	1p22	**n.a.**	1p22	**1p22**
3	1q22	**n.a.**	n.a.	**n.a.**
4	1q24	**n.a.**	n.a.	**n.a.**
5	1q41	**1q41**	1q41	**n.a.**
6	2p25.3	**n.a.**	2p25	**n.a.**
7	2q14.1	**2q14.2**	2q14.2~14.3	**n.a.**
8	2p22.3	**n.a.**	2p22~23	**n.a.**
9	2q21	**n.a.**	2q21.3	**2q21**
10	2q24.2	**2q24.2**	2q24	**n.a.**
11	2q31	**2q31**	2q31	**2q31**
12	3p26.3	**n.a.**	3p26	**n.a.**
13	3p25.3	**3p25**	3p25	**3p25.3**
14	3p22.3	**n.a.**	3p22	**n.a.**
15	3p21.31	**3p21.32**	3p21	**n.a.**
16	3p12.3	**n.a.**	n.a.	**n.a.**
17	3p11.1	**3p11.2**	3p11/q11	**n.a.**
18	3q12.1	**3q12.1**	3q12	**3q12.1**
19	3q22.1	**n.a.**	3q22	**n.a.**
20	3q25.2	**3q25.1**	3q25	**n.a.**
21	3q27.1	**3q27**	3q27	**3q27.1**
22	3q29	**3q29**	3q29	**n.a.**
23	4p12	**n.a.**	4p12	**n.a.**
24	4q22	**4q22**	4q22	**n.a.**
25	5p15.2	**n.a.**	5p15	**n.a.**
26	5p12	**n.a.**	n.a.	**5p12**
27	5q11.2	**n.a.**	5q11	**5q11.2**
28	5q21	**5q21.2**	5q21	**n.a.**
29	5q31.2	**5q31.1**	5q31.1	**5q31.2**
30	5q35.3	**5q35.3**	5q35	**n.a.**
31	6p25.3	**6p25.1**	6p25.1	**6p25.3**
32	6p21	**6p12.3~21.1**	6p21.1	**6p21**
33	6q15	**6q15**	6q15	**6q15**
34	6q21	**6q21**	6q21	**6q21**
35	7p22.3	**n.a.**	7p22	**7p22.3**

36	7p15.3	**7p15.3**	n.a.	**7p15.3**
37	7q11.1	**n.a.**	7q11.1	**7q11.1**
38	7q11.23	**7q11.23**	7q11.23	**7q11.23**
39	9q34.3	**9q34.3**	9q34	**n.a.**
40	9p24.3	**9p24.2**	9p24	**9p24.3**
41	9q33 ~ 34.1	**9q33~34.1**	9q33	**n.a.**
42	10p15.3	**n.a.**	10p15	**n.a.**
43	10p11.2	**10p11.2**	10p11.2	**10p11.2**
44	10p11.1	**10p11.1~11.21**	10p11.2	**10p11.1**
45	10q11.1	**10q11.1**	n.a.	**n.a.**
46	10q21.1	**10q21.1**	10q21	**10q21.1**
47	10q22.3	**n.a.**	n.a.	**10q22.3**
48	11p15.5	**n.a.**	n.a.	**11p15.5**
49	11p15.3	**11p15.3**	11p15.3-p15.4	**11p15.3**
50	11q12	**11q12.1**	n.a.	**n.a.**
51	12p13.33	**12p13.33**	12p13	**n.a.**
52	13q12.1	**n.a.**	n.a.	**n.a.**
53	13q14	**13q14.1**	13q14	**13q14**
54	13q32	**n.a.**	13q32	**13q32**
55	14q11.2	**n.a.**	14q11.2	**n.a.**
56	15q11.2	**15q11.2**	15q11.2	**n.a.**
57	15q26.1	**15q26.1**	15q26	**n.a.**
58	16p13.1	**16p13.1**	16p13.11	**16p13.1**
59	17p11.1	**n.a.**	17p11.1	**n.a.**
60	17q21.3	**17q21.1**	17q21	**17q21.3**
61	17q24	**17q24.1~24.2**	17q24~25	**n.a.**
62	18q21	**18q21.33~q22.1**	18q21.3 or 18q22	**n.a.**
63	19p13.2	**n.a.**	19p13.2	**n.a.**
64	19q13.2	**19q13.1~13.2**	19q13	**19q13.2**
65	19q13.43	**19q13.33~13.41**	19q13	**19q13.43**
66	20p12	**20p12**	20p12.2	**20p12**
67	20p11.1	**n.a.**	n.a.	**20p11.1**
68	20q11.1	**20q11.23**	20q11.2	**n.a.**
69	21q11.2	**21q11.21**	21q11.2	**n.a.**
70	22q11.21	**22q11.21**	n.a.	**n.a.**
71	Yp11.31	**Yp11.3**	n.a.	**n.a.**
72	Yp11.2	**Yp11.2**	n.a.	**n.a.**
73	Yq11.23	**Yq11.23**	n.a.	**n.a.**
Correlation		**64.3%**	78.1%	**43.8%**
No.	**Macaque**	**BP in human disorders**	**Human FSs**	**Monkey FSs**
1	1q23.3	**1q23.3**	1q23	**n.a.**
2	1q42.13	**1q42**	1q42	**1q42**
3	2p11.2	**2p11.2**	2p11.2	**n.a.**
4	2q11.1	**2q11.1**	2p11/2q11	**2q11.1**

5	2q14.1	**2q14.2**	2q14.2~14.3	**n.a.**
6	2q21.1	**2q14.3~21.2**	n.a.	**2q21.1**
7	2q22.1	**2q22**	2q22.3	**n.a.**
8	3p26.3	**n.a.**	3p26	**n.a.**
9	3p25.3	**3p25**	3p25	**3p25.3**
10	3p22.3	**n.a.**	3p22	**n.a.**
11	3p12.3	**n.a.**	n.a.	**n.a.**
12	3p11.1	**3p11.2**	3p11/q11	**n.a.**
13	3q12.1	**3q12.1**	3q12	**3q12.1**
14	3q22.1	**n.a.**	3q22	**n.a.**
15	3q25.2	**3q25.1**	3q25	**n.a.**
16	3q27.1	**3q27**	3q27	**3q27.1**
17	3q29	**3q29**	3q29	**n.a.**
18	4p15.3	**4p15.1**	4p15	**4p15.3**
19	4q10	**n.a.**	n.a.	**n.a.**
20	6p24	**n.a.**	n.a.	**n.a.**
21	6q25.2	**6p25.1**	6q25	**6q25.2**
22	6q21	**6q21**	6q21	**6q21**
23	6q24.3	**n.a.**	n.a.	**n.a.**
24	7p22.3	**n.a.**	7p22	**7p22.3**
25	7p22.1	**n.a.**	7p22	**7p22.1**
26	7p21.3	**7p21.1**	7p21	**n.a.**
27	7q11.23	**7q11.23**	7q11.23	**7q11.23**
28	7q21.3	**7q21.3**	n.a.	**7q21.3**
29	7q22.1	**7q22**	7q22	**7q22.1**
30	9p24.3	**9p24.2**	9p24	**9p24.3**
31	9q21.11	**9q21.1**	9q21	**n.a.**
32	9q22.33	**9q22.3**	n.a.	**9q22.33**
33	9q33.2	**9q33**	9q33	**n.a.**
34	9q34	**9q34.1~34.2**	9q34	**n.a.**
35	10q11.23	**10q11.23**	10q11.2	**n.a.**
36	10q23.2	**10q23.2**	n.a.	**n.a.**
37	11p15.4	**n.a.**	11p15.4	**11p15.4**
38	11q13.4	**11q13.3~13.5**	11q13.3	**11q13.4**
39	13q21.31	**13q21.3**	13q21.3	**13q21.31**
40	14q11.2	**14q11.1**	n.a.	**n.a.**
41	15q25	**n.a.**	15q25	**n.a.**
42	15q26.3	**15q26.3**	15q26	**n.a.**
43	16q22.1	**16q22.1**	16q22.1	**16q22.1**
44	16q22.3	**n.a.**	16q22	**16q22.3**
45	17q12	**n.a.**	n.a.	**n.a.**
46	17q21.32	**17q21.33**	17q21	**17q21.32**
47	17q23.3	**17q23.3**	n.a.	**17q23.3**
48	18q21.2	**n.a.**	n.a.	**18q21.2**

49	20p13	**20p13**	20p13	**20p13**
50	20p11.21	**n.a.**	20p11.23	**20p11.21**
51	20q11.21	**20q11.23**	20q11.2	**n.a.**
52	21q11.2	**21q11.21**	21q11.2	**n.a.**
53	22p13	**22p12~13**	n.a.	**n.a.**
Correlation		**71.7%**	75.5%	**49.05%**
No.	**CAE**	**BP in human disorders**	**Human FSs**	**Monkey FSs**
1	1q22	**n.a.**	n.a.	**n.a.**
2	1q42.3	**1q42**	1q42	**1q42.3**
3	2q12.2	**2q12**	n.a.	**n.a.**
4	3p26.3	**n.a.**	3p26	**n.a.**
5	3p25.3	**3p25**	3p25	**3p25.3**
6	3p22.3	**n.a.**	3p22	**n.a.**
7	3p12.3	**n.a.**	n.a.	**n.a.**
8	3p11.1	**3p11.2**	3p11/q11	**n.a.**
9	3q12.1	**3q12**	3q12	**3q12.1**
10	3q22.1	**n.a.**	3q22	**n.a.**
11	3q27.1	**3q27**	3q27	**3q27.1**
12	4q12	**n.a.**	4q12	**n.a.**
13	5q14.1	**n.a.**	5q14	**5q14.1**
14	6q16.1	**n.a.**	n.a.	**n.a.**
15	6q16.3	**n.a.**	6q16.3	**n.a.**
16	6q24.3	**n.a.**	n.a.	**n.a.**
17	7p22.3	**n.a.**	7p22	**7p22.3**
18	7q11.21	**7q11.21**	7q11.2	**7q11.21**
19	7q11.23	**7q11.23**	7q11.23	**7q11.23**
20	7q21.11	**7q21.11**	n.a.	**7q21.11**
21	9p24.3	**9p24.2**	9p24	**9p24.3**
22	9p11	**9p11.1~12**	n.a.	**n.a.**
23	9q11	**9q11**	n.a.	**n.a.**
24	9q22.32	**9q22.3~q31.1**	n.a.	**9q22.32**
25	10q21.3	**n.a.**	10q21	**10q21.3**
26	10q23.33	**n.a.**	10q23.3	**n.a.**
27	11p15.5	**n.a.**	n.a.	**11p15.5**
28	11q12.1	**11q12.1**	n.a.	**n.a.**
29	11q14.1	**11q14**	11q14.2	**11q14.1**
30	13q11.1	**n.a.**	n.a.	**n.a.**
31	14q11.1	**14q11.1**	n.a.	**n.a.**
32	14q13.3	**14q13**	14q13	**14q13.3**
33	15q11.1	**15q11.1**	n.a.	**n.a.**
34	15q24.1	**15q24**	15q24	**15q24.1**
35	15q26.3	**15q26.3**	15q26	**n.a.**
36	17q12	**n.a.**	n.a.	**n.a.**
37	17q25.3	**n.a.**	17q25	**17q25.3**

38	20p13	**20p13**	20p13	**20p13**
39	21q22.3	**21q22.3**	n.a.	**21q22.3**
40	21q11.1	**21q11.21**	21q11.2	**n.a.**
41	22q11.1	**22q11.1~11.21**	n.a.	**n.a.**
Correlation		**58.5%**	58.5%	**46.3%**
No.	**ACA**	**BP in human disorders**	**Human FSs**	**Monkey FSs**
1	1p22.2	**n.a.**	1p22	**1p22.2**
2	1p12	**1p12**	n.a.	**n.a.**
3	1q31.2	**1q31.2**	1q31	**n.a.**
4	2q14.3	**2q14.3**	2q14.3	**n.a.**
5	2q37.3	**2q37.1**	n.a.	**2q37.3**
6	3p26.3	**n.a.**	3p26	**n.a.**
7	3p25.3	**3p25**	3p25	**3p25.3**
8	3p21.31	**3p21.3**	3p22 or 3p21	**n.a.**
9	3p12.3	**n.a.**	n.a.	**n.a.**
10	3p11.1	**3p11.2**	3p11/q11	**n.a.**
11	3q12.1	**3q12**	3q12	**3q12.1**
12	3q22.1	**n.a.**	3q22	**n.a.**
13	3q27.1	**3q27**	3q27	**3q27.1**
14	4q26	**n.a.**	n.a.	**n.a.**
15	4q28.3	**4q28~31.1**	n.a.	**4q28.3**
16	5p15.33	**n.a.**	5p15	**n.a.**
17	5p12	**n.a.**	n.a.	**5p12**
18	5q11.2	**n.a.**	n.a.	**n.a.**
19	5q31.3	**5q31.1**	n.a.	**5q31.3**
20	5q35.3	**5q35.3**	5q35	**n.a.**
21	6p22.3	**n.a.**	n.a.	**6p22.3**
22	6p25.3	**6p25.1**	6p25	**6p25.3**
23	7p22.3	**n.a.**	7p22	**7p22.3**
24	7q11.23	**7q11.23**	7q11.23	**7q11.23**
25	7q21.11	**7q21.11**	n.a.	**7q21.11**
26	8p11.21	**8p11.22**	8p11	**n.a.**
27	8q11.21	**n.a.**	8q11	**n.a.**
28	8p23.3	**8p23.3**	8p23.3	**8p23.3**
29	9p24.3	**9p24.2**	9p24	**9p24.3**
30	9p11	**9p11.1~12**	n.a.	**n.a.**
31	9q22.32	**9q22.3~q31.1**	n.a.	**9q22.32**
32	10p11.22	**10p11.2**	10p11.2	**10p11.22**
33	10q11.22	**10q11.23**	10q11.2	**n.a.**
34	10q21.1	**10q21.1**	10q21	**10q21.1**
35	11p15.5	**n.a.**	n.a.	**11p15.5**
36	11q12.2	**11q12.1**	n.a.	**n.a.**
37	11q14.3	**11q14**	11q14.2	**11q14.3**
38	11q25	**11q25**	n.a.	**n.a.**

39	13q11.1	**n.a.**	n.a.	**n.a.**
40	14q11.1	**14q11.1**	n.a.	**n.a.**
41	15q11.1	**15q11.1**	n.a.	**n.a.**
42	15q23	**15q23**	n.a.	**n.a.**
43	15q24.1	**15q24**	15q24	**15q24.1**
44	16p13.12	**16p13.1**	16p13.11	**16p13.12**
45	16p11.1	**16p11.1**	16p11/q11	**16p11.1**
46	16q11.1	**16q11.1**	16p11/q11	**n.a.**
47	16q24.3	**16q24**	16q24	**n.a.**
48	18p11.32	**18p11.32**	18p11.3	**18p11.32**
49	20p13	**20p13**	20p13	**20p13**
50	21q11.1	**21q11.21**	21q11.2	**n.a.**
51	22q11.1	**22q11.1~11.21**	n.a.	**n.a.**
Correlation		**74.5%**	60.8%	**49%**
No.	**CAP**	**BP in human disorders**	**Human FSs**	**Monkey FSs**
1	1p12	**1p12**	n.a.	**n.a.**
2	1q31.2	**1q31.2**	1q31	**n.a.**
3	2q14.3	**2q14.3**	2q14.3	**n.a.**
4	3p26.3	**n.a.**	3p26	**n.a.**
5	3p25.3	**3p25**	3p25	**3p25**
6	3p21.31	**3p21.3**	3p22 or 3p21	**n.a.**
7	3p12.3	**n.a.**	n.a.	**n.a.**
8	3p11.1	**3p11.2**	3p11/q11	**n.a.**
9	3q12.1	**3q12**	3q12	**3q12**
10	3q22.1	**n.a.**	3q22	**n.a.**
11	3q26.33	**3q26.3**	3q26	**3q26.3**
12	5q35.3	**5q35**	5q35	**n.a.**
13	6p25.3	**n.a.**	6p25	**6p25.3**
14	6p21.33	**6p21.3~22.1**	n.a.	**6p21.33**
15	7p22.3	**n.a.**	7p22	**7p22.3**
16	7q11.23	**7q11.23**	7q11.23	**7q11.23**
17	7q21.11	**7q21.11**	n.a.	**7q21.11**
18	8p11.21	**8p11.22**	8p11	**n.a.**
19	8q11.21	**n.a.**	8q11	**n.a.**
20	9p24.3	**9p24.2**	9p24	**9p24.3**
21	9p11	**9p11.1~12**	n.a.	**n.a.**
22	9q13	**9q13**	9q13	**n.a.**
23	10p11.22	**10p11.2**	10p11.2	**10p11.22**
24	10q11.22	**10q11.23**	10q11.2	**n.a.**
25	10q23.33	**n.a.**	10q23.3	**n.a.**
26	11p15.5	**n.a.**	n.a.	**11p15.5**
27	11q12.2	**11p12~13**	n.a.	**n.a.**
28	11q25	**11q25**	n.a.	**n.a.**
29	12p13.2	**12p13.1**	12p13	**n.a.**

30	12q12	**12q12**	n.a.	**12q12**
31	13q11.1	**n.a.**	n.a.	**n.a.**
32	14q11.1	**14q11.1**	n.a.	**n.a.**
33	14q21.2	**14q21**	14q21.2	**14q21.2**
34	15q11.1	**15q11.1**	n.a.	**n.a.**
35	15q24.1	**15q24**	15q24	**15q24.1**
36	16p11.1	**16p11.1**	16p11/q11	**16p11.1**
37	16q11.1	**16q11.1**	16p11/q11	**n.a.**
38	17p13.3	**17p13.3**	n.a.	**n.a.**
39	17q12	**n.a.**	n.a.	**n.a.**
40	18p11.32	**18p11.32**	18p11.3	**18p11.32**
41	20p13	**20p13**	20p13	**20p13**
42	20q11.1	**20q11.23**	20q11.2	**n.a.**
43	21q11.1	**21q11.21**	21q11.2	**n.a.**
44	22q11.1	**22q11.1~11.21**	n.a.	**n.a.**
Correlation		**77.3%**	65.5%	**49%**
No.	**CJA**	**BP in human disorders**	**Human FSs**	**Monkey FSs**
1	1p36.33	**1p36.33**	1p36	**1p36**
2	1p12	**1p12**	n.a.	**n.a.**
3	1q31.2	**1q31.2**	1q31	**n.a.**
4	2q14.3	**2q14.3**	2q14.3	**n.a.**
5	3p26.3	**n.a.**	3p26	**n.a.**
6	3p25.3	**3p25**	3p25	**3p25**
7	3p21.31	**3p21.3**	3p22 or 3p21	**n.a.**
8	3p12.3	**n.a.**	n.a.	**n.a.**
9	3p11.1	**3p11.2**	3p11/q11	**n.a.**
10	3q12.1	**3q12**	3q12	**3q12**
11	3q22.1	**n.a.**	3q22	**n.a.**
12	3q26.33	**3q26.3**	3q26	**3q26**
13	5q35.3		5q35	**n.a.**
14	6p25.3	**6p25.1**	6p25	**6p25.3**
15	6p21.33	**6p21.3~22.1**	n.a.	**6p21.33**
16	7p22.3	**n.a.**	7p22	**7p22.3**
17	7q11.21	**7q11.21**	7q11.21	**7q11.21**
18	7q11.23	**7q11.23**	7q11.23	**7q11.23**
19	7q31.31	**n.a.**	n.a.	**7q31.31**
20	7q36.3	**7q36.3**	7q36	**n.a.**
21	8p11.21	**8p11.22**	8p11	**n.a.**
22	8q11.21	**n.a.**	8q11	**n.a.**
23	8p23.3	**8p23.3**	8p23.3	**8p23.3**
24	8q22.2	**n.a.**	n.a.	**8q22.2**
25	8q24.3	**8q24.3**	8q24.3	**8q24.3**
26	9p24.3	**9p24.2**	9p24	**9p24.3**
27	9p11	**9p11.1~12**	n.a.	**n.a.**

28	9q22.32	**9q22.3~q31.1**	n.a.	**9q22.32**
29	9q34.3	**9q34.3**	9q34	**n.a.**
30	10p11.21	**10p11.2**	10p11.2	**10p11.21**
31	10q11.22	**10q11.23**	10q11.2	**n.a.**
32	10q23.33	**n.a.**	10q23.3	**n.a.**
33	11q11.2	**11p11.2~12**	11p11.2 or 11p12	**n.a.**
34	11q12.2	**11q12.1**	n.a.	**n.a.**
35	11q14.3	**11q14**	11q14.2	**11q14.3**
36	13q11.1	**n.a.**	n.a.	**n.a.**
37	13q13.3	**13q13**	13q13.2	**13q13.3**
38	14q11.1	**14q11.1**	n.a.	**n.a.**
39	15q11.1	**15q11.1**	n.a.	**n.a.**
40	15q24.1	**15q24**	15q24	**15q24.1**
41	16p11.1	**16p11.1**	16p11/q11	**16p11.1**
42	17p13.3	**17p13.3**	n.a.	**n.a.**
43	17q25.3	**n.a.**	17q24-25	**17q25.3**
44	18p11.32	**18p11.32**	18p11.3	**18p11.32**
45	20q13.33	**20q13.32**	20q13.3	**20q13.33**
46	21q11.1	**21q11.21**	21q11.2	**n.a.**
47	22q11.1	**22q11.1~11.21**	n.a.	**n.a.**
Correlation		**78.7%**	72.3%	**48.9%**
No.	**SSC**	**BP in human disorders**	**Human FSs**	**Monkey FSs**
1	1p12	**1p12**	n.a.	**n.a.**
2	1q31.2	**1q31.2**	1q31	**n.a.**
3	2p13.1	**2p13.1**	2p13	**2p13.1**
4	2q14.3	**2q14.3**	2q14.3	**n.a.**
5	3p26.3	**n.a.**	3p26	**n.a.**
6	3p25.3	**3p25**	3p25	**3p25.3**
7	3p22.3	**n.a.**	3p22	**n.a.**
8	3p21.31	**3p21.3**	3p22 or 3p21	**n.a.**
9	3p14.1	**n.a.**	n.a.	**3p14.1**
10	3p12.3	**n.a.**	n.a.	**n.a.**
11	3p11.1	**3p11.2**	3p11/q11	**n.a.**
12	3q12.1	**3q12**	3q12	**3q12.1**
13	3q22.1	**n.a.**	3q22	**n.a.**
14	3q24	**3q24**	n.a.	**n.a.**
15	3q26.33	**3q26.3**	3q26	**3q26.33**
16	3q27.1	**3q27**	3q27	**3q27.1**
17	4q26	**n.a.**	n.a.	**n.a.**
18	4q35.2	**4q35**	4q35	**4q35.2**
19	5q34	**5q34**	5q34	**n.a.**
20	5q35.3	**5q35.3**	5q35	**n.a.**
21	6p25.3	**6p25.1**	6p25	**6p25.3**
22	6p21.33	**6p21.3~22.1**	n.a.	**6p21.33**

23	7p22.3	**n.a.**	7p22	**7p22.3**
24	7p15.3	**7p15.3**	n.a.	**7p15.3**
25	7p11.2	**7p11.2**	7p11.2	**7p11.2**
26	7q11.23	**7q11.23**	7q11.23	**7q11.23**
27	7q21.11	**7q21.11**	n.a.	**7q21.11**
28	8p11.21	**8p11.22**	8p11	**n.a.**
29	8q11.21	**n.a.**	8q11	**n.a.**
30	9p24.3	**9p24.2**	9p24	**9p24.3**
31	9q13	**9q13**	9q13	**9q13**
32	9q31.2	**9q22.3~q31.1**	9q31	**n.a.**
33	9q34.13	**9q34.1~34.2**	9q34	**n.a.**
34	9q34.3	**9q34.3**	9q34	**n.a.**
35	10p15.3	**n.a.**	10p15	**n.a.**
36	10p14	**n.a.**	n.a.	**n.a.**
37	10p11.1	**10p11.1~11.21**	10p11.2	**10p11.1**
38	10p11.22	**10p11.2**	10p11.2	**10p11.22**
39	10q11.22	**10q11.23**	10q11.2	**n.a.**
40	11p15.5	**n.a.**	n.a.	**11p15.5**
41	11q14.3	**11q14**	11q14.2	**11q14.3**
42	11q25	**11q25**	n.a.	**n.a.**
43	12p13.2	**12p13.3**	12p13	**n.a.**
44	12q12	**12q12**	n.a.	**12q12**
45	13q11.1	**n.a.**	n.a.	**n.a.**
46	14q11.1	**14q11.1**	n.a.	**n.a.**
47	14q21.2	**14q21**	14q21.2	**14q21.2**
48	14q23.1	**14q22~23**	14q22 or 14q23	**n.a.**
49	14q32.13	**14q32.1**	14q32	**n.a.**
50	14q32.22	**14q32.2**	14q32	**n.a.**
51	15q11.1	**15q11.1**	n.a.	**n.a.**
52	15q21.2	**15q21.2**	15q21	**n.a.**
53	15q23	**15q23**	n.a.	**n.a.**
54	15q24.1	**15q24**	15q24	**15q24.1**
55	16p13.3	**16p13.3**	n.a.	**16p13.3**
56	16q11.1	**16q11.1**	16p11/q11	**n.a.**
57	16q24.3	**16q24**	16q24	**n.a.**
58	18p11.32	**18p11.32**	18p11.3	**18p11.32**
59	19p13.3	**19p13.3**	n.a.	**n.a.**
60	20p13	**20p13**	20p13	**20p13**
61	20q11.1	**20q11.23**	20q11.2	**n.a.**
62	20q13.33	**20q13.32**	20q13.3	**20q13.33**
63	21q11.1	**21q11.21**	21q11.2	**n.a.**
64	22q11.1	**22q11.1~11.21**	n.a.	**n.a.**
Correlation		**81.25%**	70.3%	**42.1%**

Table 2. The distribution of cases of cancer and human diseases involving ECBs bands recorded in databases.

High frequencies ECB in chromosomal bands	No. cases in Mitelman database	No. cases in OMIM
3p25.3	434	9
3p11.1	543	7
3q12.1	375	2
3p21.31	1200	21
7q11.23	1174	51
9p24.3	540	8
9q34.3	5531	54

Table 3. The centromere positioning in OWMs and NWMs

	TCR	**Macaques**	**CAE**	**ACA**	**CAP**	**CJA**	**SSC**
Conserved centromeres (CCen)	22	22	22	10	18	14	12
Neo-centromeres (Ncen)	22	20	38	42	36	32	32
Diploid number 2n	44	42	60	52	54	46	44
% CCen	50%	52.3%	36.7%	19.2%	33.3%	30.4%	27.3%
% Ncen	50%	47.6%	63.3%	80.8%	66.7%	69.9%	72.7%

Curriculum Vitae

Family Name: Fan

Given Name: Xiaobo

Birth Data: 28.09. 1984

Birth Place: Xu Zhou City, P. R. China

Current Address: Schlegelstraße 2, 07747 Jena, Germany

E-mail: Xiaobo.Fan@med.uni-jena.de

oneshop928@hotmail.com

Education:

2011-2015 Friedrich Schiller University of Jena, Germany

Institute for Human Genetics (Ph.D. student)

Supervisor: PD Dr. rer. nat./med.habil. Thomas Liehr

2008-2011 Nan Jing Normal University, Nan Jing City, China

Zoology (Master degree)

Supervisor: Prof. Huang Yu-feng

2003-2007 Nan Jing Normal University, Nan Jing City, China

Biotechnology (Bachelor degree)

2000-2003 Xu Zhou No.1 middle school, Xu Zhou City, China

1997-2000 Xu Zhou No.2 middle school, Xu Zhou City, China

1991-1997 Shao Hua street primary school, Xu Zhou City, China

Academic exchanges and Conference:

2014.10.10-2014.10.18 National Cancer Institute of Brazil

2014.10.18-2014.10.24 The National Primate Center,

Federal University of Para, Brazil

Academic exchanges

2013.11.22-2013.11.23 Friedrich-Schiller-Universität Jena, Germany

International course on Molecular Cytogenetics

2012.4.25- 2012.4.28 20th International Colloquium on Animal Cytogenetics

And Gene Mapping (ICACGM), Cordoba, Spain

Poster Award

Research projects:

Since 2011.10- now

Ph.D. Topic: Evolutionary conserved breakpoints in Old and New World monkeys and their relation to fragile sits observed in Homo sapiens.

2009.07-2011.07

Master's Project: Application of Cytogenetics 2.7M chips on diagnosis procedure and molecular mechanisms of genetic diseases.

Experiences:

2009.07-2011.07

Institute of Laboratory Medicine, Jin Ling Hospital, Nan Jing City, China

Co-worker as clinical routine analysis of GTG Banding and Fluorescent in-situ hybridization (FISH) tests

Award:

2011-2013 China Scholarship Council (CSC)

2012.4.25- 2012.4.28 Poster Award of 20th International Colloquium on Animal Cytogenetics And Gene Mapping (ICACGM), Cordoba, Spain

Language:

Chinese: First language

English: B1, B2 and C1

(Certification: Sprachenzentrum der Friedrich-Schiller-Universität Jena)

German: A2.1

(Certification: Sprachenzentrum der Friedrich-Schiller-Universität Jena)

Publications:

1. Z Li, Q Zhang, J-H Mao, A Weise, K Mrasek, **X Fan**, X Zhang, T Liehr, KH Lu, A Balmain, W-W Cai. A HDAC1-binding domain within FATS bridges p21 turnover to radiation-induced tumorigenesis. Oncogene 2010, 29:2659-2671.

2. Kosyakova N, Hamid AB, Chaveerach A, Pinthong K, Siripiyasing P, Supiwong W, Romanenko S, Trifonov V, **Fan X**. Generation of multicolor banding probes for chromosomes of different species. Molecular Cytogenetics, 2013; 6:6.

3. Liehr T, Weise A, Hamid AB, **Fan X**, Klein E, Aust N, Othman MAK, Mrasek K, Kosyakova N. Multicolor FISH methods in current clinical diagnostics. Expert Rev Mol Diag, 2013; 13(3): 251–255.

4. **Fan X**, Pinthong K, Mkrtchyan H, Siripiyasing P, Kosyakova N, Supiwong W, Tanomtong A, Chaveerach A, Liehr T, de Bello Cioffi M, Weise A.First detailed reconstruction of the karyotype of Trachypithecus cristatus (Mammalia: Cercopithecidae). Mol Cytogenet. 2013 17;6(1):58.

5. Spittel H, Kubek F, Kreskowski K, Ziegler M, Klein E, Hamid AB, Kosyakova N, Radhakrishnan G, Junge A, Kozlowski P, Schulze B, Martin T, Huhle D, Mehnert K, Rodríguez L, Ergun M A, Sarri C, Militaru M, Stipoljev F, Tittelbach H, Vasheghani F, Cioffi MB, Hussein SS, **Fan X**, Volleth M, Liehr T. Mitotic stability of small supernumerary marker chromosomes : A study based on 93 immortalized cell lines. Cytogenet Genome Res, 2014; 142: 151-160.

6. **Fan X**, Sangpakdee W, Tanomtong A, Chaveerach A, Pinthong K, Pornnarong S, Supiwong W, Trifonov VA, Hovhannisyan GG, Aroutouinian RM, Liehr T, Weise A.

Molecular cytogenetic analysis of Thai southern pig-tailed macaque (Macaca nemestrina) by multicolor banding. Proceedings of Yerevan State University 2014, 2014:46-50.

7. **Fan X**, Sangpakdee W, Tanomtong A, Chaveerach A, Pinthong K, Pornnarong S, Supiwong W, Trifonov V, Hovhannisyan G, Loth K, Hensel C, Liehr T, Weise A. Comprehensive molecular cytogenetic analysis of Barbary macaque (Macaca sylvanus). Biol J Arm 2014, 66:98-102.

8. **Fan X**, Tanomtong A, Chaveerach A, Pinthong K, Pornnarong S, Supiwong W, Liehr T, Weise A. High resolution karyotype of Thai crab-eating macaque (Macaca fascicularis). Genetika 2014, 46:877-882.

9. Supiwong W, Liehr T, Cioffi MB, Chaveerach A, Kosyakova N, **Fan X**, Tanee T, Tanomtong A. Comparative cytogenetic mapping of rRNA genes among naked catfishes: implications for genomic evolution in the Bagridae family. Genet Mol Res. 2014 Nov 12; 13(4):9533-42.

10. Hussein SS, Kreskowski K, Ziegler M, Klein E, Hamid AB, Kosyakova N, Volleth M, Liehr T, **Fan X**, Piaszinski K. Mitotic stability of small supernumerary marker chromosomes depends on their shape and telomeres - a long term in vitro study. Gene, 2014; 552:246-248.

11. Al-Achkar W, Moassass F, Al-Ablog A, Liehr T, **Fan X**, Wafa A. Chromosomal aberration leads to recurrent pregnancy loss and partial trisomy of 5p12-15.3 in the offspring: report of a Syrian couple and review of the literature. Zhonghua Nan Ke Xue, 2015; 21(3):219-24.

12. Weise A, Kosyakova N, Voigt M, Aust N, Mrasek K, Löhmer S, Rubtsov N, Karamysheva TV, Trifonov VA, Hardekopf D, Jančušková T, Pekova S, Wilhelm K, Liehr T, **Fan X**. Comprehensive Analyses of White-Handed Gibbon Chromosomes Enables Access to 92 Evolutionary Conserved Breakpoints Compared to the Human Genome. Cytogenet Genome Res. 2015; 145(1):42-9.

13. Hamid AB, **Fan X**, Kosyakova N, Radhakrishnan G, Liehr T, Karamysheva T. New BAC probe set to narrow down chromosomal breakpoints in small and large

derivative chromosomes, especially suited for mosaic conditions. Methods Mol Biol. 2015;1227:279-87. (chapter)

14. **X Fan**, W Supiwong, A Weise, K Mrasek, N Kosyakova, A Tanomtong, K Pinthong, VA Trifonov, M de Bello Cioffi, P Grothmann, T Liehr, EHC de Oliveira. Comprehensive characterization of evolutionary conserved breakpoints in four New World Monkey karyotypes compared to Chlorocebus aethiops and Homo sapiens. Helyon 2015, Article No ~ e00042.

Jena, 20.06. 2016 Fan, Xiaobo

Acknowledgements

I want to thank PD Dr. rer. nat./ med. habil. Thomas Liehr as my supervisor. He offered me the opportunity to study in Germany. Four years ago I never forgot that moment when I sent e-mail and asked him whether I could do some researches in his lab as a Ph.D. student, and his answer was 'Yes'. He always provided the help to students in the research process as possible. During these years he gave me extremely valuable suggestions for my Ph.D. works. He supported me to attend in international conference and academic exchange. Without his supervising, I cannot achieve my experiments in time. Without his help, I cannot publish so many papers. Without his revise opinion, I cannot write a good quality of my Ph.D. thesis. He gives me so much help that words cannot adequately express my gratitude.

I would like to give my gratitude to Prof. Huang Yu-Feng and China Scholarship Council. Without his recommend, I cannot gain a scholarship in time. Also for China Scholarship Council, it plays an important role in scientific researches and academic exchange. It will be a bridge between my future work and German cooperation.

Also I would like to thank very much to my colleagues: Monika Ziegler, Katharina Kreskowski, Dr. Nadezda Kosyakova, Dr. Samarth Bhatt and Dr. Ahmed Basheer Hamid for teaching me in the lab. Dr. Anja Weise and Dr. Kristin Mrasek gave me constructive suggestions in the study of primate evolution and fragile sites. Moneeb Othman, Weerayuth Supiwong, Katharina Rittscher, Eyad Alhourani, Beate Pohle and Piaszinski Katja for making a colorful life in Jena.

I am really glad to know many friendly guests from Thailand and Brazil: Prof. Alongkoad Tanomtong, Prof. Arunrat Chaveerach, Dr. Krit Pinthong, Dr. Pornnarong Siripiyasing, Cassia Yano, Marcelo de Bello Cioffi and Prof. Edivaldo H. C. de Oliveira.

At last, I would like to say thanks to my family for taking care of me and supporting me. They give wonderful life and good education conditions to me for pursuit my dream.

Ehrenwörtliche Erklärung

Hiermit erkläre ich, dass mir die Promotionsordnung der Medizinischen Fakultät der Friedrich-Schiller-Universität bekannt ist,

ich die Dissertation selbst angefertigt habe und alle von mir benutzten Hilfsmittel, persönlichen Mitteilungen und Quellen in meiner Arbeit angegeben sind,

mich folgende Personen bei der Auswahl und Auswertung des Materials sowie bei der Herstellung des Manuskripts unterstützt haben: PD Dr. rer. nat./ med. habil. Thomas Liehr,

die Hilfe eines Promotionsberaters nicht in Anspruch genommen wurde und dass Dritte weder unmittelbar noch mittelbar geldwerte Leistungen von mir für Arbeiten erhalten haben, die im Zusammenhang mit dem Inhalt der vorgelegten Dissertation stehen,

dass ich die Dissertation noch nicht als Prüfungsarbeit für eine staatliche oder andere wissenschaftliche Prüfung eingereicht habe und

dass ich die gleiche, eine in wesentlichen Teilen ähnliche oder eine andere Abhandlung nicht bei einer anderen Hochschule als Dissertation eingereicht habe.

Jena, 20.06.2016 Fan, Xiaobo